PHD

Post-receptor signalling in the insulin regulation of glucose uptake

Liu, Simon C. H.

Award date:
1997

Awarding institution:
University of Bath

Post-receptor Signalling in the Insulin Regulation of Glucose Uptake

submitted by Simon C.H. Liu
for the degree of PhD
of the University of Bath
1997

ProQuest LLC
789 East Eisenhower Parkway
P.O. Box 1346
Ann Arbor, MI 48106-1346

CONTENTS

ABSTRACT

The potential involvement of the PH domain of IRS-1 in the stimulation of glucose uptake by insulin has been investigated. Exogenous IRS-1 PH domain - produced using a GST fusion protein system - was introduced into permeabilized 3T3-L1 adipocytes prior to insulin stimulation. The exogenous protein was able to partially block insulin-stimulated tyrosine phosphorylation of IRS-1, but only if the stimulation time with 100 nM insulin was reduced from 10 min to 2 min. However, insulin stimulation of PI 3-K activity and of glucose uptake - both events have been implicated to be downstream of IRS-1 phosphorylation - were not affected. The results are consistent with the view that the PH domain is involved in targeting IRS-1 to the insulin receptor. However the nature of this process is not clear. Binding studies using either biotinylated IRS-1 PH domain or immobilized IRS-1 PH domain did not reveal a protein ligand for this structural domain.

Insulin stimulation of glucose uptake and of PKB activity appear to occur via PI 3-K. Evidence was obtained in support of the view that PKB is downstream of PI 3-K and involved in insulin-stimulated glucose uptake in 3T3-L1 adipocytes. First, activation of PKB is less sensitive to insulin stimulation than elevation of glucose uptake. Thus, the potential signal from PKB to increase transport activity may be amplified. Second, following insulin treatment, maximal stimulation of PKB activity occurs before that of glucose transport activity. Third, following the addition of wortmannin - an inhibitor of PI 3-K - to insulin-stimulated cells, PKB activity declines more rapidly than glucose uptake. Fourth, chronic treatment of cells with insulin down-regulates both cell surface GLUT4 and PKB activity. Further, in rat adipocytes, metformin can counteract the effects of prolonged insulin stimulation on both parameters.

The characteristics of insulin stimulation of PKB activity were also investigated in 3T3-L1 adipocytes. First, measurements of PKB activity in subcellular fractions revealed that only the activity in the cytoplasm is stimulated by insulin. Second,

PP2A has a partial role to play in the deactivation of PKB. Thus, if okadaic acid - an inhibitor of PP2A - is present during insulin stimulation prior to wortmannin treatment, then the inhibition of PKB activity is partially blocked. Further, okadaic acid also reduces the rate at which wortmannin inhibits insulin-stimulated glucose uptake. However, it is likely that okadaic acid also acts on proteins other than PKB to cause this effect.

The expression of a constitutively active form of PKB in 3T3-L1 adipocytes leads to an elevation of basal glucose uptake (without an effect on the maximal insulin-stimulated response). The ATB-BMPA photolabel label was used to assess the relative contributions from GLUT1 and GLUT4. In the basal state, cell surface levels of both GLUT1 and GLUT4 are higher than those in control basal cells. In the insulin-stimulated state, only cell surface levels of GLUT1 are greater than those in control insulin-stimulated cells. Also, glucose transport and GLUT4 translocation are similarly increased by constitutively active PKB in basal cells, but to less than half the maximal insulin-stimulated response (38.9% and 37% respectively). Thus, it is likely that GLUT4 is the major contributor to the elevated glucose uptake induced by constitutively active PKB.

ACKNOWLEDGEMENTS

I am grateful to Geoff Holman for supervising my PhD and the critical reading of this thesis. I would also like to thank past and present members of Geoff's lab for all their help and advice during my time at Bath.

I am also grateful to the BBSRC for the funding of my PhD studentship.

ABBREVIATIONS

AEBSF	4-(2-aminoethyl)benzenesulfonylfluoride
AP-IC	Intracellular Buffer Supplemented with ATP and Pyruvate (*Methods 2.3.2*)
β-Ark	β-Adrenergic Receptor Kinase
ATB-BMPA	2-*N*-4-(1-azi-2,2,2-trifluoroethyl)benzoyl-1,3-bis(D-mannos-4-yloxy)-2-propylamine
BSA	Bovine Serum Albumin
DMEM	Dulbecco's Modification of Eagle's Medium
DTT	DL-Dithiothreitol
EGF	Epidermal Growth Factor
FBS	Foetal Bovine Serum
Gα	α-subunit of Trimeric G Protein
Gβ	β-subunit of Trimeric G Protein
Gβγ	βγ-subunit of Trimeric G Protein
GST	Glutathione *S*-transferase
GDPβS	Guanosine 5'-O-(2-thiodiphosphate)
GSK-3	Glycogen Synthase Kinase-3
GTPγS	Guanosine 5'-O-(3-thiotriphosphate)
HDM	High Density Microsome
HRP	Horseradish Peroxidase
IC Buffer	Intracellular Buffer (*Methods 2.3.2*)
IGF-II	Insulin-like Growth Factor II
Ins 1,4,5-P_3	Inositol 1,4,5-trisphosphate
IRS-1/2/3	Insulin Receptor Substrate-1/2/3
k_{en}	Rate of Endocytosis
k_{ex}	Rate of Exocytosis
KRH	Krebs-Ringers-HEPES (*Methods 2.2.2* and *2.3.1*)
KRM	Krebs-Ringer-MES (*Methods 2.3.4*)
LDM	Low Density Microsome
MAPK	Mitogen-activated-protein Kinase
MAPKK	Mitogen-activated-protein Kinase Kinase
NCS	Newborn Calf Serum
NIDDM	Non-insulin Dependent Diabetes Mellitus
NSF	N-ethylmaleimide Sensitive Fusion
PBS	Phosphate-buffered Saline (*Methods 2.1.3*)
PDGF	Platelet-derived Growth Factor

PH Domain	Pleckstrin Homology Domain
PI	Phosphatidylinositol
PI 3-K	Phosphoinositide 3-kinase
PI 3-P	Phosphatidylinositol 3-phosphate
PI 4-P	Phosphatidylinositol 4-phosphate
PI 3,4-P_2	Phosphatidylinositol 3,4-bisphosphate
PI 3,4,5-P_3	Phosphatidylinositol 3,4,5-trisphosphate
PI 4,5-P_2	Phosphatidylinositol 4,5-bisphosphate
PKB	Protein Kinase B
PKC	Protein Kinase C
PLC	Phospholipase C
PM	Plasma Membrane
PMA	Phorbol 12-myristate 13-acetate
PMSF	Phenylmethylsulfonyl Fluoride
PP1	Protein Phosphatase 1
PP2A	Protein Phosphatase 2A
$pp70^{S6k}$	70 kDa Ribosomal S6 Kinase
$pp90^{rsk}$	90 kDa Ribosomal S6 Kinase
PTB Domain	Phosphotyrosine-binding Domain
SDS-PAGE	Sodium Dodecyl Sulphate - Polyacrylamide Gel Electrophoresis
SH2 Domain	Src Homology 2 Domain
SH3 Domain	Src Homology 3 Domain
SLO	Streptolysin O
SNAP	Soluble NSF Attachment Protein
SNARE	Soluble NSF Attachment Protein Receptor
TBS	Tris-buffered Saline (*Methods 2.7.4*)
TBS-T	Tris-buffered Saline with Tween 20 (*Methods 2.7.4*)
TES	Tris-EDTA-Sucrose (*Methods 2.6.1*)
TGR	*trans*-Golgi Reticulum

1.0 INTRODUCTION

Glucose is a major metabolic substrate. First, it is the starting point for the generation of ATP via glycolysis, the citric acid cycle and oxidative phosphorylation. Second, its conversion to glycogen allows it to act as an energy store. Third, it is involved in cellular biosynthesis via the generation of NADPH and ribose 5-phosphate in the pentose phosphate pathway. Levels of glucose in human blood are maintained between 80 and 120 mg per 100 ml (4.4 to 6.7 mM). One of the regulatory mechanisms involved is the control of glycogen metabolism in the liver by levels of hormones and glucose in the circulation: glucose can be released or taken up by the liver depending on the circumstances. One of the regulatory hormones that induce glycogen synthesis, insulin, can also act on muscle and adipose cells to encourage uptake of glucose via glucose transporters. These are integral membrane proteins that allow glucose to cross the plasma membrane.

The mechanism of insulin action involves altering the distribution of glucose transporters between intracellular membranes and the plasma membrane, such that there is an increase in the number of cell surface transporters. To have a greater understanding of insulin-stimulated glucose uptake, investigations are required in several key areas: the nature of the transporters that allow glucose transport; the nature of the intracellular compartments that contain glucose transporters; the mechanism of the subcellular trafficking of glucose transporters; the mechanism by which insulin stimulation leads to a change in the cellular distribution of glucose transporters. Studies of this kind will be of benefit in the treatment of non-insulin dependent diabetes mellitus (NIDDM), where a defect of the transporters or in the response to insulin stimulation may be responsible.

Insulin communicates with the cell by binding to and activating the transmembrane insulin receptor at the cell surface. Insulin receptor substrate-1 (IRS-1) is subsequently phosphorylated, enabling it to associate with and activate phosphoinositide 3-kinase (PI 3-K). Present at the the N-terminus of IRS-1 is the

pleckstrin homology (PH) domain, which is not directly involved in the enzyme activation. The increased kinase activity of PI 3-K appears to lead to a rise in glucose uptake via translocation of glucose transporters, though the mechanism involved is not known. However, several downstream enzymes are known to be regulated by PI 3-K, one of them being protein kinase B (PKB). The studies described in this thesis have investigated the possible involvement of the IRS-1 PH domain and of PKB in insulin-regulated glucose uptake in adipocytes.

1.1 Facilitative Glucose Transporters

The presence of glucose transporters in the plasma membrane of adipocytes provide a means for the movement of glucose across the cell surface. They are important with regards to insulin-stimulated glucose uptake, since the rate at which glucose is transported by them represents the end-point of the action of insulin on the cell. Glucose transporters are integral membrane proteins that allow passive facilitated diffusion of glucose (reviewed by Gould and Holman, 1993). Thus, a glucose concentration gradient across the plasma membrane provides the driving force for glucose to enter or exit the cell via the transporter. The glucose transporter is specific for D-glucose and has kinetic properties that can be described by the Michaelis-Menten equation. Thus, transport is characterized by two values: K_m, the concentration of glucose at which transport is half the maximal rate, V_{max}. From a family of glucose transporters that has been identified in mammalian cells, the isoforms that exist in adipocytes are GLUT1, GLUT4 and GLUT5. Only GLUT1 and GLUT4 will be described in further detail, as GLUT5 is a fructose transporter.

1.1.1 GLUT1

A cDNA clone for GLUT1 was isolated by Mueckler *et al.* (1985), using anti-serum raised against the purified transporter from erythrocytes. A cDNA library prepared from the HepG2 cell line (derived from a human hepatoma) was screened. The

sequence of the cDNA clone reveals a polypeptide of 492 residues with a molecular weight of 54 kDa. A hydropathy plot of the amino acid sequence suggests the presence of 12 transmembrane domains. As tryptic digestion of the erythrocyte transporter occurs only on the cytoplasmic side of the membrane, the hydrophilic loop between the sixth and seventh transmembrane domains and the C-terminal tail were predicted to be located in the cytoplasm. The *N*-glycosylation site was predicted to be at residue Asn-45, which follows the first transmembrane domain; thus, the N-terminal tail is likely to be cytosolic as well. A cDNA clone for GLUT1 was also isolated by Birnbaum *et al.* (1986) from a cDNA library from rat brain. A polypeptide of 492 residues was also predicted, with 97.6% homology to the HepG2 transporter. Further, the tissue distribution of GLUT1 was investigated by blot hybridization of total RNA: the transporter was also detected in kidney and adipose tissue, but not in the liver.

Human erythrocytes have also been used to determine the kinetics of glucose transport for GLUT1 (Lowe and Walmsley, 1986). Using D-[^{14}C]glucose, transport was determined in terms of net flux, where the influx or efflux of labelled sugar into a sugar-free comparment was measured. The value of the K_m for the efflux of glucose was determined to be greater than that for its influx. Thus, at 0 °C, the former is 12-fold greater than the latter, whereas at 20 °C it is 3-fold. Thus, the GLUT1 transporter is kinetically asymmetrical. It was proposed that this property allows GLUT1 to effectively act like a unidirectional transporter under conditions of low extracellular glucose and high glucose demand (Gould and Holman, 1993).

1.1.2 GLUT4

A cDNA clone for GLUT4 was isolated by five independent groups in 1989. This was achieved by screening cDNA libraries from rat skeletal muscle (Birnbaum, 1989, and Charron *et al.*, 1989), human skeletal muscle (Fukumoto *et al.*, 1989), rat adipocyte and heart (James *et al.*, 1989) and mouse 3T3-L1 adipocytes (Kaestner *et al.*, 1989) with GLUT1 cDNA. The sequence reveals a polypeptide of 509 residues

(510 for mouse GLUT4) with a molecular weight of 55 kDa. The amino acid sequence is about 65% identical to that of GLUT1. Similarity is greatest within the predicted transmembrane domains, apart from the third from the N-terminus. Differences are more apparent in the predicted cytoplasmic domains for the N- and C-terminal tails and for the central cytoplasmic loop. The putative *N*-glycosylation site in the exofacial loop following the first transmembrane domain is also present at residue Asn-57. The tissue distribution of GLUT4 was also investigated by Northern blot analysis of total RNA from rat tissue using GLUT4 cDNA as the probe (Birnbaum, 1989, Charron *et al.*, 1989, and James *et al.*, 1989). RNA for this isoform is abundant in insulin-responsive heart, skeletal muscle and adipose tissue. This observation was confirmed by immunoblotting with a monoclonal antibody for GLUT4 (James *et al.*, 1989). The expression of GLUT4 following differentiation of mouse 3T3-L1 fibroblasts into adipocytes was also observed (James *et al.*, 1989, and Kaestner *et al.*, 1989). mRNA for the isoform does not appear until 3 days after induction of differentiation.

The cloning of GLUT1 and GLUT4 allowed kinetic studies to be performed in *Xenopus* oocytes expressing glucose transporters (Keller *et al.*, 1989). Transport of 3-*O*-methyl-D-glucose was determined under equilibrium exchange conditions, where the concentration of unlabelled sugar inside the cell is the same as that of external ^{3}H-labelled sugar. From their studies, the K_m for GLUT4 is 1.8 mM, which is lower than that for GLUT1, in which the K_m is 21.3 mM. In similar studies by Nishimura *et al.* (1993), cell surface transporters were also quantitated by photolabelling with 2-*N*-4-(1-azi-2,2,2-trifluoroethyl)benzoyl-1,3-bis(D-mannos-4-yloxy)-2-propylamine (ATB-BMPA) (*Introduction 1.2.2*). It was determined that the K_m is 26.2 and 4.3 mM for GLUT1 and GLUT4 respectively, whereas the turnover number (V_{max}/Number of transporters) is about 20 000 min^{-1} for both isoforms. It has been suggested that the relatively low value for the K_m of GLUT4, compared with that of GLUT1, allows the former to transport glucose at close to its V_{max} under physiological conditions (Gould and Holman, 1993).

Studies on transport via GLUT4 have been performed using rat adipocytes (Whitesell and Gliemann, 1979). When transport of 3-*O*-methyl-D-glucose was measured under equilibrium exchange conditions, insulin stimulation was found to increase V_{max} by about 6-fold without a significant change in the K_m. The net influx of 3-*O*-methyl-D-glucose into a sugar-free cell was also determined, with a K_m of 2.5 to 5 mM. This value is similar to that obtained under equilibrium exchange conditions (K_m of 3.1-3.5 mM), indicating that the transporter exhibits symmetrical kinetic properties. The study led to the question as to whether the increase in V_{max} is due to an increase in the number of cell surface transporters, or to an increase in the turnover number of the transporters.

1.2 Insulin-stimulated Translocation of Glucose Transporters

The regulation of glucose uptake by insulin occurs via the alteration of the distribution of glucose transporters in the cell. To understand how signalling from the insulin receptor leads to this cellular effect, knowledge is required of: the relative roles of GLUT1 and GLUT4; the membrane compartments that contain these transporter isoforms; the mechanisms involved in the movement of the transporters between these comparments. The locus (or loci) of insulin action in this subcellular trafficking system for glucose transporters thus forms (or form) the end-point (or end-points) of the insulin signalling pathway.

1.2.1 Subcellular Localization of Glucose Transporters

The translocation of GLUT4 from the microsome fraction to the plasma membrane following insulin stimulation of rat adipocytes was discovered in 1980 by two independent groups. Studies by Cushman and Wardzala (1980) were based on the use of cytochalasin B, which is a competitive inhibitor of D-glucose transport. Plasma membrane and microsome fractions were prepared from homogenized rat adipocytes. Following insulin stimulation, they found that the number of D-glucose-inhibitable cytochalasin B-binding sites increased in the former and decreased in the latter. Suzuki and Kono (1980) measured the cytochalasin B-sensitive glucose transport activity of transporters reconstituted into a cell-free system. Crude microsomal fractions were further fractionated by sucrose density gradient centrifugation. Fractions were then either subjected to an assay of marker enzymes, or they were reconstituted into liposomes prior to assay of transport activity. Fractions corresponding to the peaks for 5'-nucleotidase (a plasma membrane marker) and UDPGal:*N*-acetylglucosamine galactosyltransferase (representing an intracellular membrane compartment) were also found to contain the peaks for transport activity. Upon insulin stimulation, there appeared to be an increase in activity associated with

the plasma membrane and a decrease in that found in the intracellular membrane fraction.

The characterization of subcellular membrane fractions isolated from rat adipocytes by differential ultracentrifugation has been described by Simpson *et al.* (1983). Four fractions termed the plasma membrane, the high density microsome (HDM), the low density microsome (LDM), and mitochondria and nuclei were obtained, each enriched with marker proteins for the plasma membrane, endoplasmic reticulum, Golgi apparatus and mitochondria respectively. The levels of D-glucose-inhibitable cytochalasin B-binding sites per mg protein are greatest in the LDM. Insulin stimulation decreases the levels present in this fraction, together with a concomitant increase in the HDM and plasma membrane. GLUT1 and GLUT4 were later identified as the transporters in the LDM fraction of rat adipocytes (Zorzano *et al.*, 1989). An antibody raised against GLUT4 was conjugated to protein A agarose and used to immunoadsorb the LDM fraction. From immunoblotting studies, it was found that 80% of GLUT4-containing vesicles were adsorbed, while more than 90% of GLUT1-containing vesicles remained in the supernatant. Following insulin stimulation, both isoforms were found to increase in number in the plasma membrane and decrease in the LDM. It was concluded that insulin-stimulated glucose transport occurs via the tranlocation of the two transporter isoforms from two or more intracellular pools. This conclusion was supported by Piper *et al.* (1991). Homogenates from 3T3-L1 adipocytes were spun to remove the crude plasma membrane fraction, before fractionation by sucrose density gradient centrifugation. Immunoblotting of fractions showed that the peak for GLUT4 occurs at a denser fraction than that for GLUT1; both peaks decrease following insulin stimulation. Also, cells labelled with antibodies against GLUT1 and GLUT4, before observation by confocal immunfluorescence microscopy, revealed distinct populations of both isoforms.

The subcellular distribution of GLUT4 was also investigated by immunoelectron microscopy of brown adipose tissue (Slot *et al.*, 1991). In basal cells, most of the GLUT4 transporters are present in tubulo-vesicular structures, either in the *trans-*

Golgi reticulum (TGR) or throughout the cytoplasm. In insulin-stimulated cells, there is an increase in GLUT4 at the plasma membrane (from 1% total cell number to 40%), with a concomitant decrease in the tubulo-vesicular structures. Further, the transporter is also present in coated pits and vesicles following insulin stimulation. Immunolabelling of albumin to detect early endosomes demonstrated that GLUT4 is present in these structures in insulin-treated cells. The early endosomes were also found in association with tubulo-vesicular structures containing GLUT4, where separation of the two proteins appeared to occur between the two compartments. Late endosomes were defined by the appearance of albumin and cathepsin D: these contain little GLUT4. The increase in GLUT4 in the coated pits and early endosomes in the insulin-stimulated state was seen as an indication that recycling from the plasma membrane occurs during insulin stimulation. Further, the accumulation of GLUT4 in these structures suggested that insulin acts by increasing the exocytosis of GLUT4, rather than by decreasing its endocytosis.

The co-localization of GLUT1 with endosomal-TGR markers supports the idea that the transporter is part of a recycling pathway between this compartment and the plasma membrane (Tanner and Lienhard, 1989). GLUT1 and receptors for transferrin and insulin-like growth factor II (IGF-II) all translocate to the plasma membrane upon insulin stimulation of 3T3-L1 adipocytes. Binding and immunoblotting studies showed an increase in these proteins in the crude plasma membrane fraction (1.5-fold, 1.2-fold and 2.5-4.5-fold respectively) and their decrease in the microsomal fraction. GLUT1-containing vesicles were prepared by mixing the microsomal fraction with *Staphylococcus aureus* cells conjugated to an anti-GLUT1 antibody. Binding studies revealed that the content of tranferrin receptors were similar in microsomal membranes and GLUT1 vesicles under basal and insulin-stimulated conditions. Also, immunoadsorption of GLUT1 vesicles extracted similar percentages of GLUT1 and IGF-II receptors from the microsomal membrane. This was also observed when IGF-II-containing vesicles were prepared instead. However, these markers do not appear to co-localize with GLUT4 in the same vesicles (Zorzano *et al.*, 1989). Vesicles prepared by immunoadsorption of the LDM fraction from rat adipocytes with anti-

GLUT4 were immunoblotted with an antibody against the IGF-II receptor. Little depletion of this receptor from the LDM was observed.

Taken together, these studies indicate the recycling of GLUT1 and GLUT4 between intracellular membranes and the plasma membrane. While insulin stimulation appears to cause the translocation of GLUT1, transferrin receptors and IGF-II receptors from the same intracellular compartment, it appears that GLUT4 is translocated from a distinct pool. This is based on two observations. First, GLUT4 can be isolated in vesicles that do not contain these other proteins. Second, the insulin-stimulated increase in cell surface GLUT4 is much greater than that for GLUT1 and the endosomal-TGR markers.

1.2.2 Kinetic Studies of GLUT4 Translocation

In order to assess the relative roles of GLUT1 and GLUT4 in insulin-stimulated glucose uptake, it is necessary to be able to quantitate the levels of both transporters in the plasma membrane, before and after insulin stimulation. Further, in order to determine the kinetics of the movement of glucose transporters between membrane compartments, a method of tagging these transporters is required. The ATB-BMPA photolabel was developed for these purposes (Clark and Holman, 1990). This compound is composed of two D-mannose groups linked to 2-propylamine via their C-4 hydroxy groups. The photolabile ATB group is attached to the bridge between the two sugar groups. The D-mannose groups interact with the transporter, where upon irradiation with 300 nm light, the label is incorporated into the transporter. As ATB-BMPA is membrane impermeable, then only cell surface transporters are detected.

The quantification of cell surface GLUT1 and GLUT4 by ATB-BMPA photolabelling was first undertaken in 3T3-L1 adipocytes (Calderhead *et al.*, 1990). Immunoblotting of cell lysate with antibodies against each isoform revealed GLUT1 to be the more dominant of the two transporters (4:1). After photolabelling of cells with ATB-

BMPA, tagged transporters were immunoprecipitated and resolved on a sodium dodecyl sulphate polyacrylamide gel electrophoresis (SDS-PAGE) gel. Following insulin stimulation, the ratio of GLUT1 to GLUT4 in the plasma membrane decreased from 4.6 to 1.6. However, the fold-increase was 6.5 and 17.1 for GLUT1 and GLUT4 respectively. The affinity of the transporters for the probe was not considered to be changed by insulin treatment, since there was no change in its dissociation constant for the inhibition of 2-deoxy-D-glucose transport. Insulin stimulation was found to increase 2-deoxy-D-glucose transport by 21-fold. As GLUT1 was still the predominant transporter under insulin-stimulated conditions, it was concluded that translocation would only account for the rise in transport if GLUT4 had a higher intrinsic activity. Similar experiments were performed using rat adipocytes (Holman *et al.*, 1990). Under basal conditions, it was determined that the level of GLUT4 transporters in the plasma membrane was about twice that of GLUT1. Upon insulin stimulation, there was a 5- and 15-20-fold increase in cell surface GLUT1 and GLUT4 respectively, leading to GLUT4 as 90% of both transporters. Insulin-stimulated 3-*O*-methyl-D-glucose transport was found to be 20-30-fold greater than in basal cells. As this increase was similar to that for GLUT4 translocation, it was similarly concluded that the intrinsic activity of GLUT4 was greater than that for GLUT1. Further, unlike 3T3-L1 adipocytes, GLUT1 is not a major contributor to transport activity in rat adipocytes.

ATB-BMPA was used in further studies to compare changes in glucose transport activity with levels of cell surface transporters in rat adipocytes (Clark *et al.*, 1991). Following insulin stimulation, transport of 3-*O*-methyl-D-glucose increases with a half-time of 3.2 min, but with a time lag of 47.1 s. However, the appearance of GLUT1 and GLUT4 at the cell surface occur with half-times of 2.32 and 2.17 min respectively and with no time lag. Transport activity and cell surface transporters were also determined following the removal of insulin from stimulated cells. The former declines with a half-time of 10.9 min, whereas the latter decreases with similar half-times of 11.7 and 12.3 min for GLUT1 and GLUT4 respectively. Similar studies were undertaken in 3T3-L1 adipocytes (Yang *et al.*, 1992). Likewise, there is also a lag between the appearance of cell surface transporters and the increase in transport

activity, while the decline in both parameters following insulin removal are similar. In subsequent studies, it was observed that the half-time for the appearance of cell surface GLUT4 is faster when determined by immunoblotting instead of ATB-BMPA photolabelling (Satoh *et al.*, 1993). Thus, these data support the idea that transporters can exist in partially occluded or occluded vesicles in the plasma membrane. It was further postulated that these vesicles are associated with trafficking proteins and cannot participate in glucose transport.

The recycling of ATB-BMPA-labelled transporters between the plasma membrane and the LDM in rat adipocytes was demonstrated by Satoh *et al.* (1993). Cells stimulated to a steady state of glucose transport activity were treated with collagenase to remove the insulin present. Immunodetectable and labelled GLUT4 in the plasma membrane and transport activity all declined to below 20% of the original response with similar half-times. In the continuous presence of insulin, while cell surface immunodetectable GLUT4 and transport activity remained constant, labelled GLUT4 declined with a half-time similar to that following collagenase treatment, but to a higher steady state level. Restimulation of collagenase-treated cells restored cell surface immunodetectable GLUT4, labelled GLUT4 and transport activity to steady state levels observed in cells continuously treated with insulin. The half-times for the first two were similar and slightly faster than that for the last. Thus, the data indicates that insulin affects the rate constant for the exocytosis (k_{ex}) of GLUT4, and not that for its endocytosis (k_{en}). Values for these constants were calculated assuming that there are only two pools of GLUT4: the plasma membrane and the LDM. It was estimated that k_{ex} increases about 10-fold following insulin stimulation, whereas k_{en} remains constant. These experiments were repeated again, but with measurements of GLUT4 in the LDM instead. It was observed that labelled GLUT4 that had returned to the LDM from the plasma membrane following collagenase treatment, could be reduced following restimulation with insulin to a steady state level found in cells continuously treated with insulin. Thus, the data indicates that total cellular GLUT4 is involved in subcellular trafficking. Similar experiments were carried out in 3T3-L1 adipocytes (Yang and Holman, 1993). Basal and maximally insulin-stimulated cells were labelled with ATB-BMPA before further incubation at these steady states, during

which the decline in labelled GLUT1 and GLUT4 in the plasma membrane was determined. In the insulin-stimulated state, both transporters share a similar value for k_{ex} and for k_{en}. A steady state is reached where half the labelled transporters are present in the plasma membrane. In the basal state, k_{en} for both transporters are similar, while k_{en} in insulin-stimulated cells are about 30% slower. Further, in the basal state, labelled GLUT4 is internalized to a greater extent than GLUT1. Thus, 8% of original cell surface labelled transporter remain, compared with 21%. This observation is reflected in k_{ex}, where the value for GLUT1 is 3.5-times greater than that for GLUT4. Insulin stimulation was determined to raise GLUT1 and GLUT4 exocytosis by 3-fold and 9-fold respectively.

In the two-pool model, the half-time for the insulin-stimulated appearance of cell surface GLUT4 should be the same as that for the internalization of cell surface GLUT4 during continuous insulin stimulation, as both depend on the same values for k_{ex} and k_{en}. However, this is not observed experimentally (Satoh *et al.*, 1993): the former has a faster half-time (2.7 min) than that for the latter (10.6 min). This data was found to be better explained by the computer simulation of a three-pool model (Holman *et al.*, 1994). Here, there are two intracellular pools: the tubulo-vesicular system and the early endosomes. The former would allow the initial rapid translocation of GLUT4 without a major contribution from k_{en} on the half-time for this process. The latter would account for the slower half-time for the recycling of GLUT4 in the presence of insulin.

From these studies with ATB-BMPA, it is now known that GLUT4, and not GLUT1, is the major insulin-responsive transporter isoform. This conclusion is based on the relatively large insulin-stimulated increase in cell surface GLUT4, compared with that of GLUT1, in adipocytes. The cause of this appears to be the insulin stimulation of a greater increase in k_{ex} for GLUT4 than that for GLUT1. Further, the translocation of GLUT4 is the major contributor to glucose transport activity. Subsequent studies have demonstrated that GLUT4 has a greater intrinsic activity (Turnover number/K_m) than that of GLUT1 (Nishimura *et al.*, 1993). The kinetic studies with ATB-BMPA labelled-transporters support previous biochemical and morphological studies in two

areas. First, the kinetic data also indicates that there is distinct pool of GLUT4 inside the cell, ready for rapid translocation to the cell surface. Second, the kinetic data is consistent with a role for GLUT4 exocytosis as the major mechanism of GLUT4 translocation.

1.2.3 Targeting of GLUT4

In 3T3-L1 adipocytes, the rate of exocytosis of GLUT4 is lower in the basal state than in the insulin-stimulated state, whereas for GLUT1, the difference is not as great (Yang and Holman, 1993). This observation implies that there must be a sequence or structure present in the former that enables it to be retained in the cell more efficiently in the basal state. An approach to determine the sites in GLUT4 responsible for this property has been to observe the subcelluar distribution of chimeras of GLUT1 and GLUT4. Piper *et al.* (1992) expressed transporter constructs in CHO cells. Their subcellular distribution was detected by immunoelectron and immunofluorescence microscopy. Wild-type GLUT4 was detected mainly in intracellular tubulo-vesicles, while wild-type GLUT1 was found mainly in the plasma membrane. A chimera where the C-terminal 25 residues of GLUT4 were replaced with those of GLUT1 showed the same intracellular localization as wild-type GLUT4. Likewise, exchanging the C-terminal 25 residues of GLUT1 with those of GLUT4 had no effect on its cell surface localization. However, when the N-terminal 41 residues of the latter chimera were replaced with those of GLUT4, intracellular localization was observed. Further studies (Piper *et al.*, 1993) demonstrated that the deletion of 8 amino acids from the N-terminus of GLUT4, or the deletion of residue phe-5, was sufficient to cause localization at the plasma membrane. The motif is PSGFGGI.

However, similar experiments by Czech *et al.* (1993) showed that the C-terminus of GLUT4 is important for intracellular sequestration. A hemagglutinin epitope was inserted into an exofacial loop of transporter constructs, which were then expressed in COS-7 cells. Tagged constructs were detected by immunofluorescence microscopy. A chimera where the C-terminal 30 residues of GLUT4 were substituted into GLUT1

was detected intracellularly, but not at the cell surface. The converse chimera, where the 29 C-terminal residues of GLUT1 were substituted into GLUT4, was observed at the cell surface. Intracellular localization of the former was also observed in CHO cells. Further experiments in CHO and COS-7 cells by Corvera *et al.* (1994) demonstrated that the dileucine motif (residues leu-489 and leu-490) in GLUT4 was the critical component of C-terminal-mediated sequestration. Thus, its mutation to a double alanine in the chimera of GLUT1 substituted with the C-terminal 30 residues of GLUT4 led to levels at the cell surface similar to those of wild-type GLUT1.

It has been argued that the use of transfected CHO and COS-7 cells may not be adequate for investigating the targeting sequences of GLUT4 (Holman and Cushman, 1994). First, they are unresponsive to insulin and thus may not possess the molecular mechanisms for sequestration of GLUT4. Second, expression of constructs at a high level may overcome the ability of the cell to maintain the transporters intracellularly. Further work was carried out on chimeras and mutants expressed in 3T3-L1 cells. Verhey *et al.* (1995) produced chimeric transporters with an epitope tag in the central cytoplasmic loop. These were expressed in 3T3-L1 adipocytes at levels that were less than 2-fold of that of endogenous GLUT4. Cell surface transporters were detected by immunofluorescence microscopy of plasma membrane sheets. A chimera of GLUT1 substituted with the N-terminal 183 residues of GLUT4 was not present in the plasma membrane under basal conditions. Following insulin stimulation, there was only a slight increase in the levels of this chimera at the cell surface. However, for a chimera of GLUT1 substituted with the C-terminal 30 residues of GLUT4, insulin treatment led to levels in the plasma membrane that were equivalent to those obtained with cells expressing endogenous GLUT4 or tagged-GLUT4. This chimera was absent from the cell surface in the basal state. Contrary to previous data, mutation of the dileucine motif in the latter construct to a double alanine did not affect intracellular localization. Further experiments demonstrated that this mutation reduced the rate of internalization of the transporter following removal of insulin stimulation.

Marsh *et al.* (1995) expressed C-terminal epitope-tagged GLUT4 constructs in 3T3-L1 adipocytes. The distribution of transporters between the plasma membrane and the

LDM was quantitated by immunoblotting. Expression levels were defined as low (similar to endogenous GLUT4) or high (4-fold the levels of endogenous GLUT4). Mutation of phe-5 to alanine led to accumulation of GLUT4 at the plasma membrane, giving a high ratio of cell surface to intracellular transporters (PM/LDM ratio). Insulin stimulation caused a further slight increase of this transporter at the cell surface. Mutation of the dileucine motif to a double alanine gave different results depending on the expression level. At low levels, the transporter had a similar PM/LDM ratio to that of endogenous or tagged- GLUT4, in both basal and insulin-stimulated states. At high levels, the ratio increased for basal cells, but was not as high as that for the phe-5 mutant. Additional transporters could be recruited to the cell surface upon insulin treatment.

As both groups had used different sets of transporter constructs in their experiments, it is difficult to make direct comparisons between their work. Verhey *et al.* (1995) concluded that the C- and N-terminus are important for intracellular sequestration, though the latter is not involved in targeting to an insulin-sensitive pool. Further, the dileucine motif appears to be important for the rate of internalization only. Marsh *et al.* (1995) inferred that as both N- and C-terminal mutants were still capable of insulin-stimulated translocation, other sequences must be involved in this process. Both agreed that the dileucine motif is not involved in intracellular sequestration. However, while these studies have identified sequences in GLUT4 that contribute to its intracellular sequestration, the cellular mechanisms involved in this process are not yet known.

1.2.4 Fusion of GLUT4 Vesicles at the Plasma Membrane

The exocytosis of GLUT4-containing vesicles to the plasma membrane has been compared to the fusion of neurotransmitter-containing vesicles at synaptic membranes. It has been proposed that the proteins involved in the latter process may also be involved in GLUT4 translocation (Holman and Cushman, 1994). The model is as follows. Present in the vesicular and plasma membranes are Soluble N-

ethylmaleimide Sensitive Fusion (NSF) Attachment Protein Receptors (SNAREs) (v-SNARE for the former, t-SNARE for the latter). A complex is formed, consisting of these two proteins plus Soluble NSF Attachment Proteins (SNAPs). The binding of NSF protein to the assembly drives the fusion of the vesicle with the plasma membrane. The presence of these proteins in rat adipocytes and their ability to form complexes with each other *in vitro* was demonstrated by Timmers *et al.* (1996). Plasma membrane and GLUT4 vesicles were isolated from rat adipocytes, solubilized, and mixed with recombinant α-SNAP and *myc*-epitope-tagged NSF plus ATP and EDTA. The resulting complex was immunoprecipitated with an anti-*myc* antibody, before elution of SNAREs with Mg^{2+}. The proteins detected by immunoblotting were syntaxin 4 (a t-SNARE), VAMP2 and VAMP3 (v-SNAREs), and α-SNAP.

A functional role for the SNARE proteins in GLUT4 translocation was studied by Cheatham *et al.* (1996). Compounds were introduced into permeabilized 3T3-L1 adipocytes prior to determination of insulin-stimulated GLUT4 translocation. These were: botulinum neurotoxin D (an endopeptidase specific for VAMPs 2 and 3); IgA protease (which cleaves VAMP2, but not VAMP3); glutathione *S*-transferase (GST) fusion proteins of the soluble portion of syntaxin 4 or VAMP2. All were found to inhibit exocytosis of GLUT4 following insulin treatment, as determined by immunofluorescence microscopy of plasma membrane sheets. Similar studies were undertaken by Olson *et al.* (1997) in 3T3-L1 adipocytes infected with recombinant vaccinia virus. The expression of the cytoplasmic domains of syntaxin 4, VAMP2, or VAMP3, but not syntaxin 3, led to a reduction in insulin-stimulated GLUT4 translocation, as determined by immunoblotting or immunofluorescence microscopy of plasma membrane sheets. Further, the presence of syntaxin 4 did not affect GLUT1 translocation. Thus, both groups indicate that VAMP2 and syntaxin 4 could have a role to play in the docking and fusion of GLUT4 vesicles with the plasma membrane.

1.3 Insulin Signalling

The recognition of the hormone insulin at the cell surface ultimately leads to the translocation of glucose transporters, especially GLUT4, to the plasma membrane. To have a greater understanding of insulin action, the signalling mechanisms that link these two events need to be determined. Several studies have mapped the molecular events that occur in the cell following the binding of insulin to its receptor. The discovery of insulin-regulated proteins, such as IRS-1 and PKB, warrant investigations into their potential role in insulin-stimulated glucose uptake and are the subject of studies described in this thesis. Some studies have demonstrated that the activation or inhibition of certain cellular proteins can influence glucose transport activity. These include G proteins, protein kinase C (PKC), and protein phosphatases 1 and 2A (PP1 and PP2A). How these proteins are involved in the normal insulin-stimulated response remains to be determined.

1.3.1 The Insulin Receptor

The insulin receptor is a heterotetramer consisting of a pair of disulphide bond-linked α-subunits, each disulphide bond-linked to a β-subunit (reviewed by White and Kahn, 1994). The α-subunit is extracellular and binds the ligand insulin. The β-subunit is a transmembrane protein which possesses insulin-regulatable tyrosine kinase activity. A cDNA clone for the human insulin receptor precursor was isolated by two independent groups in 1985. Ullrich *et al.* (1985) deduced a polypeptide consisting of an N-terminal 27 residue signal sequence, followed by a 719 residue α-subunit sequence, a 4 residue cleavage site and a 620 residue β-subunit sequence. Ebina *et al.* (1985) had identified a different isoform of the receptor precursor, where the α-subunit was found to consist of 731 residues. The α-subunit is hydrophilic with 15 putative *N*-glycosylation sites and a region rich in cysteine residues. The β-subunit is composed of an N-terminal extracellular domain with four putative *N*-glycosylation sites and four cysteine residues, a hydrophobic transmembrane domain and a C-

terminal cytosolic domain. The intracellular domain can be further subdivided into the juxtamembrane region, the kinase region and the C-terminal region.

The ability of insulin to stimulate tyrosine phosphorylation of the insulin receptor was described by Kasuga *et al.* (1982) in a cell-free system. Partially purified insulin receptor from solubilized rat membrane was incubated with or without insulin before the addition of [γ-^{32}P]ATP. Insulin was found to induce the incorporation of phosphate into the β-subunit on its tyrosine residues, indicating autophosphorylation of the receptor. The role of putative autophosphorylation sites in the β-subunit were investigated by Murakami and Rosen (1991), where they mutated tyrosine residues to phenylalanine. The cDNA constructs were stably transfected into CHO cells. Mutation of tyr-1146, -1150 and -1151 in the kinase region impaired the insulin-stimulated kinase activity of the receptor. Whereas mutation of tyr-960 in the juxtamembrane region did not affect receptor kinase activity, it did reduce the sensitivity to stimulation of glucose uptake and thymidine incorporation. Mutation of tyr-953 in the juxtamembrane region and tyr-1316 and tyr-1322 in the C-terminal tail had no effect on the above parameters. Thus, autophosphorylation of the receptor is required for normal insulin-stimulated kinase activity and for the ability to effect downstream events in the cell.

The importance of tyrosine phosphorylation of the insulin receptor for the subsequent phosphorylation of substrate proteins was determined by Yonezawa *et al.* (1994), using CHO cells overexpressing wild-type and mutant insulin receptors. First, mutation of lys-1018 to arginine in the kinase region abolished both insulin-stimulated autophosphorylation and phosphorylation of the substrate proteins IRS-1 and Shc. Second, whilst mutation of tyr-960 to alanine attenuated phosphorylation of IRS-1 and Shc, the deletion of the C-terminal 82 residues (containing tyr-1316 and tyr-1322) impaired Shc phosphorylation only. Thus, receptor tyrosine kinase activity and the autophosphorylation of certain tyrosine residues are both required in order for phosphorylation of endogenous substrates to occur.

1.3.2 Substrates of the Insulin Receptor

1.3.2.1 IRS-1

The tyrosine phosphorylation of IRS-1 by the insulin receptor *in vivo* was first identified in the hepatoma cell line Fao by White *et al.* (1985). Cells previously labelled with ^{32}P-orthophosphate were immunoprecipitated with anti-phosphotyrosine antibodies. Following insulin stimulation, a protein of 185 kDa was observed. The protein, termed pp185, was later purified from rat liver (Rothenberg *et al.*, 1991) with anti-phosphotyrosine. Purified pp185 was subjected to tryptic digestion, after which, one of the fragments was used to raise an antibody specific for the protein. This work enabled the generation of cDNA probes for pp185, which were used to identify cDNA clones for the protein (Sun *et al.*, 1991). IRS-1 (pp185) is a hydrophilic protein of 131 kDa with potential phosphorylation sites: there are 35 for serine/threonine kinases (based on motifs for known kinases of this type) and at least 10 for tyrosine kinases (six possessing the YMXM motif, three with YXXM and one with EYYE). Another group (Keller *et al.*, 1991 and 1993) were able to purify IRS-1 (pp160) from mouse 3T3-L1 cells and to clone its cDNA. The protein has a molecular weight of 131 kDa and is 97.6% identical to rat IRS-1; the number of residues are 1231 compared with 1235 for rat. Two N-terminal domains in IRS-1 have also been identified. The first is the PH domain (Musacchio *et al.*, 1993) at residues 13-115 of rat IRS-1. The second is the phosphotyrosine-binding (PTB) domain, a 156-residue domain in mouse IRS-1 that is C-terminal to the PH domain (Sun *et al.*, 1995).

The multiple phosphorylation of IRS-1 by the insulin receptor was observed in CHO cells expressing human insulin receptor and rat liver IRS-1 (Sun *et al.*, 1992). Tryptic digestion of phosphorylated IRS-1 from basal cells revealed 12 fragments containing phosphoserine, four with phosphothreonine and one with phosphotyrosine. Following insulin stimulation, eight further phosphoserine and one further phosphothreonine were observed; also seen were at least six phosphotyrosines. The same study suggested direct phosphorylation of IRS-1 by the insulin receptor. Partially purified IRS-1 from Sf9 cells expressing its cDNA was incubated with [γ-^{32}P]ATP and Mn^{2+}.

The addition of partially purified activated insulin receptor from CHO cells led to an increase in phosphorylation of the protein on tyrosine residues only. Sun *et al.* (1991) suggested that IRS-1 functions as a multisite docking protein for other proteins involved in signal transduction. This was based on their observation that PI 3-K activity was present on IRS-1 immunoprecipitates following insulin stimulation of CHO cells expressing the insulin receptor. It was predicted that the src homology 2 (SH2) domains (of which there are two) of the regulatory subunit (p85) of PI 3-K bind to the phosphotyrosine residues on IRS-1.

The mechanism of the activation of PI 3-K was investigated by Backer *et al.* (1992). Recombinant IRS-1 was incubated with p85 immunoprecipitates (containing the p110 catalytic subunit) from quiescent CHO cells before assaying for PI 3-K activity. An increase in activity was observed if IRS-1 was phosphorylated beforehand. Activation seemed to occur via the phosphorylated YXXM motif, as phosphopeptides from IRS-1 sequences were also capable of raising kinase activity if they contained this motif. Further, tryptic phosphopeptides containing tyr-608 or tyr-939 of IRS-1 were found to bind most strongly to the SH2 domains of p85 (Sun *et al.*, 1993); both peptides contain the YMXM motif. Thus, activation of PI 3-K appears to occur upon association of its SH2 domains with the phosphorylated YXXM motifs of IRS-1. Further, Rordorf-Kikolic *et al.* (1995) demonstrated the need for both SH2 domains of p85 for maximal activation of PI 3-K. A point mutation in either or both of the SH2 domains to inhibit phosphopeptide binding was made. Activation of PI 3-K activity in the p85/p110 heterodimer by tyrosine-phosphorylated IRS-1 was found to be reduced by about 50% for a single mutation and by 100% for a double mutation.

The association of phosphotyrosine residues in IRS-1 with other signalling proteins also occurs (Figure 1.3.1) (reviewed by Keller and Lienhard, 1994). The first is Grb2, which possesses a single SH2 domain that is thought to bind to try-895 (YVNI). Grb2 associates with Sos, a protein which causes GDP release from the G protein Ras. The second is the phosphotyrosine phosphatase Syp (SH-PTP2), which possesses two N-terminal SH2 domains, one of which is believed to bind to tyr-1172 (YIDL). The

third is Nck, which has a single SH2 domain. Thus, the binding of an SH2 domain-containing protein appears to occur via sequences in IRS-1 specific for that protein.

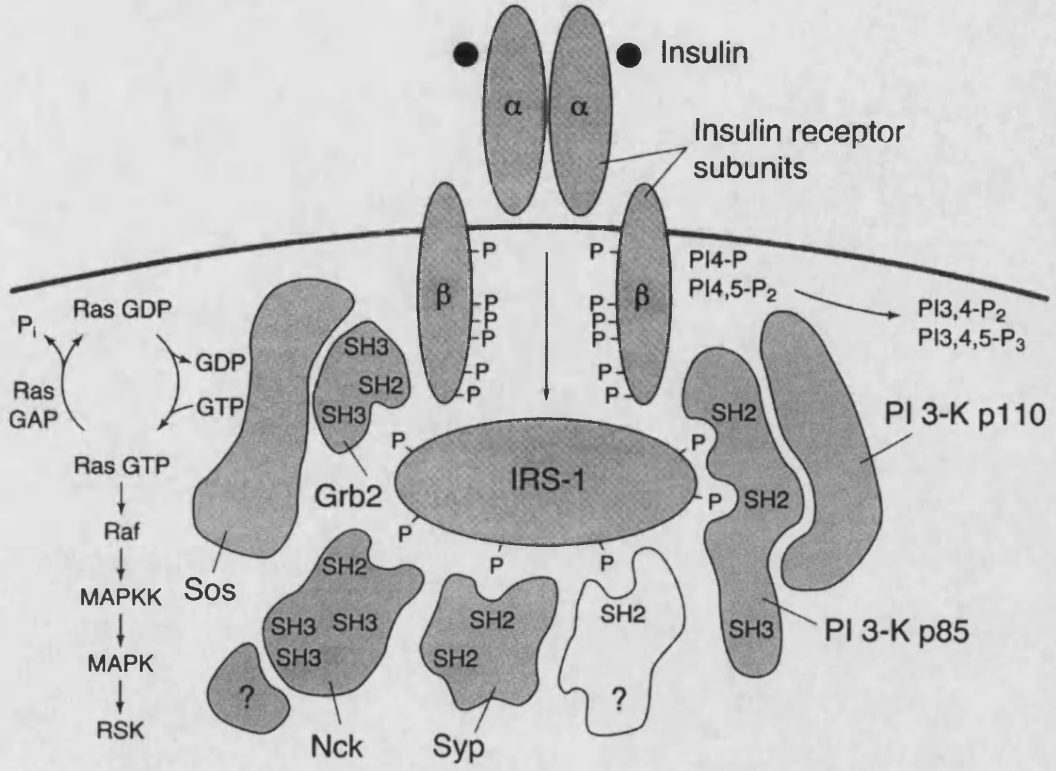

Figure 1.3.1. The Interaction of Tyrosine-phosphorylated IRS-1 with SH2 Domain-containing Proteins (Keller and Lienhard, 1994).

The importance of the serine/threonine phosphorylated state of IRS-1 was demonstrated by Tanti *et al.* (1994). Pre-treatment of 3T3-L1 adipocytes with okadaic acid prior to insulin stimulation led to a reduction in the tyrosine phosphorylation of IRS-1, but not of the insulin receptor, as determined by immunoblotting with anti-phosphotyrosine. Also, there was an observed decrease in the electrophoretic mobility of IRS-1 following okadaic acid treatment. This appeared to be due to an increase in serine/threonine phosphorylation, since cells labelled with [γ-^{32}P]orthophosphate demonstrated an increase in phosphorylated IRS-1 that could not be immunoblotted or immunoprecipitated with anti-phosphotryosine. Further, when immunoprecipitated IRS-1 was incubated with purified insulin receptor, phosphorylation of the former was

reduced if the cells had previously been treated with okadaic acid. Thus, serine/threonine phosphorylation of IRS-1 appears to modulate phosphorylation at the tyrosine residues.

1.3.2.2 IRS-2

The protein 4PS was purified and cloned from murine myeloid progenitor cells (Sun *et al.*, 1995) and subsequently designated IRS-2 due to its similarity to IRS-1. The IRS-2 cDNA reveals a polypeptide of 145 kDa. In common with IRS-1 is the N-terminal PH domain (69% identical), followed by the PTB domain (75% identical). Though the C-terminus is 35% identical to that of IRS-1, about 20 putative tyrosine phosphorylation motifs are present: nine of these are YXXM, of which four are YMXM. IRS-2 was detected in insulin-stimulated murine liver by Tobe *et al.* (1995). Phosphotyrosine immunoblotting revealed a faint 190 kDa band, relative to that for IRS-1. Further, it was shown that IRS-2 phosphorylation is enhanced in IRS-1-deficient mice. Patti *et al.* (1995) were able to immunoprecipitate IRS-2 from murine muscle and liver, where upon insulin stimulation, they detected increased tyrosine phosphorylation and the binding of p85 with associated PI 3-K activity. Further, it was found that these effects are more noticeable in IRS-1-deficient mice, and that they are due to enhanced phosphorylation of IRS-2, as its expression level is unchanged. IRS-2 appears to be the major alternative substrate to IRS-1 in insulin-stimulated IRS-1-deficient mice in terms of activation of PI 3-K, since removal of IRS-2 from tissue homogenates virtually depletes phosphotyrosine-associated activity (Patti *et al.*, 1995).

1.3.2.3 IRS-3

A 60 kDa protein (pp60) that binds PI 3-K following tyrosine phosphorylation, due to insulin stimulation of rat adipocytes, was identified by Lavan and Lienhard (1993). Following insulin stimulation, anti-phosphotyrosine immunoblotting showed the appearance of a band of 60 kDa. Further, anti-phosphotyrosine immunoblotting of p85 immunoprecipitates from insulin-stimulated cells showed the presence of a 60 kDa protein. This protein was not observed in IRS-1 immunoprecipitates, indicating

that its association with PI 3-K is not via IRS-1. Also, GST fusion proteins of the N- and C-terminal SH2 domains of PI 3-K were found to bind to tyrosine-phosphorylated pp60, indicating that association is via this domain.

The purification of pp60 and the cloning of its cDNA from a rat adipocyte cDNA library was later described by Lavan *et al.* (1997). The sequence reveals a polypeptide of 494 residues with a molecular weight of 55.3 kDa. As with IRS-1 and IRS-2, the protein has an N-terminal PH domain (50% and 45% identical respectively), followed by a PTB domain (48% and 53% identical respectively), followed by putative tyrosine phosphorylation sites (four with YXXM motifs). Thus, based on its similarity to IRS-1 and IRS-2, pp60 was designated IRS-3. A study by Kelly and Ruderman (1993), in which p85 immunoprecipitates from rat adipocyte membrane fractions were immunoblotted with anti-phosphotyrosine, revealed a 60 kDa band located predominantly in the plasma membrane. This is in contrast to a 185 kDa band found mainly in the LDM. Assuming this 60 kDa protein is IRS-3, then its plasma membrane localization indicates that it has a different role to play in insulin signalling.

1.3.2.4 Shc

The phosphorylation of the SH2 domain-containing protein Shc by the insulin receptor was described by Pronk *et al.* (1993). Shc immunoprecipitates from insulin-stimulated CHO cells overexpressing the insulin receptor were immunoblotted with anti-phosphotyrosine. Two bands of 52 and 46 kDa were observed, whereas Skolnik *et al.* (1993a) also detected a 66 kDa band. The association of tyrosine-phosphorylated Shc with Grb2 was demonstrated by Skolnik *et al.* (1993a). Immunoprecipitates of Grb2 from insulin-stimulated CHO cells (overexpressing the insulin receptor) that were immunoblotted with anti-Shc revealed the presence of the 52 and 66 kDa bands of Shc. Skolnik *et al.* (1993a) also detected Grb2 on IRS-1 immunoprecipitates from the same cell system following insulin stimulation. Thus, there is a convergence of signalling pathways towards Grb2.

Grb2 was found to be able to bind to Sos, as determined by immunoblotting with anti-Sos of Grb2 immunoprecipitates from L6 myoblast cells overexpressing Grb2 (Skolnik *et al.*, 1993b). Further, IRS-1 and Shc were also detected in the immunoprecipitated complex following insulin stimulation. A role for Sos in promoting the exchange of bound GDP on the G protein Ras for GTP was shown by Baltensperger *et al.* (1993). COS-1 cells transfected with cDNAs for Sos and Ras were radiolabelled with [γ-^{32}P]orthophosphate: the amount of GTP-bound Ras present was 10-fold greater than if Sos cDNA was absent. It has been suggested that insulin stimulation activates Ras either by localizing cytosolic Grb2/Sos to membrane-bound Ras, or by increasing the intrinsic activity of Sos (Skolnik *et al.*, 1993b).

1.3.3 Downstream of the Insulin Receptor Substrates

1.3.3.1 Phosphoinositide 3-Kinase

PI 3-K is a heterodimer of a p85 regulatory subunit and a p110 catalytic subunit (reviewed by Kapeller and Cantley, 1994). Two isoforms have been identified for each subunit: α and β. The p85 subunit is composed of an N-terminal src homology 3 (SH3) domain, followed by a Bcr homology domain sandwiched between a pair of proline-rich sequences, followed by an inter-SH2 region that is sandwiched between two SH2 domains. The association of p85 with p110 occurs via the inter-SH2 region. In mouse 3T3-L1 adipocytes, insulin-stimulated PI 3-K activity is observed in p85α immunoprecipitates, but not in those of p85β; also, the latter is not detected by immunoblotting (Baltensperger *et al.*, 1994).

The lipid kinase activity of PI 3-K leads to the phosphorylation of phosphatidylinositol (PI), phosphatidylinositol 4-phosphate (PI 4-P) and phosphatidylinositol 4,5-bisphosphate (PI 4,5-P_2) to form phosphatidylinositol 3-phosphate (PI 3-P), phosphatidylinositol 3,4-bisphosphate (PI 3,4-P_2) and phosphatidylinositol 3,4,5-trisphosphate (PI 3,4,5-P_3) respectively, as determined with p85 immunoprecipitates from rat adipocytes (Kelly and Ruderman, 1993). However,

extracted lipids from rat adipocytes show that only PI 3,4-P_2 and PI 3,4,5-P_3 levels are elevated following insulin stimulation (Kelly and Ruderman, 1993).

Two inhibitors of PI 3-K have been used to determine the role of the kinase in insulin-stimulated glucose uptake: wortmannin and LY294002. Wortmannin is a membrane permeable fungal metabolite that inhibits the kinase activity of PI 3-K at nanomolar concentrations (IC_{50} ~3 nM) by binding non-competitively and irreversibly to p110 (Ui *et al.*, 1995). It is a relatively specific inhibitor, as it can block other kinases at concentrations greater than 1 μM (Ui *et al.*, 1995). Clarke *et al.* (1994) demonstrated that the stimulation of glucose uptake by 100 nM insulin in 3T3-L1 adipocytes can be inhibited by wortmannin in a dose-dependent manner. Insulin-stimulated transport activity is reduced to basal levels with 1 μM wortmannin. The observed lack of transport activity is due to the inhibition of the translocation of GLUT1 and GLUT4 to the plasma membrane, as determined by ATB-BMPA photolabelling of cell surface transporters. In further experiments, the loss of cell surface transporters following the addition of wortmannin to insulin-stimulated 3T3-L1 adipocytes was determined by ATB-BMPA photolabelling (Yang *et al.*, 1996). Estimation of the rate constants for the endocytosis and exocytosis of transporters revealed that wortmannin blocks the exocytotic pathway. LY294002 is another membrane permeable compound; it is a specific competitive inhibitor at the ATP-binding site of PI 3-K (IC_{50} ~1.4 μM) (Vlahos *et al.*, 1994). Pre-treatment of 3T3-L1 adipocytes with this compound (100 μM) prior to 100 nM insulin stimulation blocks the increase in glucose uptake. Further, this correlates with an absence of GLUT4 at the cell surface (Cheatham *et al.*, 1994).

An alternative method to block PI 3-K activity has been the transient expression by adenovirus of dominant negative p85α in 3T3-L1 adipocytes (Katagiri *et al.*, 1997). Insulin action was affected in three ways. First, maximal insulin-stimulated PI 3-K activity in anti-phosphotyrosine immunoprecipitates was reduced to 6%. Second, maximal insulin-stimulated 2-deoxy-D-glucose transport was decreased to 27%. Third, insulin-stimulated GLUT4 translocation was blocked, as determined by

immunoblotting of subcellular fractions. Thus, the data supports a role for PI 3-K in insulin-stimulated GLUT4 translocation.

To show that PI 3-K is required for insulin-stimulated GLUT4 translocation, it is also necessary to demonstrate that the activation of the kinase is sufficient for this process. Several groups have expressed a constitutively active form of p110 in 3T3-L1 adipocytes: this was either p110 with the inter-SH2 region fused to the N-terminus (Martin *et al.*, 1996) or p110 that was co-expressed with the inter-SH2 region (Frevert and Kahn, 1997). For the former, immunofluorescence microscopy of microinjected cells showed cell surface GLUT4 that was 75% of that in non-injected insulin-stimulated cells. For the latter, immunoblotting of membrane fractions from adenovirus-infected cells showed that there was a 3-fold increase in cell surface GLUT4 over that in control infected basal cells. However, this increase was less than the 4-fold increase upon insulin stimulation of control and experimental cells.

An explanation for the lack of maximal GLUT4 translocation in 3T3-L1 adipocytes expressing constitutively active p110 may be that the construct is not properly targeted to a membrane site (Klippel *et al.*, 1996). In their studies, the transient expression of constitutively active PI 3-K (p110 with an N-terminal inter-SH2 region) in COS-7 cells stimulated downstream PKB activity by 4-fold. However, the addition of either an N-terminal myristoylation sequence or a C-terminal farnesylation sequence to the constitutively active kinase had two effects. First, the construct was located mainly in the membrane fractions. Second, the construct stimulated a greater fold-increase in PKB activity (7-20-fold). Thus, it is possible that the expression of membrane-localized constitutively active PI 3-K in 3T3-L1 adipocytes could stimulate maximal GLUT4 translocation.

The importance of membrane localization of PI 3-K activity was suggested by Ricort *et al.* (1996) and Nave *et al.* (1996a). Though both platelet-derived growth factor (PDGF) and insulin stimulation of 3T3-L1 adipocytes increase PI 3-K activity in anti-phosphotyrosine immunoprecipitates (50- and 17-fold respectively), insulin exerts a greater effect on glucose uptake (11-fold compared with 2-fold) than PDGF.

Moreover, PDGF has no effect on GLUT4 translocation. Subcellular fractionation reveals that PDGF has a greater effect than insulin on PI 3-K activity in anti-phosphotyrosine immunoprecipitates from the plasma membrane (37-fold versus 7-fold). However, this situation is reversed for activity determined in the microsomal membrane fraction: 4.6-fold versus 2.3-fold. The basis of the different effects of insulin and PDGF stimulation was demonstrated by immunoblotting studies. First, insulin stimulation leads to the appearance of phosphorylated IRS-1 predominantly in the LDM, whereas phosphorylated PDGF receptor is present mainly in the plasma membrane. Second, insulin exerts a greater translocation of p85 to the LDM than PDGF, whereas the opposite is true for the plasma membrane. Thus, it appears that insulin, and not PDGF, is able to induce GLUT4 translocation because it can elevate PI 3-K activity in the microsomal membranes. The idea that PI 3-K acts at an intracellular membrane site is supported by Heller-Harrison *et al.* (1996). Immunoadsorbed GLUT4 vesicles from the LDM of 3T3-L1 adipocytes were found to be associated with IRS-1 immunoprecipitates that demonstrated an increase in PI 3-K activity upon insulin stimulation.

Investigations have also been undertaken to determine if IRS-1 is required for the regulation of glucose uptake by insulin-activated PI 3-K. One approach has been the generation of transgenic mice lacking the gene for IRS-1 (Tamemoto *et al.* and Araki *et al.*, 1994). Insulin resistance is evident, as the injection of insulin does not produce as great a drop in blood glucose as that seen in control mice. Also, insulin-stimulated glucose uptake is impaired in adipocytes isolated from the transgenic mice. However, blood glucose levels are normal and insulin-activated PI 3-K activity can be measured in anti-phosphotyrosine immunoprecipitates, later shown to be due to IRS-2 (Patti *et al.*, 1995). Thus, IRS-1 independent pathways are capable of regulating insulin-stimulated glucose uptake. A role for IRS-2 as the alternative insulin receptor substrate was also observed in adipocytes from patients with NIDDM (Rondinone *et al.*, 1997). Compared with control subjects, immunoblotting revealed a reduction of IRS-1 by 50-90%, with no changes in the level of IRS-2. Again, PI 3-K activity was found to be associated with tyrosine-phosphorylated IRS-2. In non-diabetic subjects, immunoblotting of IRS-1 and IRS-2 showed that p85 binds preferentially to the

former. This is reflected in insulin-stimulated PI 3-K activity, where the activity on IRS-1 immunoprecipitates was found to be 70% of that in the sum of both IRS immunoprecipitates. Thus, IRS-1 appears to be the major docking protein for PI 3-K.

An alternative approach to determine the role of IRS-1 in the regulation of glucose uptake has involved the disruption of the interaction between IRS-1 and the insulin receptor (Morris *et al.*, 1996). This was achieved by microinjecting the PTB domain of IRS-1 or an NPXY phosphopeptide into 3T3-L1 adipocytes (both to block the binding of the IRS-1 PTB domain to the NPXY motif of the insulin receptor). Immunofluorescence studies revealed that insulin-stimulated GLUT4 translocation was not perturbed. Also, submaximal stimulation of translocation was not affected. The viability of this technique was demonstrated by the partial inhibition of other insulin-stimulated cellular events: membrane ruffling and mitogenesis. Thus, it was concluded that an IRS-1 independent pathway can regulate glucose transport. Assuming that IRS-2 phosphorylation is perturbed as well, since it also has a PTB domain, a possibility is that PI 3-K activation can occur directly via the association of p85 with the insulin receptor. In binding studies with GST fusion proteins of the N-terminal SH2 domain of p85, interaction with the insulin receptor was disrupted if a C-terminal insulin receptor peptide containing the YTHM motif (tyr-1322) was also present, indicating interaction via this sequence (Staubs *et al.*, 1994). Further, activity in p85 immunoprecipitates could be increased if they were incubated with insulin-stimulated partially purified insulin receptor. However, this was not observed if the C-terminal (containing the Y(1322)THM motif) was deleted, thus indicating activation of PI 3-K via phosphorylated tyr-1322 of the insulin receptor (Van Horn *et al.*, 1994).

Taking all these studies into consideration, it appears that PI 3-K is involved in insulin-stimulated GLUT4 translocation. Thus, inhibition of the kinase blocks this cellular effect. However, the expression of constitutively active PI 3-K leads to submaximal GLUT4 translocation. Thus, it is possible that other pathways are also involved in this process. However, the role of IRS-1 is unclear. Though PI 3-K signalling and increased glucose uptake occur in its absence, a role for IRS-1 under

normal conditions cannot be ruled out, since other pathways may be able to compensate for IRS-1 deficiency. Further, the nature of the IRS-1 independent pathway(s) need to be determined. Thus, it would be interesting to investigate the effects of IRS-2 deficiency or mutation of the Y(1322)THM motif, or combinations of these with IRS-1 deficiency.

1.3.3.2 Ras

The activation of Ras by the insulin receptor initiates a signalling pathway consisting of Raf, mitogen-activated-protein kinase kinase (MAPKK), mitogen-activated-protein kinase (MAPK) and 90 kDa ribosomal S6 kinase ($pp90^{rsk}$), where each component is activated by the preceding one (reviewed by Denton and Tavare, 1995). As insulin stimulation leads to activation of these proteins, several groups have investigated their roles in the regulation of glucose uptake. The role of Ras in insulin-stimulated glucose transport was determined by the microinjection of constitutively active and dominant inhibitory forms of the protein into 3T3-L1 adipocytes (Hausdorff *et al.*, 1994). Cell surface transporters were then quantitated by immunofluorescence microscopy. While the former mimics the effects of chronic (20 hour) insulin treatment by elevating the expression of cell surface GLUT1, the latter blocks insulin stimulation of this response. However, for acute (15 min) insulin treatment, neither construct affects basal and insulin-stimulated levels of cell surface GLUT4. Thus, Ras appears to be involved in regulating GLUT1 expression, but not GLUT4 translocation.

An activated form of Raf also appears to have the same effects as those of Ras (Fingar and Birnbaum, 1994a). Constitutively active Raf was expressed in 3T3-L1 adipocytes. While total cellular GLUT1 levels were increased, those of GLUT4 were unchanged. Further, immunofluorescence studies of plasma membrane sheets revealed elevated cell surface levels of GLUT1 that could not be further increased with chronic insulin treatment. However, acute insulin-stimulated GLUT4 translocation was found to be unaffected. A potential role for MAPK and $pp90^{rsk}$ was also determined by Fingar and Birnbaum (1994b). While the treatment of 3T3-L1

adipocytes with insulin, epidermal growth factor (EGF) or foetal bovine serum (FBS) were found to increase MAPK and $pp90^{rsk}$ activity to a similar extent, only insulin was capable of stimulating an increase in glucose transport activity. Similar studies by Gould *et al.* (1994) showed that while EGF, PDGF and insulin could activate MAPK, only insulin was able to cause GLUT4 translocation in 3T3-L1 adipocytes, as determined by ATB-BMPA photolabelling. Thus, neither activated Raf, MAPK or $pp90^{rsk}$ appear to be sufficient for stimulation of GLUT4 translocation.

1.3.4 Downstream of Phosphoinositide 3-Kinase

1.3.4.1 Protein Kinase B

A cDNA clone for a novel serine/threonine kinase was isolated by Jones *et al.* (1991), who termed it rac, and by Coffer and Woodgett (1991), who termed it protein kinase B (PKB). It was also identified as the cellular homologue of v-*akt*, and thus is also known as Akt (Bellacosa *et al.*, 1991). Human PKB is a polypeptide of 480 residues (molecular weight ~55.7 kDa) with a C-terminal catalytic domain that is 73% and 68% similar to those of PKC and cAMP-dependent protein kinase (Jones *et al.*, 1991). A PH domain at the N-terminus is also present (Musacchio *et al.*, 1993). PKB was later renamed PKBα due to the discovery of two other isoforms, PKBβ (Cheng *et al.*, 1992) and PKBγ (Konishi *et al.*, 1995). Human PKBβ is 481 residues long and 91% homologous to PKBα, whereas PKBγ is 454 residues long. Though there are three identified isoforms of PKB, most studies have focused on the α-isoform only. The insulin stimulation of PKB activity was first described by Kohn *et al.* (1995). In insulin receptor-overexpressing CHO cells that are transiently transfected with PKBα cDNA, the insulin-stimulated increase in activity is 12-fold. Further, activation appears to occur via PI 3-K: wortmannin inhibits insulin-stimulated activity *in vivo*, but not *in vitro* (Kohn *et al.*, 1995).

PKB has been implicated in the regulation of two kinases. The first is 70 kDa ribosomal S6 kinase ($pp70^{S6k}$). The expression of a constitutively active form of

PKBα in Rat-1 fibroblasts was found to increase $pp70^{S6k}$ phosphorylation and activity (Burgering and Coffer, 1995). The second PKB-regulated kinase is glycogen synthase kinase-3 (GSK-3). Immunoprecipitated PKBα from insulin-stimulated L6 myotubes was found to be able to phosphorylate and inactivate GSK-3 *in vitro* (Cross *et al.*, 1995). Subsequent PKB assays have utilized a peptide based on the phosphorylation sequence from GSK-3, termed Crosstide (GRPRTSSFAEG) (Cross *et al.*, 1995).

A role for PKB in stimulating glucose uptake was indicated by Kohn *et al.* (1996b), using 3T3-L1 adipocytes expressing a constitutively active form of PKBα. The PKBα construct was a PH domain deletion mutant with an N-terminal *src* myristoylation signal sequence. As a control, there was a point mutation in the signal sequence. Retroviral infection of fibroblasts with the construct allows the cells to spontaneously differentiate into adipocytes. Basal glucose transport activity was found to be 70% of that in insulin-stimulated cells. The cause of this was attributed to GLUT1 and GLUT4. First, immunoblotting revealed increased GLUT1 expression (55%) compared with control cells, but no change in GLUT4 levels. Second, cell surface GLUT4 (as determined by immunofluorescence microscopy of plasma membrane sheets and by anti-*myc* antibody binding of epitope-tagged GLUT4) was found to be indistinguishable between the basal and insulin-stimulated state. However, only the long-term effects of PKB activation are represented here: it remains to be seen whether PKB is sufficient for acute stimulation of glucose uptake. Further, it needs to be established whether PKB is necessary for insulin stimulation of glucose transport.

1.3.4.2 $pp70^{S6k}$

The identification of $pp70^{S6k}$ as a target for PI 3-K was described by Chung *et al.* (1994). In HepG2 cells, the stimulation of PI 3-K and $pp70^{S6k}$ activity by PDGF are both inhibited by wortmannin with a similar IC_{50}. Since wortmannin does not inhibit $pp70^{S6k}$ activity *in vitro*, this therefore indicates that the kinase is downstream of PI 3-K. Chung *et al.* (1994) also demonstrated that the activation of $pp70^{S6k}$ can be inhibited by the drug rapamycin, which itself does not inhibit PI 3-K activity.

The elevation of $pp70^{S6k}$ activity in response to insulin stimulation of 3T3-L1 adipocytes was demonstrated by Fingar *et al.* (1993). They found that while pre-incubation of cells with rapamycin before insulin treatment inhibited this rise in activity, there was no effect of the inhibitor on the translocation of GLUT1 and GLUT4 as determined by immunofluorescence microscopy of plasma membrane sheets. Thus, $pp70^{S6k}$ does not appear to be required for insulin-stimulated glucose uptake.

1.3.5 Potential Regulators of Glucose Transport

1.3.5.1 Protein Kinase C

The involvement of PKC in the regulation of GLUT4 translocation has been investigated using the phorbol ester, phorbol 12-myristate 13-acetate (PMA), a known stimulator of PKC activity (Holman *et al.*, 1990). Treatment of rat adipocytes with this compound raises cell surface levels of GLUT1 and GLUT4 by 5.7- and 4-fold respectively. Though the translocation of GLUT1 is comparable to that seen with insulin treatment, the same cannot be said for GLUT4, where the insulin-stimulated increase in cell surface levels is 15-20-fold. A similar observation was made in 3T3-L1 adipocytes, in which PMA-stimulated cell surface GLUT1 and GLUT4 levels are 40% and 10% respectively of that following insulin stimulation (Gibbs *et al.*, 1991). Further, down-regulation of PKC by chronic treatment of 3T3-L1 adipocytes with PMA prevents elevation of glucose transport by acute and chronic PMA stimulation, but does not inhibit that by insulin stimulation (Gibbs *et al.*, 1991). Thus, PMA-sensitive PKC appears to be neither sufficient nor necessary for insulin-stimulated GLUT4 translocation. However, a role for PKC cannot be entirely ruled out, as PMA appears to activate PKC differently from insulin stimulation (Farese *et al.*, 1992). In immunoblotting studies of cytosolic and total membrane fractions from rat adipocytes, PMA and insulin treatment were found to stimulate the translocation of PKC isoforms to different extents. For example, while insulin stimulates the rapid tranlocation of PKCβ to the plasma membrane, PMA does not.

Nave *et al.* (1996b) demonstrated that insulin and PMA stimulation are both able to increase levels of PI 3,4,5-P_3 in 3T3-L1 adipocytes. They observed that the fold-increase in phospholipid by either compound correlated with the observed fold-increase in glucose transport. Further, wortmannin was found to block the stimulatory action of both insulin and PMA on PI 3,4,5-P_3 production and glucose uptake. Gibbs *et al.* (1991) showed that the effects of PMA on glucose transport are not additive with maximal stimulatory concentrations of insulin, though an additive effect occurs at lower insulin doses. Thus, both studies are consistent with the idea that the PMA-stimulated pathway converges with that from the insulin receptor via the production of PI 3,4,5-P_3. However, factors other than the production of this phospholipid must be required for GLUT4 translocation, since PMA stimulation only gives an insulin-like response in terms of GLUT1 translocation (Holman *et al.*, 1990).

Phorbol ester-insensitive PKCζ has been shown to be activated by PI 3,4,5-P_3 *in vitro* (Nakanishi *et al.*, 1993), thus indicating regulation by PI 3-K. Farese *et al.* (1992) immunoblotted cytosolic and membrane fractions from rat adipocytes and found that insulin stimulation decreases cytosolic levels of PKCζ, while increasing those in the total membrane fraction. Although similar experiments by Frevert and Kahn (1996) were unable to show insulin-stimulated translocation of PKCζ, they did demonstrate that the isoform is present in the LDM fraction, unlike the phorbol ester-sensitive isoforms. To determine a role for PKCζ in the regulation of glucose transport, the enzyme was stably transfected into 3T3-L1 adipocytes (Bandyopadhyay *et al.*, 1997). Their findings were as follows. Overexpression of wild-type PKCζ by 2-fold also doubled basal glucose uptake, but was without an additive effect on the 7-fold response seen in insulin-stimulated control transfected cells. Similar overexpression of dominant negative PKCζ had no effect on basal glucose uptake, though it did attenuate the insulin-stimulated response (a 4-fold maximum response was observed). There was no change in the expression of total cellular GLUT1 and GLUT4, while immunoblotting of subcellular fractions revealed translocation of both isoforms in cells overexpressing PKCζ. Thus, PKCζ is a putative component of the insulin signalling pathway that regulates glucose transport.

1.3.5.2 Protein Phosphatases 1 and 2A

A role for PP1 and PP2A in the regulation of glucose transport was first suggested by Haystead *et al.* (1989), from studies with the specific inhibitor okadaic acid. This compound was shown to increase the phosphorylation state of many cellular proteins in hepatocytes and adipocytes. They observed that the treatment of rat adipocytes with 1 μM okadaic acid increased uptake of 2-deoxy-D-glucose, though with a 5 min time lag that was not observed with insulin stimulation. The effects of okadaic acid on glucose transport were further investigated by Lawrence *et al.* (1990). Rat adipocytes were maximally stimulated with either insulin or okadaic acid prior to the measurement of 2-deoxy-D-glucose uptake. The former elicited an 8-fold response, whereas the response induced by the latter was 4-fold. However, treatment with both agents led to a submaximal insulin response (5-fold). The cause of this effect was investigated by Corvera *et al.* (1991). They found that while okadaic acid and insulin both elevated 3-*O*-methyl-D-glucose transport and cell surface levels of GLUT4, the rate of glucose uptake induced by the former appeared to be lower than expected for the number of transporters present. Further, while the addition of okadaic acid to insulin-stimulated cells led to a reduction in 3-*O*-methyl-D-glucose transport, this was not associated with a significant decrease in cell surface GLUT4. Thus, it was suggested that okadaic acid both stimulates GLUT4 translocation and causes a reduction in its intrinsic activity.

PP1 and PP2A are not specific for a particular protein. As such, the sites of action for okadaic acid are likely to be located at different points in the insulin signalling pathway. The effect of okadaic acid on PI 3-K activity in 3T3-L1 adipocytes and muscle was determined by Jullien *et al.* (1993). While okadaic acid treatment of 3T3-L1 adipocyes and muscle has no effect on PI 3-K activity in anti-phosphotyrosine immunoprecipitates, it does however attenuate the increase observed with insulin stimulation. Further experiments revealed that while okadaic acid does not affect insulin-induced receptor autophosphorylation, it does block the subsequent step of tyrosine phosphorylation of IRS-1. Thus, inhibition of PI 3-K activation may account, at least partly, for the attenuation of insulin-stimulated glucose uptake by okadaic

acid. Further, okadaic acid stimulation of glucose transport is also likely to occur via action at sites downstream of PI 3-K.

1.3.5.3 G Proteins

A role for G proteins in the regulation of glucose uptake can be demonstrated by using the non-hydrolyzable GTP analogue, GTPγS (Clarke *et al.*, 1994). Its introduction into permeabilized 3T3-L1 adipocytes increases glucose uptake levels. Further, when insulin-treated cells are incubated with wortmannin, a stimulated response is observed if GTPγS is still present, indicating that G proteins may be acting downstream of PI 3-K, or via a different pathway. Further, a role for G proteins in the exocytosis and endocytosis of GLUT4 vesicles in rat adipocytes was demonstrated by Shibata *et al.* (1995). If the internalization of GLUT4 is blocked by treatment with a major histocompatibility complex class I-derived peptide, GTPγS is still able to stimulate translocation of transporters to the plasma membrane, indicating a role for G proteins in the exocytosis of GLUT4. The endocytosis of GLUT4 was determined by maximally stimulating adipocytes with insulin before ATP-deprivation with potassium cyanide and trypsin treatment. The internalization of trypsin-cleaved GLUT4 is blocked if GTPγS is present. Also, if insulin stimulation of adipocytes is reversed, the rate of decline of transport activity is increased if GTP is present and is decreased if GDPβS is present. Thus, it appears that GTP hydrolysis is involved in the endocytosis of GLUT4 vesicles.

1.4 The PH Domain and the PTB Domain

1.4.1 Structure and Function of the PH Domain

The PH domain is so-called because it was first identified in pleckstrin, a substrate of PKC in platelets. It has subsequently been detected in other proteins, including IRS-1 and PKB (Musacchio *et al.*, 1993). The structures of the PH domains for β-spectrin and pleckstrin have been determined (reviewed by Gibson *et al.*, 1994) (Figure 1.4.1). The domain consists of an anti-parallel β-sheet made up of seven strands (forming a β-barrel), followed by a long α-helix at the C-terminal end. The first four β-strands form a sheet that is at an angle to the sheet formed by the last three β-strands. The PH domains of different proteins vary in the length of the loops between the strands of the β-sheet. A cleft is present in the domain, bounded by β-strands b, c and d (the strands are named from a to g). A cluster of positive charges is associated with this cleft (due to loops a-b and e-f): this may be of functional importance, as it is conserved in many PH domains.

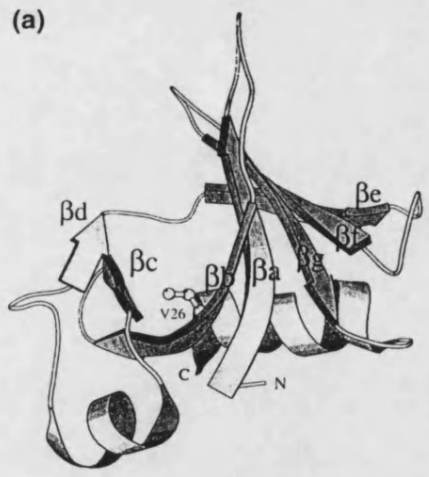

Figure 1.4.1. Structure of the β-spectrin PH Domain (Gibson *et al.*, 1994).

The β-strands are labelled (from the N-terminus) from a to g.

Three ligands have been shown to bind to the PH domain. The first is PI 4,5-P_2 (Harlan *et al.*, 1994). By using a centrifugation assay, it was found that vesicles

containing PI 4,5-P_2 were able to bind - in a concentration dependent manner - to the PH domain of the different proteins tested, which included those of pleckstrin and β-adrenergic receptor kinase (β-Ark). NMR studies indicated that PI 4,5-P_2 binds to the N-terminal half of the PH domain, involving residues found in loop a-b and β-strands c and d. As these residues include several positively charged lysines, it was suggested that they bind to the negatively charged phosphates of PI 4,5-P_2. However, the hydrophobic core of the β-barrel does not appear to be able to bind to the fatty acid chains of PI 4,5-P_2. It is likely that the affinity of the PH domain for PI 4,5-P_2 will vary between proteins. The dissociation constant (K_d) for the binding of PI 4,5-P_2 to the pleckstrin PH domain is 30 μM (Harlan *et al.*, 1994), whereas it is 1.7 μM for the PH domain from phospholipase C (PLC) δ_1 (Lemmon *et al.*, 1995). Also, inositol 1,4,5-trisphosphate (Ins 1,4,5-P_3) binds to the PLC δ_1 PH domain with a lower K_d of 210 nM (Lemmon *et al.*, 1995). It is also likely that PH domains from different proteins are specific for particular phosphoinositides. Frech *et al.* (1997) were able to demonstrate the association of PI 3,4-P_2 and PI 3,4,5-P_3 with the PH domain of PKBα, with K_d values of 570 and 400 nM respectively. Since PI 4,5-P_2 was found to bind with a K_d of 2.5 μM, it appears that PKBα has a preference for PI 3,4-P_2 and PI 3,4,5-P_3.

A second potential ligand for the PH domain is the βγ subunit of trimeric G proteins (Gβγ) (Touhara *et al.*, 1994). In their study, GST fusion proteins were produced, with sequences for PH domains from several proteins (including IRSI and β-Ark). From direct Gβγ binding assays, it was found that all of the PH domains tested could bind to Gβγ, but to varying extents. The presence of Gα inhibits this interaction, demonstrating that the same site on Gβγ is responsible for binding the PH domain or Gα. By using GST fusion proteins that contained different sections of the PH domain, it was found that the portion of the PH domain that binds to Gβγ is the C-terminal region (corresponding to β-strands d-g and the α-helix) plus sequences distal to it.

The third potential PH domain-binding protein is PKC. The association of the PH domain of PKB with three PKC isoforms (α, δ and ζ) was identified by Konishi *et al.* (1995). GST fusion proteins of the PKB PH domain were immobilized on glutathione

sepharose beads and incubated with cell lysate from COS-7 cells expressing one of the three PKC isoforms. Binding was detected by immunoblotting with isoform-specific antibodies. However, the functional significance of the interaction between the two kinases is unclear, as no changes in the enzyme activity of PKB were observed upon binding of PKC.

From an examination of the nature of the ligands that bind the PH domain, it is possible to suggest that the domain may enable a protein to associate with membranes. This has been shown to be the case for PLC δ_1 (Paterson *et al.*, 1995), which has an N-terminal PH domain. Constructs of this enzyme were microinjected into Madin Darby canine kidney cells, with the subcellular distribution determined by immunofluorescence microscopy. Deletion mutants that lacked the PH domain were found to be present only in the cytoplasm, unlike the full length and N-terminal constructs, which were membrane-bound. Concomitant studies showed that the deletion mutants lacking the the proposed PI 4,5-P_2 binding site of the PH domain were also unable to bind Ins 1,4,5-P_3 (the polar head group of PI 4,5-P_2), implying that membrane interaction is via this phospholipid. Another possible method of membrane binding is via Gβγ (reviewed by Inglese *et al.*, 1995). The enzyme β-Ark down-regulates G-protein-coupled receptors (GPCR) by phosphorylating them. Association of β-Ark with the plasma membrane occurs when the GPCR effects the dissociation of trimeric G proteins into Gα and Gβγ. The enzyme is then able to bind to Gβγ, and is thereby localized near its substrate. The region of β-Ark which interacts with Gβγ includes the PH domain.

1.4.2 Structure of the PTB Domain

The crystal structure of the IRS-1 PTB domain is similar to that of the PH domain (Eck *et al.*, 1996). Thus, it consists of a seven-stranded β-sandwich (one face formed by the first four β-strands in an anti-parallel β-sheet) followed by a C-terminal α-helix. Unlike the PH domain, the cluster of positive charges that bind inositol phosphates is absent. All nine residues of the insulin receptor peptide LYASSNPAY

bind to the PTB domain via hydrogen bonds and hydrophobic interactions. The first five residues of the peptide form an anti-parallel β-strand with the domain.

1.4.3 Function of the N-terminal Domains of the IRS Proteins

A role for the PH domain of IRS-1 in coupling the protein to the insulin receptor was first described by Myers Jr. *et al.* (1995). Rat IRS-1 was expressed in 32D cells, which lack endogenous IRS proteins. The deletion of the PH domain (residues 13-115) virtually inhibited insulin-stimulated tyrosine phosphorylation of IRS-1. However, overexpression of the insulin receptor prevented this from occurring. The nature of the interaction between the IRS-1 PH domain and the insulin receptor is unclear, as binding of the latter to a GST fusion protein of the former could not be achieved. The findings by Myers Jr. *et al.* (1995) were supported by Voliovitch *et al.* (1995). In their study, the N-terminal 61-residues of the PH domain in IRS-1 were deleted. The construct was transiently expressed in COS-7 cells along with the insulin receptor. Anti-phosphotyrosine immunoblotting showed that insulin-stimulated phosphorylation of the deletion mutant was significantly reduced, compared with that observed for full-length IRS-1. The data by Voliovitch *et al.* (1995) also suggest that the IRS-1 PH domain interacts with a phospholipid, since only the N-terminal residues of the PH domain were deleted in their study. This region of the PH domain has been shown to be involved in PI 4,5-P_2 binding (Harlan *et al.*, 1994).

However, a direct interaction between the insulin receptor and IRS-1 has been located at the PTB domain (Wolf *et al.*, 1995). A GST fusion protein of human IRS-1 PTB domain (residues 144-316) was able to precipitate phosphorylated purified insulin receptor. This interaction was inhibited if tyr-960 of the receptor was mutated to phenylalanine, or if an insulin receptor phosphopeptide with the NPXY motif (containing tyr-960) was present. Further, phosphopeptide binding studies revealed the importance of hydrophobic residues at positions 6, 7 and 8, N-terminal to tyr-960. For IRS-2, another domain, in addition to the PTB domain, was found to interact with the insulin receptor (Sawka-Verhelle *et al.*, 1996). Using the yeast two-hybrid system,

an association between murine IRS-2 PTB domain (191-350) and the insulin receptor was detected, but not if tyr-960 was mutated to phenylalanine. However, an interaction between full length IRS-2 and the same mutant insulin receptor was also observed. The sequence responsible was located to residues 591-786. Further, it was found that tyr-1146, -1150 and -1151 of the insulin receptor were required, as the mutation of any of these residues to phenylalanine inhibited binding of the domain.

The role of the PTB domain in receptor-mediated phosphorylation of IRS-1 was investigated by Yenush *et al.* (1996) in 32D cells expressing IRS proteins. Unlike IRS-1 constructs lacking the PH domain, the deletion of the PTB domain did not affect maximum insulin stimulation of IRS-1 tyrosine phophorylation. However, at lower insulin doses, IRS-1 phosphorylation of the construct was affected. When the insulin receptor was overexpressed, only the phosphorylation of IRS-1 lacking both domains was found to be affected at all insulin concentrations. However, the absence of either domain did not perturb IRS-1 phosphorylation. In similar studies (Backer *et al.*, 1997), where the insulin receptor and IRS-1 were co-expressed (5:1) in CHO cells, mutation of tyr-960 to alanine in the insulin receptor did not affect IRS-1 tyrosine phosphorylation. Further, *in vitro* studies revealed that whilst the solubilized form of the same mutant receptor bound similarly to IRS-1 as the wild-type, the deletion of the PH domain virtually blocked association of IRS-1 with the insulin receptor.

From the available data, it appears that the PH domain is more sensitive than the PTB domain in terms of coupling IRS-1 to the insulin receptor. However, both domains are required for full IRS-1 phosphorylation to occur. Despite the greater importance of the PH domain, the mechanism of its function has not yet been determined.

1.4.4 Role of the PH Domain in the Activation of PKB

The activation of PKB appears to occur via two mechanisms. The first involves the binding of PI 3,4-P_2 to the N-terminal PH domain (Franke *et al.*, 1997). In CHO cells expressing hemagglutinin epitope-tagged PKBα, the immunoprecipitated activity

increases if the cells are treated with either PDGF or PI 3,4-P_2. This effect is not observed if the PKBα constructs have a point or partial deletion mutation of the PH domain. The second activation mechanism involves the phosphorylation of PKB (Kohn *et al.*, 1995). Kinase activity was measured in insulin receptor-overexpressing CHO cells that transiently express PKBα. Alkaline phosphatase treatment of immunoprecipitates from stimulated cells was found to reduce PKB activity to basal levels. It is likely that the PH domain is responsible for membrane localization of PKB in order to facilitate its activation by a regulatory kinase (Kohn *et al.*, 1996a). A construct of PKBα lacking the PH domain, but with a *src* myristoylation signal sequence fused to the N-terminus, is constitutively active when expressed in CHO cells. This is due to a higher phosphorylated state. A possibility is that the generation of PI 3,4-P_2 by PI 3-K provides the signal for the membrane association of PKB. This idea is consistent with the observation that the expression of constitutively active PI 3-K leads to continuous activation of PKB (Didichenko *et al.*, 1996). Also, it is likely that phosphorylation is the major mechanism for the direct activation of PKB, as dephosphorylation of the constitutively active PKBα construct with phosphatase inhibitors reduces activity by 76% (Kohn *et al.*, 1996a). Further, stimulation of purified hemagglutinin epitope-tagged PKBα from unstimulated COS-1 cells with PI 3,4-P_2 leads to a 2.5-fold increase in activity, whereas the activity in immunoprecipitates from stimulated cells is about 19-fold over basal levels (Frech *et al.*, 1997). Thus, the phospholipid cannot fully activate PKB activity on its own.

The phosphorylation sites on PKBα were identified as two residues: ser-473 and thr-308 (Alessi *et al.*, 1996). For hemagglutinin-tagged constructs expressed in 293 cells, the mutation of thr-308 to alanine leads to inhibition of the insulin-stimulated increase in activity. For a similar mutation of ser-473, 15% of the insulin-induced response occurs. This indicates that the phosphorylation of both residues are required for the synergistic and full activation of PKB. An upstream kinase for PKB phosphorylation was identified by Alessi *et al.* (1997), and termed PI 3,4,5-P_3-dependent protein kinase-1 (PDK-1) based on its requirement for the phospholipid in *in vitro* kinase assays with PKB as the substrate. Phosphorylation was found to be at only thr-308 of PKBα. The dephosphorylation of PKB may occur via PP2A, as immunoprecipitates

of PKB from stimulated Swiss 3T3 cells can be inactivated by treatment with the phosphatase (Andjelkovic *et al.*, 1996).

1.5 Insulin Resistance

NIDDM is characterized by two defects (Kahn, 1994). The first is insulin resistance, where the hormone is unable to fully effect glucose disposal. Thus, there is a defect in insulin-stimulated glucose uptake and insulin-inhibited glucose production in the liver. The second is relative insulin deficiency, where the pancreas is unable to produce enough insulin to compensate for this resistance. The development of NIDDM is caused by a combination of genetic and environmental factors (Kahn, 1994). Studies in subjects of parents with NIDDM demonstrate that low insulin sensitivty is inherited, and that this factor precedes and predicts the development of NIDDM. A reduction in insulin sensitivity leading to NIDDM can also be caused by obesity. Further, this factor has a greater effect on subjects with diabetic parents.

Since insulin resistance is associated with the onset of NIDDM, it is likely that a defect (or defects) in the pathway from the insulin receptor to the glucose transporter is (or are) responsible for the disease. Though some defective genes have been identified, such as that for the insulin receptor, these do not account for the majority of cases of NIDDM (Kahn, 1994). Thus, a common defective gene for NIDDM has not been discovered. One approach to determine defects in insulin action is in models of insulin resistance. One such model is adipocytes made insulin resistant by chronic treatment with insulin (see below). This model is useful since it is comparable to the pre-diabetic state of NIDDM patients, in which insulin resistance is associated with hyper-insulinaemia. Though this model may not represent the genetic cause of NIDDM, it does however enable identification of factors that may be involved in insulin-regulated glucose uptake.

1.5.1 Insulin Resistance Induced by Chronic Treatment of Adipocytes with Insulin

Chronic treatment of 3T3-L1 adipocytes with insulin induces a state of insulin resistance (Kozka *et al.*, 1991). Following a 24 h 500 nM insulin treatment, total

cellular GLUT1 increases 6-fold, whereas GLUT4 levels rise only 1.4-fold. ATB-BMPA photolabelling of cell surface transporters demonstrates that levels of GLUT1 increase by 4-fold over those in acute (30 min) insulin-stimulated cells, whereas for GLUT4, levels are about half of the maximum response. This down-regulation of cell surface GLUT4 is associated with resistance to further insulin stimulation. Thus, an acute insulin treatment of washed cells (previously chronically insulin-treated) does not further increase cell surface GLUT1 and GLUT4.

This state of insulin resistance is not associated with a change in insulin binding (Kozka *et al.*, 1991). However, Pryor *et al.* (1997) have observed a 70% reduction in the tyrosine phosphorylation of the insulin receptor following chronic treatment of rat adipocytes with insulin, compared with that for acute insulin-stimulated cells. Other groups have observed the down-regulation of IRS-1 following chronic treatment of 3T3-L1 adipocytes with insulin. Immunoblotting studies by Rice *et al.* (1993) show that 24 h 1 μM insulin treatment leads to a virtual absence of IRS-1 (10% of maximum levels), while there is a slight increase in p85 (20%). Ricort *et al.* (1995) determined PI 3-K activity in anti-phosphotyrosine immunoprecipitates following 10 h 100 nM insulin treatment. They found that activity was 2-fold over basal levels, compared with a maximum 60-fold for control acute insulin-stimulated cells. Restimulation after washing only produced a maximum response that was 30% of the maximum in the control cells. Thus, a factor responsible for the insulin resistance following chronic treatment with insulin appears to be down-regulation of IRS-1, which affects the downstream signalling of PI 3-K. However, the decreased expression of other signalling proteins cannot be ruled out.

The drug metformin has been shown to counteract the insulin resistance that is induced by chronic treatment with insulin (Kozka and Holman, 1993). If metformin is present during chronic treatment of rat adipocytes with insulin, down-regulation of cell surface GLUT4 is prevented. Thus, the proportion of total cellular GLUT4 present is 60% (compared with 49% for acute insulin-stimulated cells). Further, resistance to insulin stimulation is not observed. Thus, if the cells are washed and

restimulated, resulting levels of cell surface GLUT1 and GLUT4 are comparable to those in acute insulin-stimulated cells.

1.6 Experimental Aims of Work Described in the Thesis

Work has focused on two components of the insulin signalling pathway: the PH domain of IRS-1 and PKB. Investigations were undertaken to examine the possibility that the PH domain may act to target IRS-1 to a membrane site. IRS-1 PH domain was produced using the GST fusion protein system. The construct was introduced into permeabilized 3T3-L1 adipocytes to determine if it would affect interactions between IRS-1 and the insulin receptor or the LDM. A number of methods have also been used to search for a potential protein ligand of the IRS-1 PH domain.

An enzyme assay for PKB was developed. Then, several studies with 3T3-L1 adipocytes were undertaken to confirm that PKB is downstream of insulin-regulated PI 3-K, and also, to determine if PKB may be involved in insulin-stimulated glucose uptake. First, the insulin stimulation of PKB activity was measured as a function of time and dose. The response observed could then be compared with that for insulin-stimulated glucose uptake. Second, the time-course for wortmannin inhibition of insulin-stimulated PKB activity was determined, and then compared with that for insulin-stimulated glucose uptake. Third, the effects of chronic stimulation of adipocytes with insulin on PKB activity was determined, since this treatment regime down-regulates cell surface GLUT4. Fourth, the ability of Crosstide to inhibit insulin-stimulated glucose uptake was investigated. Studies with 3T3-L1 adipocytes were also undertaken to characterize insulin stimulation of PKB activity. First, kinase activity was determined in subcellular fractions in order to locate the site of action of PKB. Second, okadaic acid was used to determine if PP2A is involved in the inactivation of PKB *in vivo*.

In addition, the ATB-BMPA photolabel was used to quantitate cell surface glucose transporters in 3T3-L1 adipocytes expressing constitutively active PKB (Kohn *et al.*, 1996b). Thus, this would allow an assessment of the relative contributions of GLUT1 and GLUT4 to the elevated glucose transport activity induced by the constitutively active enzyme.

2.0 METHODS

2.1 Materials

2.1.1 Laboratory Chemicals

Unless otherwise indicated, general laboratory chemicals and solvents were from Sigma-Aldrich Company Ltd. (Poole, Dorset), Fisons Scientific UK Ltd. (Loughborough) or BDH Laboratory Supplies (Merck Ltd., Poole, Dorset).

- Monocomponent porcine insulin was a gift from Dr R. Chance (Lilly Research Laboratories, Indianapolis, IN);

- Radiochemicals and ECL Western blotting detection reagents were from Amersham International plc (Little Chalfont, Buckinghamshire);

- 2-*N*-4-(1-azi-2,2,2-trifluoroethyl)benzoyl-1,3-[^{3}H]bis-(D-mannos-4-yloxy)-2-propylamine (ATB-[2-^{3}H]BMPA) (≈ 10 Ci/mmol) was synthesized by Professor G.D. Holman (University of Bath, Bath) (Clark and Holman, 1990);

- Crosstide was synthesized by Mrs S. Phillips (University of Bath, Bath) (Cross *et al.*, 1995);

- Thesit® ($C_{12}E_9$) was from Boehringer Mannheim UK Ltd. (Lewes, East Sussex);

- 4-(2-aminoethyl)benzenesulfonylfluoride (AEBSF) was from Calbiochem-Novabiochem (UK) Ltd. (Nottingham);

- Bovine serum albumin (BSA) (Bovuminar Cohn Fraction V) was from Intergen Company (Purchase, NY);

- Collagenase was from Worthington Biochemical Corporation (Freehold, NJ);

- Inositol 1,4,5-trisphosphate and okadaic acid were from Alexis Corporation (UK) Ltd. (Nottingham).

2.1.2 Antibodies

- Rabbit antisera against GLUT1 and GLUT4 were kindly provided by Dr S.W. Cushman (National Institutes of Health, Bethesda, USA); they were raised against C-terminal peptides produced in our laboratory (Holman *et al.*, 1990);

- Monoclonal anti-IRS-1 (ID6) (Yang *et al.*, 1996) was a gift from Dr M. Kasuga (Kobe University School of Medicine, Kobe, Japan);

- Mouse monoclonal anti-phosphotyrosine (clone 4G10) and rabbit polyclonal anti-Rac-CT were from Upstate Biotechnology, Inc. (Lake Placid, NY);

- Goat polyclonal anti-Akt1(C-20) was from Santa Cruz Biotechnology, Inc. (Santa Cruz, CA).

2.1.3 Cell Culture

Unless stated otherwise, all cell culture materials were purchased from Sigma.

- The following were purchased from GibcoBRL (Life Technologies, Paisley, Renfrewshire): Newborn Calf Serum (NCS); Foetal Bovine Serum (FBS); 0.25% (w/v) Trypsin (in Gibco solution A - 0.4 g/L KCl, 2.2 g/L $NaHCO_3$, 6.8

g/L NaCl, 1.0 g/L glucose, 0.005 g/L Phenol Red); Cell Culture Freezing Medium (glycerol in DMEM with FBS and NCS); and Nunclon™ Δ Dishes and Δ Flasks;

- Dulbecco's Modification of Eagle's Medium (DMEM) and 0.4% (w/v) Trypan Blue solution were from ICN Biomedicals Ltd. (Thame, Oxfordshire);

- Cryogenic vials (2.0 ml) were from Corning Costar Corporation (Cambridge, MA);

- Universal containers (30 ml) were from Bibby Sterilin Ltd. (Stone, Staffordshire);

- Phosphate Buffered Saline (PBS) (Dulbecco 'A') (0.2 g/L KCl, 0.2 g/L NaH_2PO_4, 8 g/L NaCl, 1.15 g/L Na_2HPO_4, pH 7.3) was from Oxoid (Unipath Ltd., Basingstoke, Hampshire).

2.2 Culture of Adipocyte Cells

2.2.1 Culture of 3T3-L1 Adipocytes

Preparation of Medium. DMEM (with 4.5 g/l glucose and without L-glutamine) was supplemented with 1% (v/v) L-glutamine (200 mM in tissue culture grade water), 2% (v/v) penicillin-streptomycin solution (5000 units penicillin and 5 mg streptomycin per ml in 0.9% (w/v) NaCl), and either 10% (v/v) newborn calf serum or 10% (v/v) foetal bovine serum (Myoclone Super Plus) to give DMEM-NCS or DMEM-FBS. Sera were heat-inactivated by incubation at 56 °C for 30 min before addition to media.

Culturing Conditions. Media and PBS were pre-warmed to 37 °C before use. Cells were grown in an automatic CO_2 incubator (LEEC, Nottingham) calibrated for dry

operation. The temperature was set at 37 °C with CO_2 levels at 10%. Dishes of cells were stored with 100 mm dishes of water inside sandwich boxes which were covered with a clingfilm lid.

Preparation of Frozen Stocks of 3T3-L1 Fibroblasts. 3T3-L1 fibroblasts were purchased from American Type Culture Collection (Rockville, MD). Cell number was increased by culture in 175 cm^2 flasks (see below) before frozen storage. Pelleted cells were resuspended in Cell Culture Freezing Medium (0.5×10^6 cells per 0.5 ml) and transferred to cryogenic vials on ice. The cells were slowly cooled above liquid nitrogen for 24 h, before eventual storage in liquid nitrogen.

Seeding 3T3-L1 Fibroblasts from Frozen Stocks. The frozen fibroblasts were removed from liquid nitrogen storage and rapidly thawed at 37 °C, before addition to 20 ml DMEM-NCS. The cells were pelleted by spinning at 1500 rpm for 3 min. The medium was removed and the cells resuspended in 2 ml DMEM-NCS using a needle and syringe (21 g), before transfer to 40 ml DMEM-NCS in a 175 cm^2 flask. The cells were grown to near-confluence, with medium being replaced every two days.

Harvesting 3T3-L1 Fibroblasts. The subconfluent fibroblasts were washed twice with 10 ml PBS, before treatment with 4 ml trypsin at 37 °C for 3 min. The cells were detached by knocking before dilution with 16 ml DMEM-NCS. The cells were pelleted and resuspended as above. Cell number was determined using a haemocytometer, where the cells were mixed 1:1 (v/v) with 0.4 % (w/v) Trypan Blue. Cells were seeded in 35 mm dishes at a density of 0.05×10^6 cells per 2 ml DMEM-NCS per dish. 175 cm^2 flasks were seeded with $0.1\text{-}0.2 \times 10^6$ cells in 40 ml DMEM-NCS. Medium was replaced every two days. Cells were passaged 7 times.

Differentiation of 3T3-L1 Fibroblasts into Adipocytes. Three days after the fibroblasts in the 35 mm dishes had grown to confluence, the cells were differentiated into adipocytes. DMEM-NCS was replaced with DMEM-FBS containing 0.25 μM dexamethasone, 0.5 mM 3-isobutyl-1-methylxanthine and 0.2 μM insulin. Two days later, the medium was replaced with DMEM-FBS containing 0.2 μM insulin, and

thereafter every two days with DMEM-FBS. Cells were fully differentiated on day nine and were usable until day thirteen.

2.2.2 Isolation and Culture of Rat Adipocytes

Epididymal fat pads were removed from male Wistar rats (180-200 g), washed in rat BSA-Krebs-Ringers-HEPES buffer (rat BSA-KRH buffer) (140 mM NaCl, 4.7 mM KCl, 2.5 mM $CaCl_2.2H_2O$, 1.25 mM $MgSO_4.7H_2O$, 2.5 mM $NaH_2PO_4.2H_2O$, 10 mM HEPES, pH 7.6, 1% (w/v) BSA) and chopped up with scissors. Three fat pads were digested in 3.5 ml digestion buffer (rat KRH buffer with 3.5% (w/v) BSA, 0.9 mg/ml glucose and 0.7 mg/ml collagenase) for 50 min in a 37 °C shaking water bath. Undigested connective material was removed by filtration through a nylon gauze. Cells were washed with rat BSA-KRH buffer and made up to 40% cytocrit. Then, the cells could either be used immediately, or they could be cultured for 24 h. For the former, 40% cytocrit suspensions were treated with or without 20 nM insulin. For the latter, 2 ml cells was added to 40 ml DMEM (with 1% (w/v) BSA, 25 mM HEPES, pH 7.6, 2 mM L-glutamine, 100 U/ml penicillin and 100 μg/ml streptomycin) in 100 ml disposable containers (Sarstedt Ltd., Leicester). Incubation was at 37 °C 5% CO_2 for 24 h in the absence or presence of 500 nM insulin with or without 1 mM metformin.

BSA stocks were prepared as follows. 100 g of powder was dissolved in 500 ml double-distilled water and dialyzed for 24 h at 4 °C with two changes of ten volumes of double-distilled water. The BSA solution was made up to 10% (w/v) and filtered through a Millipore filter (type AA, pore size 0.8 μm) (Millipore Corporation, Bedford, MA). The BSA solution was adjusted to pH 7.4 with 10 M NaOH and stored in frozen aliquots at -20 °C.

2.3 Treatment of Adipocytes with Insulin

2.3.1 Insulin Treatment of 3T3-L1 Adipocytes

Two hours prior to insulin stimulation, each dish of 3T3-L1 adipocytes was washed twice with 2 ml PBS at 37 °C before incubation in 2 ml DMEM with 2 mM L-glutamine, 100 U/ml penicillin and 100 μg/ml streptomycin (serum-free DMEM) for 2 h at 37 °C 10% CO_2. Each dish was then washed 3 times with 2 ml Krebs-Ringers-HEPES (KRH) buffer (136 mM NaCl, 4.7 mM KCl, 1.25 mM $CaCl_2.2H_2O$, 1.25 mM $MgSO_4.7H_2O$, 10 mM HEPES, pH 7.4) at 37 °C before incubation in 1 ml KRH (0.95 ml for glucose transport assays) at 37 °C with or without insulin. The usual treatment was 100 nM insulin for 20 min.

2.3.2 Insulin Treatment of Permeabilized 3T3-L1 Adipocytes

After incubation in serum-free DMEM, each dish of 3T3-L1 adipocytes was washed 3 times at 37 °C with 2 ml intracellular (IC) buffer (20 mM HEPES, 5 mM NaCl, 5 mM EGTA, 5 mM $MgCl_2.6H_2O$, 140 mM L-glutamate, pH 7.4) before incubation in 0.5 ml IC buffer containing 0.4 I.U. streptolysin O (SLO) (Murex Diagnostics Ltd., Dartford) for 5 min at 37 °C. Each dish was then washed 3 times at 37 °C with 2 ml IC buffer before incubation in 0.95 ml (0.94 ml for insulin-stimulated cells) IC buffer supplemented with 10 mM ATP and 3 mM pyruvate (AP-IC); also present was the compound to be introduced into the cells. After a period of time (indicated in the figure legends - up to 20 min) at 37 °C, cells were further incubated with or without 10 or 100 nM insulin.

2.3.3 Chronic Insulin Treatment of 3T3-L1 Adipocytes

Twenty-four hours before an experiment, 2 ml DMEM-FBS with 500 nM insulin was added to each dish of 3T3-L1 adipocytes. This concentration of insulin was maintained in subsequent incubations with serum-free DMEM and KRH buffer.

2.3.4 Restimulation of 3T3-L1 Adipocytes following Culture with Insulin Treatment

After incubation in serum-free DMEM, each dish of 3T3-L1 adipocytes was washed 3 times at 37 °C with 2 ml Krebs-Ringers-MES (KRM) buffer (salts as for KRH buffer plus MES, pH 6.0) before incubation in 1 ml MES with 25 mM D-glucose at 37 °C for 1 h. Each dish of cells was then washed and insulin-stimulated as before (*Methods 2.3.1*). Control dishes were maintained in KRH (with 25 mM D-glucose) instead of KRM buffer.

2.3.5 Insulin Treatment of Rat Adipocytes Maintained in Primary Culture

After 24 h culture, cells were washed with rat BSA-KRH buffer (*Methods 2.2.2*) containing 500 nM insulin in the absence or presence of 1 mM metformin as appropriate. After resuspension to 40% cytocrit, cells were incubated with or without 20 nM insulin, or with 500 nM insulin with or without 1 mM metformin.

2.4 Glucose Transporter Studies

2.4.1 Assay of 2-deoxy-D-glucose Uptake in 3T3-L1 Adipocytes

To each dish of 3T3-L1 adipocytes containing 0.95 ml KRH buffer was added 50 µl of 0.3 µCi 2-deoxy-D-[2,6-^{3}H]glucose (50 µM final concentration). Cells were incubated for 5 min at 37 °C before each dish was washed twice with 3 ml ice-cold KRH buffer. Each dish of cells was solubilized in 1 ml 1% (v/v) Triton X-100 before addition of 8 ml scintillation cocktail. Samples were counted in the ^{3}H channel (0-12 keV) of a liquid scintillation counter; standard counts were determined from 50 µl of 0.3 µCi 2-deoxy-D-[2,6-^{3}H]glucose in 1 ml 1% (v/v) Triton X-100. Uptake of 2-deoxy-D-glucose was taken to be linear over 5 min and expressed as pmoles transported per minute per dish (pmoles/min/dish).

2.4.2 Assay of 2-deoxy-D-glucose Uptake in Permeabilized 3T3-L1 Adipocytes

Each dish of 3T3-L1 adipocytes containing 0.95 ml AP-IC buffer was given 50 µl of radiolabelled sugar (50 nmoles 2-deoxy-D-glucose, 0.6 µCi 2-deoxy-D-[2,6-^{3}H]glucose, 0.12 µCi [U-^{14}C]sucrose). Cells were incubated for 5 min at 37 °C before each dish was washed twice with 3 ml ice-cold IC buffer. Cells from each dish were solubilized in 1 ml 1% (v/v) Triton X-100 before the addition of 8 ml scintillation cocktail. Samples were counted in a dual channel program for ^{3}H (0-12 keV) and ^{14}C (12-156 keV); standard counts were determined from 50 µl radiolabelled sugar in 1 ml 1% (v/v) Triton X-100. The uptake of [U-^{14}C]sucrose was used to determine the extent of non-specific uptake of 2-deoxy-D-glucose through permeabilized cell membrane.

2.4.3 ATB-BMPA Photolabelling of Cell Surface Glucose Transporters in 3T3-L1 Adipocytes

Each dish of 3T3-L1 adipocytes was washed 3 times with 2 ml KRH buffer at 18 °C before the addition of 290 µl 18 °C KRH buffer containing 200 µCi ATB-[2-^{3}H]BMPA. Following irradiation for 1 min in a Rayonet photochemical reactor, each dish was washed 4 times with 2 ml KRH buffer at 18 °C. Cells were solubilized in 1 ml detergent buffer (2% (w/v) Thesit, 5 mM $Na_2HPO_4.12H_2O$, pH 7.2, and 1 µg/ml antipain, aprotinin, leupeptin and pepstatin A) on ice for 20 min before centrifugation at 20 000 g_{max} for 20 min at 4 °C. The supernatant was subjected to GLUT1, and then GLUT4, immunoprecipitation (50 µl anti-serum conjugated to 5 mg protein A sepharose) for 2 h each at 4 °C on a rotating wheel. Immunoprecipitates were washed 3 times with 1 ml detergent buffer containing 1% (w/v) Thesit and once in 1 ml detergent buffer containing 0.1% (w/v) Thesit, before 160 µl sample buffer (*Methods 2.7.2*) was added for 20 min at room temperature. Samples were resolved on 10% SDS-PAGE gels. After staining and destaining, lanes from the gels were cut into sixteen 6.5 mm slices and dried individually in open scintillation vials in an 80 °C oven. Dried gel slices were solubilized with 500 µl 2% (v/v) NH_4OH in 30% (w/w) H_2O_2 in sealed vials at 80 °C, before ^{3}H counts were determined in 8 ml scintillation cocktail. A graph of slice number (*x*-axis) against d.p.m. (*y*-axis) was constructed. Radioactivity associated with the labelled transporter was determined by adding up the counts from the slices that formed the peak and subtracting the counts from a same number of slices that contained no label (background counts).

2.5 Immunoprecipitation and Assay of Kinase Enzymes

2.5.1 Assay for PI 3-K Activity in 3T3-L1 Adipocytes

Each dish of 3T3-L1 adipocytes was washed twice with 3 ml before solubilization in 1 ml of 5 mM $Na_2HPO_4.12H_2O$, pH 7.2, 0.4 mM Na_3VO_4, 1% (v/v) Triton X-100, and 1

μg/ml antipain, aprotinin, leupeptin and pepstatin A, for 20 min on ice before centrifugation at 20 000 g_{max} for 20 min. Insoluble fat was removed by passing lysate through 0.2 μm Minisart filters (Sartorius). Beforehand, anti-IRS-1 was bound to protein G sepharose (200 μl ID6 per 30 μl beads for 3 h at 4 °C). The beads were mixed with cell lysate (30 μl beads per sample) for 2 h at 4 °C. The beads were then washed twice with 12.5 mM $Na_2HPO_4.12H_2O$, pH 7.2, 154 mM NaCl, 1% (v/v) Triton X-100, 1 mM DL-dithiothreitol (DTT), then twice with 0.1 M Tris, pH 7.4, 0.5 M LiCl, 1 mM DTT, and finally twice with 10 mM Tris, pH 7.4, 0.1 M NaCl, 1 mM DTT (1 ml volume for each wash). As much buffer as possible was removed before the kinase activity was assayed.

For the PI 3-K assay, each sample was resuspended in 50 μl buffer (20 mM HEPES, pH 7.1, 0.4 mM EGTA, 0.4 mM $Na_2HPO_4.12H_2O$, 10 mM $MgCl_2.6H_2O$, 0.2 mg/ml phosphatidylinositol, 40 μM ATP and 5-10 μCi [γ-^{32}P]ATP). The samples were incubated with the phospholipid for 5 min at room temperature before the Mg^{2+} and ATP were added. After 20 min, 30 μl 4 M HCl was added to stop the reaction; 130 μl 1:1 (v/v) chloroform/methanol was then added, before the samples were vortexed and spun at 13 000 rpm for 10 min to separate the phases.

TLC polyester plates coated with silica gel (layer thickness 250 μm, particle size 5 to 17 μm, pore size 60 Å) were pre-treated with 0.91% (w/v) *trans*-1,2-diaminocyclohexane-N,N,N',N'-tetraacetic acid (CDTA) in 0.6% (v/v) 10 M NaOH, 66% (v/v) ethanol. Plates were soaked for 10 s and left to air-dry before baking in an 80 °C oven for 1 h. Samples from the lower phase (see above) were spotted onto the TLC plate. Lipids were then separated using the following solvent: 7.5 ml water, 3 ml 88% (v/v) formic acid, 0.375 g 2,6-di-*tert*-butyl-4-methylphenol (BHT), and 75 μl ethoxyquin mixed with 75 ml methanol, 60 ml chloroform, 45 ml pyridine and 12 g dissolved boric acid. After separation, the plates were dried before exposure to autoradiography film. Labelled phosphatidylinositol was then cut out and counted in 8 ml scintillation cocktail in the ^{32}P channel (5-1700 keV) of a liquid scintillation counter.

2.5.2 Assay for PKB Activity in 3T3-L1 Adipocytes

Each dish of 3T3-L1 adipocytes was washed twice with 3 ml ice-cold lysis buffer (50 mM HEPES, pH 7.6, 1% (v/v) Triton X-100, 1 mM Na_3VO_4, 10 mM NaF, 30 mM $Na_4P_2O_7$, 150 mM NaCl, 1 mM EDTA, 100 μM AEBSF, and 1 μg/ml antipain, aprotinin, leupeptin and pepstatin A) before solubilization in 1 ml. Samples were transferred to eppendorf tubes and left on ice for 10 min, before centrifugation at 14 000 rpm for 5 min at 4 °C. Insoluble fat was removed by passing lysate through 0.2 μm Minisart filters (Sartorius). PKB from each dish was immunoprecipitated by mixing lysate with 2 μg anti-Akt1(C-20) conjugated to 10 μl protein G sepharose for 2 h at 4 °C. Immunoprecipitates were washed 3 times with 1 ml lysis buffer and 3 times with 1 ml kinase assay buffer (50 mM Tris, pH 7.5, 10 mM $MgCl_2.6H_2O$). As much buffer as possible was removed before assaying for kinase activity.

Immunoprecipitates were incubated in 50 μl kinase assay buffer containing 1 mM DTT, 100 ng protein kinase A (PKA) inhibitor peptide, 25 μg protamine sulphate, 5 μM ATP and 2 μCi [γ-^{32}P]ATP for 5 min. The reaction was started by the addition of the radiolabelled ATP. Samples were incubated for 20 min at 30 °C, after which 50 μl supernatant was removed. To the remaining beads, 40 μl 2% (w/v) sodium dodecyl sulphate (SDS) was added for 10 min. The two supernatants were combined and from this, 20 μl was spotted onto a 2 cm × 2 cm area of P81 phosphocellulose paper (Whatman International Ltd., Maidstone, Kent). After the spots had dried, the phosphocellulose was washed 5 times with 500 ml 75 mM phosphoric acid in a sandwich box on a shaking table. The phosphocellulose was then rinsed once in water and once in acetone. Once dried, the phosphocellulose was put into scintillation vials containing 8 ml scintillation cocktail. Counts were determined using the ^{32}P channel (5-1700 keV) of a liquid scintillation counter. Background counts were determined from 10 μl protein G sepharose that was treated in the same way as the immunoprecipitates.

2.6 Subcellular Fractionation of Adipocytes

2.6.1 Subfractionation of 3T3-L1 Adipocytes

Each dish of 3T3-L1 adipocytes was washed twice with 3 ml ice-cold TES (10 mM Tris, pH 7.2, 5 mM EDTA, 250 mM sucrose, 100 μM AEBSF, and 1 μg/ml antipain, aprotinin, leupeptin and pepstatin A) before the cells were removed in 1 ml TES with a cell scrapper. Phosphatase inhibitors were included in TES for those studies in which PKB was assayed (1 mM Na_3VO_4, 10 mM NaF and 30 mM $Na_4P_2O_7$). Following 15 strokes in a 5 ml homogenizer, the homogenate was subjected to sequential centrifugation with a TLA-100.3 fixed angle rotor (Beckman TL-100 ultracentrifuge) at 4 °C. The first spin was at 15 000 rpm (12 000 g_{max}) for 15 min to obtain the crude plasma membrane pellet. The supernatant was then spun at 17 000 rpm (16 000 g_{max}) for 15 min to pellet the high density microsomes (HDM). The supernatant from this was spun at 100 000 rpm (541 000 g_{max}) for 17 min to obtain the low density microsomes (LDM). The crude plasma membrane pellet was resuspended in 300 μl TES and spun at 35 000 rpm (105 000 g_{max}) for 20 min (TLS-55 swinging bucket rotor, Beckman TL-100) on 600 μl of a 38% sucrose cushion (1.12 M sucrose, 10 mM Tris, pH 7.2, 10 mM EDTA). The sucrose layer was then spun with 2 ml TES at 37 000 rpm (74 000 g_{max}) for 9 min (TLA-100.3 rotor) to obtain the plasma membrane fraction (PM). Membrane fractions were resuspended in 5 mM $Na_2HPO_4.12H_2O$, pH 7.2, and assayed for protein content.

2.6.2 Subfractionation of Rat Adipocytes

After washing 2 ml 40% cells once in TES at 20 °C, they were resuspended in 2 ml TES at 18 °C. Following 10 strokes in a 55 ml homogenizer, the homogenate was spun at 1000 rpm for 1 min. From this, the infranatant was removed with a syringe and needle (21 g) before it was subjected to sequential centrifugation with a TLA-100.3 rotor (Beckman TL-100). The first spin at 18 000 rpm (18 000 g_{max}) for 20 min

gave the crude plasma membrane pellet. The supernatant was taken and spun at 30 000 rpm (49 000 g_{max}) for 30 min to obtain the HDM fraction. The remaining supernatant was spun at 100 000 rpm (541 000 g_{max}) for 17 min to obtain the LDM fraction. The crude plasma membrane pellet was homogenized in 2 ml TES with 5 strokes in a 10 ml homogenizer before recentrifugation at 18 000 rpm for 20 min. The PM fraction was then obtained as above (*Methods 2.6.1*). Membrane fractions were resuspended in TES and assayed for protein content.

2.7 Protein Biochemistry Techniques

2.7.1 Bio-Rad Protein Assay

The Bio-Rad Protein Assay (Bio-Rad Laboratories Ltd., Hemel Hempstead, Hertfordshire) was used to quantitate the protein content of samples. Samples were made up to 160 µl with 5 mM $Na_2HPO_4.12H_2O$, pH 7.2, and mixed with 40 µl Dye Reagent Concentrate (Bio-Rad) in the wells of Microplates (Labsystems, Helsinki, Finland). A calibration curve was constructed using 1-5 µg BSA. Absorption at 595 nm was measured in a spectrophotometer.

2.7.2 SDS-Polyacrylamide Gel Electrophoresis (SDS-PAGE)

Protein samples were mixed with sample buffer (2% (w/v) SDS, 115 mM Tris, pH 6.8, 1 mM EDTA, 10% (v/v) glycerol, 400 µg/ml bromophenol blue and 10% (v/v) 2-mercaptoethanol) such that the volume of the latter was at least 75% of the total volume, before heating at 95 °C for 5 min. Four-times and two-times concentrates of sample buffer were used for larger volumes of protein samples.

Discontinuous polyacrylamide gels (lower resolving gel and upper stacking gel) were set up on either the Mini-PROTEAN II electrophoresis cell or the PROTEAN II xi slab cell (both Bio-Rad). Gels were prepared according to the manuals with the

following solutions: acrylamide/bis (30% T, 2.7% C) (National Diagnostics, Flowgen, Lichfield, Staffordshire), resolving gel buffer (1.5 M Tris, pH 8.8, 0.4% (w/v) SDS), stacking gel buffer (0.5 M Tris, pH 6.8, 0.4% (w/v) SDS), 10% (w/v) ammonium persulfate (Bio-Rad) and N,N,N',N'-tetramethylethylenediamine (TEMED) (Bio-Rad). For the Mini-PROTEAN II cell, the resolving gel was made to 0.375 M Tris and 0.1% (w/v) SDS with acrylamide concentrations of 7-13%, while the stacking gel was made to 0.125 M Tris and 0.1% (w/v) SDS with 5% acrylamide. For the PROTEAN II cell, the method was modified to give 0.5 M Tris and 0.133% (w/v) SDS for the resolving gel, and 0.156 M Tris, 0.125% (w/v) SDS and 6.375% acrylamide for the stacking gel.

After the upper and lower buffer chambers were filled with electrode buffer (0.025 M Tris, 0.1% (w/v) SDS, 0.192 M glycine, pH 8.3), protein samples were loaded using either a Gilson pipetter or a Hamilton syringe. Gels were run until the dye front had reached the bottom. After electrophoresis, protein bands were detected by staining for 30 min with 0.2% (w/v) Coomassie Blue R-250 in fixative (30% (v/v) methanol, 10% (v/v) glacial acetic acid) and destaining for a few hours with fixative only.

2.7.3 Electrotransfer of Protein from SDS-PAGE Gels to Nitrocellulose

After SDS-PAGE, the 1.5 mm gel was soaked in transfer buffer (0.0375% (w/v) SDS, 48 mM Tris, 39 mM glycine, pH 8.8) for 5 min. The gel was laid on top of a piece of BioTrace® nitrocellulose blotting membrane (Gelman Sciences Ltd., Northampton) and sandwiched between two layers (nine sheets thick) of electrode paper (Pharmacia Biotech, St. Albans, Hertfordshire). The nitrocellulose and electrode paper were soaked in transfer buffer beforehand with air bubbles smoothed out. The assembly was placed between the pre-wet electrode plates of a Multiphor II NovaBlot electrophoretic transfer unit (Pharmacia). Current was run at 0.8 mA/cm^2 for 105 min. After electrotransfer, the nitrocellulose was rinsed in water before staining with 0.1% (w/v) Ponceau S in 3% (w/v) trichloroacetic acid.

2.7.4 Western Blotting

The nitrocellulose was rinsed briefly in TBS-T (10 mM Tris, pH 7.4, 0.9% (w/v) NaCl, 0.1% (v/v) Tween 20) before blocking with 5% (w/v) Marvel dried skimmed milk (Premier Beverages, Stafford) in TBS-T for 30 min. After a brief wash, the nitrocellulose was incubated with the primary antibody (1:1000 or 1:4000) in TBS-T with 3% (w/v) Marvel for 90 min. After 6× 3 min washes with TBS-T, the nitrocellulose was incubated with the secondary antibody (1:4000 anti-rabbit (Sigma), anti-goat (Sigma) or anti-mouse (Amersham) IgG conjugated to horseradish peroxidase) in TBS-T with 3% (w/v) Marvel for 30 min. After 6× 3 min washes with TBS-T, the nitrocellulose was incubated for 1 min with ECL detection reagent (Amersham). The nitrocellulose was placed between two transparency sheets before exposure to autoradiography film.

All incubations were carried out at room temperature on a shaking table. For phosphotyrosine immunoblotting, 3% (w/v) and 1% (w/v) BSA were used in the blocking and antibody incubations respectively.

2.8 Expression and Purification of a GST Fusion Protein

2.8.1 PH Domain/GST Fusion Protein Construct

The vector pGEX-2T (Smith and Johnson, 1988) encoding the fusion protein of glutathione *S*-transferase and PH domain (with a thrombin cleavage site) was a gift from Dr Kamran Salim (Ludwig Institute for Cancer Research, UCL, London). The PH domain was amplified from rat IRS-1 cDNA and extended at the C-terminal end from residue 120. The sequence is as follows:

1 MASPPDTDGF SDVRKVGYLR KPKSMHKRFF VLRAASEAGG PARLEYYENE

51 KKWRHKSSAP KRSIPLESCF NINKRADSKN KHLVALYTRD EHFAIAADSE

101 AEQDSWYQAL LQLHNRAKAH HDGAGGG

2.8.2 Transformation of Bacterial Cells

Epicurian Coli® SURE® competent cells (Stratagene, La Jolla, California) were transformed with the pGEX-2T vector. The cells were thawed before 100 µl was aliquoted into a 1.9 ml eppendorf and mixed with 1.7 µl of 1.42 M β-mercaptoethanol. The cells were incubated on ice for 10 min with gentle swirling every 2 min, before 10 ng plasmid was added for 30 min on ice. The cells were then heated at 42 °C for 45 s before incubation for 2 min on ice. Pre-heated (42 °C) 0.9 ml SOC medium (20 g/l tryptone, 5 g/l yeast extract, 0.5 g/l NaCl, 10 mM $MgCl_2.6H_2O$, 10 mM $MgSO_4$ and 20 mM glucose) was added before the cells were shaken at 37 °C for 1 h. The cells (5 µl in 200 µl SOC medium) were spread on 100 mm LB-ampicillin agar (10 g/l NaCl, 10 g/l tryptone, 5 g/l yeast extract, 20 g/l agar, pH to 7.0 with 5 M NaOH, 50 mg/l ampicillin) plates and incubated at 37 °C overnight.

2.8.3 Culture and Lysis of Bacterial Cells

An aliquot of 5 ml LB Broth (50 µg/ml ampicillin) was inoculated and shaken at 37 °C overnight. The culture was then transferred to 500 ml LB Broth (100 µg/ml ampicillin) before shaking at 37 °C during the day (about 7 h). From this culture, 100 ml was added to 1000 ml LB Broth (100 µg/ml ampicillin), which was then shaken at 37 °C until absorbance at 600 nm was 0.6-1.0. Fusion protein production was induced by incubation with 0.1 mM isopropyl β-D-thiogalactopyranoside (IPTG) at 25 °C overnight. The cells were pelleted by spinning at 6000 rpm for 10 min at 4 °C before resuspension in 12.5 ml ice-cold lysis buffer (50 mM Tris, 50 mM NaCl, 5 mM $MgCl_2.6H_2O$, 1 mM DTT, 1 mM phenylmethylsulfonyl fluoride (PMSF), pH 7.5). The cells were sonicated on ice with 8× 10 s pulses, using a 19 mm diameter probe. The lysed cells were spun at 30 000 rpm for 30 min at 4 °C and the supernatant saved.

2.8.4 Purification and Cleavage of GST Fusion Protein

The supernatant from lysed cells was mixed with 1 ml glutathione sepharose 4B beads (Pharmacia) (equilibrated with several bed volumes of lysis buffer) for 30 min at 4 °C in 2× 12 ml polystyrene conical test tubes (Sarstedt). The beads were then washed 3 or 4 times with 10 ml lysis buffer (minus PMSF) per tube. The beads were then equilibrated with one bed volume of thrombin resuspension buffer (TRB) (50 mM Tris, 150 mM NaCl, 5 mM $MgCl_2.6H_2O$, 2.5 mM $CaCl_2.2H_2O$, 1 mM DTT, pH 8). The fusion protein was cleaved with 1.5 units thrombin per ml beads at 4 °C overnight. The supernatant was collected and mixed with 10 µl p-aminobenzamidine agarose beads at 4 °C for 30 min (to bind thrombin); the supernatant from this was saved. The glutathione sepharose beads were washed 2 or 3 times with TRB to remove any remaining unbound cleaved protein. The washes were combined with the supernatant and concentrated with Microsep™ centrifugal concentrators (Flowgen). PD-10 columns (Pharmacia) were used to replace TRB with the buffer of choice. The purity of the final product was determined by SDS-PAGE.

2.9 Analysis of Data

Data was plotted on GraphPad PRISM™ (Version 2.0) (GraphPad Software, Inc., San Diego, CA). Statistical analysis was carried out using the PRISM™ program with unpaired t tests (two-tail P values).

Autoradiograms were scanned with a Bio-Rad GS-670 Imaging Densitometer. The density of protein bands were determined using Molecular Analyst™ Software (Bio-Rad).

3.0 RESULTS AND DISCUSSION

3.1 Studies with the PH Domain of IRS-1

3.1.1 Searching for the Binding-protein of the IRS-1 PH Domain

So far, the only protein found to associate with the PH domain of IRS-1 is Gβγ (Touhara *et al.*, 1994). However, the functional significance of this interaction has not been demonstrated *in vivo*. Further, though the tyrosine-phosphorylated residues of IRS-1 are known to activate multiple signalling proteins - including PI 3-K, which appears to be involved in insulin-regulated glucose uptake - the purpose of the PH domain is not as clear (reviewed by Keller and Lienhard, 1994). Thus, in an attempt to further understand the role of the IRS-1 PH domain in insulin signalling and in relation to stimulation of glucose transport, cell lysate from 3T3-L1 adipocytes was screened for a binding-protein for this domain. The identification of such a protein may help determine the function of the IRS-1 PH domain. The probe used was an IRS-1 PH domain construct, produced using the GST fusion protein system (*Methods 2.8*). Separate experiments had demonstrated that the protein was functional, as it was able to attenuate the tyrosine phosphorylation of IRS-1 by the insulin receptor in permeabilized 3T3-L1 adipocytes (*Results and Discussion 3.1.3*). Thus, these experiments indicate that the bacterially-expressed IRS-1 PH domain has a similar conformation to that *in vivo*. Two techniques were used to attempt to identify a PH domain-binding protein. The first involved a modification of the Western blotting procedure, where biotinylated IRS-1 PH domain was used to detect binding-proteins on nitrocellulose. The second involved affinity chromatography with the GST fusion protein of the IRS-1 PH domain immobilized on glutathione sepharose beads.

A probe for proteins that bind the IRS-1 PH domain was made by covalently linking biotin to the IRS-1 PH domain protein from purified GST-PH domain. The biotinylation reagent was ImmunoPure® NHS-LC-Biotin (sulfosuccinimidyl-6-

(biotinamido)-hexanoate) (Pierce & Warriner (UK) Ltd., Chester). It was linked by incubating a 100-fold excess with IRS-1 PH domain in 0.1 M $Na_2B_4O_7.10H_2O$, pH 8.5, at 4 °C for 24 h. Unreacted biotin was removed by the addition of Tris and dialysis with PBS. Biotinylated IRS-1 PH domain was detected with streptavidin linked to horseradish peroxidase (streptavidin-HRP) (Figure 3.1.1).

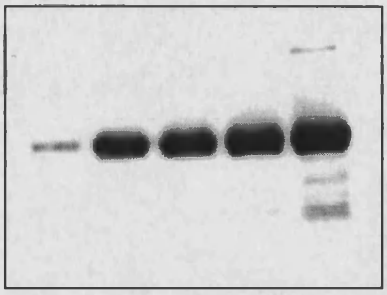

10 100 250 500 1000

Figure 3.1.1. Detection of Biotinylated IRS-1 PH Domain with Streptavidin Linked to Horseradish Peroxidase.

Biotinylated IRS-1 PH domain (**10**, **100**, **250**, **500** and **1000** ng) was resolved on a 13% SDS-PAGE gel, transferred to nitrocellulose and incubated with streptavidin-HRP (1:4000) in TBS, before detection with ECL Western blotting detection reagent (*Methods 2.7*).

To identify proteins that may bind to the IRS-1 PH domain, lysate from 3T3-L1 adipocytes was run on a SDS-PAGE gel and transferred to nitrocellulose, before incubation with biotinylated IRS-1 PH domain and then streptavidin-HRP (Figure 3.1.2). For the controls, samples on nitrocellulose were either incubated with streptavidin-HRP only, or they were incubated with an excess of unbiotinylated IRS-1 PH domain before incubation with the biotinylated probe. No difference was observed between the control and experimental samples. As streptavidin-HRP was able to detect protein on its own, attempts were made to block any biotin-containing proteins on the nitrocellulose prior to incubation with biotinylated IRS-1 PH domain, using either anti-biotin antibody (Sigma) or streptavidin (Pierce) (both 1:4000). Neither method prevented the bands from appearing (data not shown).

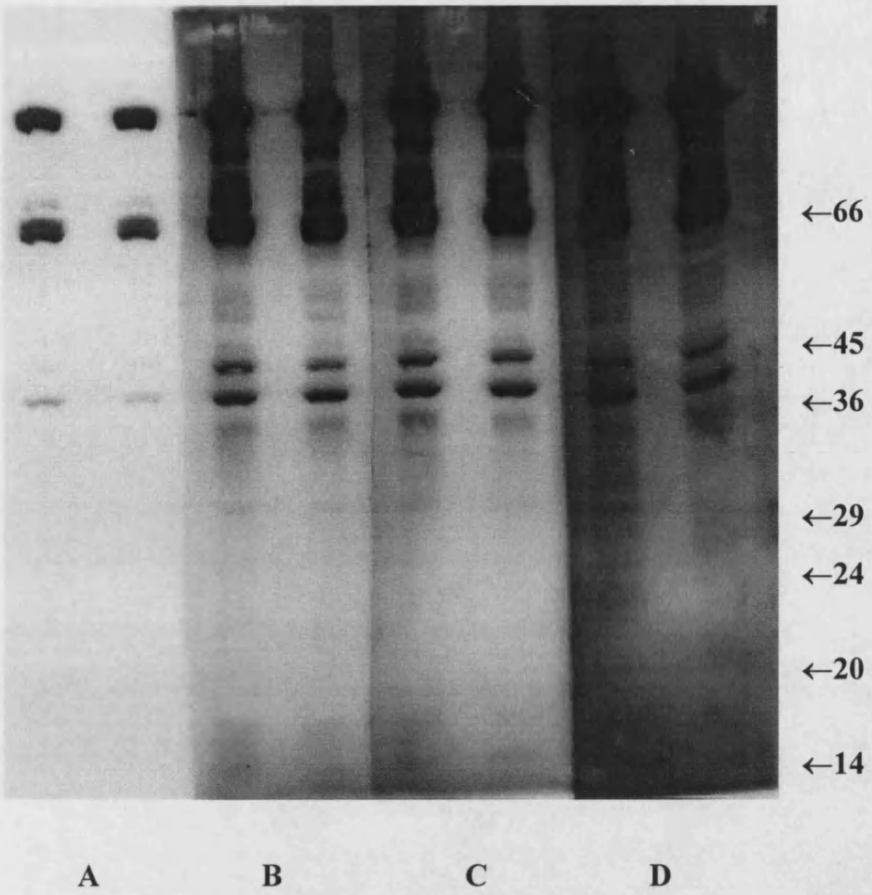

Figure 3.1.2. Western Blotting of Lysate from 3T3-L1 Adipocytes with Biotinylated IRS-1 PH Domain.

Each dish of 3T3-L1 adipocytes was solubilized in 500 µl sample buffer, of which 50 µl was run on a 10% SDS-PAGE gel before transfer to nitrocellulose (*Methods 2.7.2* and *2.7.3*). Three duplicate lanes were prepared and blocked with 5% (w/v) Marvel in TBS (no Tween 20) for 30 min before the following incubations: (**A**) Incubation with streptavidin-HRP only; (**B**) Incubation with 1:100 IRS-1 PH domain for 30 min and then 1:1000 biotinylated IRS-1 PH domain for 90 min; (**C**) As for **B**, except pre-incubation with 1:45 IRS-1 PH domain; (**D**) Incubation with 1:1000 biotinylated IRS-1 PH domain for 90 min. After extensive washing with TBS, samples were incubated with 1:4000 streptavidin-HRP for 30 min before detection with ECL Western blotting detection reagent (*Methods 2.7.4*). All incubations were in 1% (w/v) BSA/TBS. Markers show molecular weights in kDa.

An advantage of this modified Western blotting technique is that a signal from the biotinylated probe can be amplified using streptavidin linked to horseradish peroxidase. However, a PH domain-binding protein was not detected with this method. It is difficult to determine whether failure was due to a fault with the technique, as the ability to identify Gβγ as a control was not examined. Since the

IRS-1 PH domain has been shown to be functional, then the cause of the failure to detect a binding-protein is probably not due to the probe itself. Using a similar method, Wang *et al.* (1994) resolved purified G protein β-subunit (Gβ) on SDS-PAGE before transfer to nitrocellulose and detection with a PH domain construct. Thus, the use of purified protein instead of cell extract may aid detection as more of the desired protein is present. Further, in this study, the inability to detect Gβ itself in the cell extract may reflect the low specificity of the interaction between this protein and the IRS-1 PH domain. Thus, the binding of Gβγ with the GST fusion protein of the IRS-1 PH domain is weaker than with that of the β-Ark PH domain (Touhara *et al.*, 1994). Another possible reason for the failure to detect novel proteins in the cell extract may be the disruption of protein conformation caused by denaturation with SDS treatment. Thus, a way to overcome this problem may be to run proteins on polyacrylamide gels under non-denaturing conditions prior to transfer to nitrocellulose.

An alternative method to identify proteins that bind the PH domain was to mix immobilized IRS-1 PH domain with cell lysate, before elution with sample buffer and detection by Coomassie Blue stain following SDS-PAGE. GST or GST-PH domain were bound to glutathione sepharose beads before incubation with lysate from 3T3-L1 adipocytes. Originally, a band between 29 and 36 kDa and another two between 24 and 29 kDa were detected in GST-PH domain beads, but not in GST beads. To examine the possibility that these bands were degradation products of GST-PH domain, the experiment was repeated again, in which a 100-fold excess of unbound PH domain was present during the incubation of bound GST-PH domain with cell lysate (Figure 3.1.3). This procedure did not eliminate the additional bands, indicating that they were indeed likely to be degradation products of the GST-PH domain.

This method of searching for a binding-protein for the IRS-1 PH domain - where a GST fusion protein of the IRS-1 PH domain was immobilized on glutathione sepharose beads - was advantageous over the previous method in that it did not require the denaturation of cellular proteins. Also, it had the potential to allow the mixing of a relatively large amount of cell lysate with the IRS-1 PH domain construct.

Thus, this feature was also an advantage over the earlier method, in which there is a limit to the volume of protein that can be loaded onto a SDS-PAGE gel.

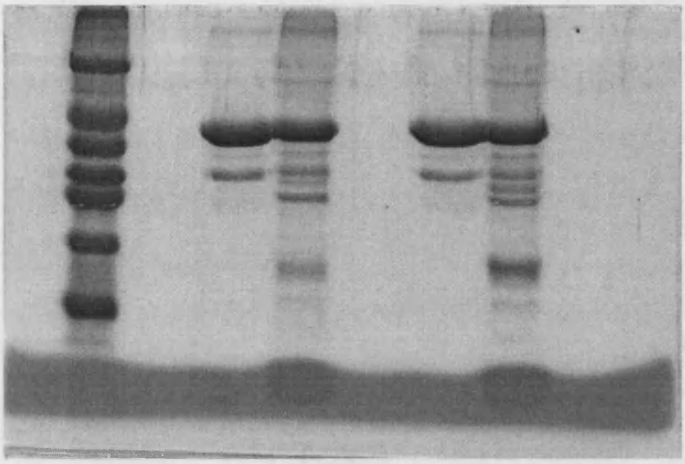

Figure 3.1.3. Incubation of GST-PH Domain Immobilized on Glutathione Sepharose Beads with Lysate from 3T3-L1 Adipocytes.

GST-PH domain was produced from a litre culture and immobilized on 500 µl glutathione sepharose beads (*Methods 2.8*). Lysate was produced by solubilizing each dish of 3T3-L1 adipocytes in 1 ml lysis buffer (20 mM Tris, 150 mM NaCl, 1 mM EDTA, 1% (v/v) Triton X-100, 1 mM PMSF, 1 mM Na_3VO_4, and 1 µg/ml antipain, aprotinin, leupeptin and pepstatin A) for 30 min on ice before centrifugation at 49 000 g_{max} for 30 min. To 2.5 µl beads was added 10 ml lysate; incubation was at 4 °C for 24 h on a rotating wheel. The beads were then washed 5 times with the lysis buffer. Protein was eluted with 30 µl sample buffer and resolved on a 13% SDS-PAGE gel (*Methods 2.7.2*). GST-PH domain was either: (**A** and **C**) Untreated with cell lysate; (**B**) Mixed with cell lysate; (**D**) Mixed with cell lysate in the presence of a 100-fold excess of unbound PH domain protein. Molecular weight (**MW**) markers (from the top) are: 66, 45, 36, 29, 24, 20 and 14 kDa.

However, no binding-proteins for the IRS-1 PH domain were detected with this technique. A possible reason is that the detection of proteins with Coomassie Blue stain is less sensitive than by Western blotting. Indeed, Konishi *et al.* (1995) were able to find an association between PKC and a GST fusion protein of the PH domain of PKB by both using cell lysate from cells overexpressing PKC and by detection with PKC antibodies. Thus, a way of overcoming the problem may be to use even more cell lysate from 3T3-L1 adipocytes. However, with the quantities used in this study, a

faint background of non-specifically bound protein was already observed, though this may be eliminated by pre-incubation of lysate with glutathione sepharose beads bound to GST only. As a potential control, any proteins bound to the IRS-1 PH domain could be immunoblotted with antibodies against PKC or Gβγ.

Despite the lack of success in finding a binding-protein for the IRS-1 PH domain, the absence of such a protein cannot be ruled out. One of the reasons for why it cannot be said that a PH domain-binding protein does not exist, is that the techniques used did not have a positive control to check their feasibility. Also, further modifications of the described protocols can be made. Given that the binding of phosphoinositides and inositol phosphates to the PH domain have been observed (Harlan *et al.*, 1994, and Lemmon *et al.*, 1995), it would also be worth investigating if this interaction occurs for the IRS-1 PH domain.

3.1.2 Investigating the Role of the IRS-1 PH Domain in Insulin-stimulated Glucose Uptake

A proposed role of the IRS-1 PH domain in insulin signalling is the targeting of activated PI 3-K - bound to IRS-1 - to an intracellular membrane site so that it can enhance GLUT4 exocytosis. This idea is supported by two observations. First, insulin-activated PI 3-K is present mainly at an intracellular membrane location - the LDM - in 3T3-L1 adipocytes (Yang *et al.*, 1996). Second, insulin stimulation of 3T3-L1 adipocytes leads to the appearance of tyrosine-phosphorylated IRS-1 in the LDM, together with translocation of p85 to the same compartment (Ricort *et al.*, 1996). To investigate the possibility that the IRS-1 PH domain acts to target IRS-1 to the LDM fraction, a method of blocking the function of the PH domain of endogenous IRS-1 in 3T3-L1 adipocytes was required. In this study, one of two compounds were introduced into permeabilized 3T3-L1 adipoyctes. The first was the IRS-1 PH domain, which could compete with endogenous IRS-1 for endogenous binding sites. The second was Ins 1,4,5-P_3, which could bind to the PH domain of endogenous IRS-1. This inositol phosphate is known to bind the PH domain of PLC δ_1 (Lemmon *et*

al., 1995). The insulin-stimulated cellular responses that were measured following treatment with these compounds were glucose uptake and PI 3-K activity in the LDM.

If the PH domain does target the IRS-1/PI 3-K complex to the LDM where it may act to cause GLUT4 translocation, then the presence of exogenous IRS-1 PH domain - which may compete for endogenous binding sites - could result in a reduction in insulin-stimulated glucose transport. Permeabilized 3T3-L1 adipocytes were pre-incubated with 3.5 μM IRS-1 PH domain for 15 min prior to a 10 nM insulin stimulation for 20 min (Figure 3.1.4). Insulin-stimulated 2-deoxy-D-glucose transport was the same regardless of whether the permeabilized cells were pre-treated with IRS-1 PH domain or not.

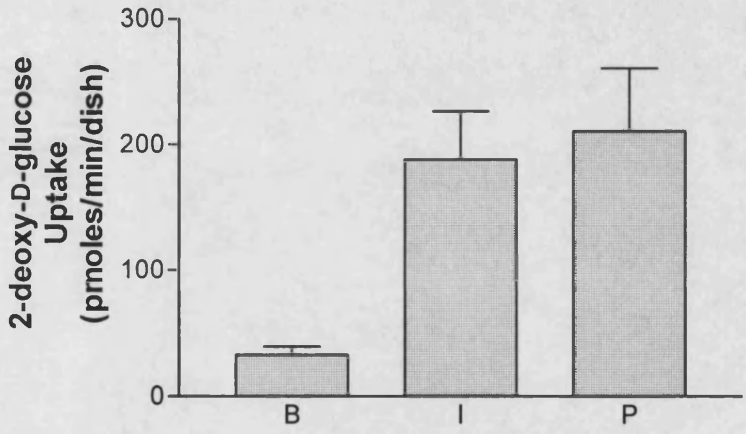

Figure 3.1.4. Insulin-stimulated 2-deoxy-D-Glucose Uptake in Permeabilized 3T3-L1 Adipocytes Following Incubation with IRS-1 PH Domain.

Each dish of 3T3-L1 adipocytes was permeabilized and pre-incubated for 15 min before treatment without (**B**) or with (**I**) 10 nM insulin for 20 min (*Methods 2.3.2*); one group was pre-incubated with 3.5 μM IRS-1 PH domain prior to insulin stimulation (**P**). Uptake of 2-deoxy-D-glucose was measured as in *Methods 2.4.2*. Values are the means ± S.E.M. from three independent experiments done in duplicate (n = 6).

A possible alternative method of blocking the function of the IRS-1 PH domain, and perhaps insulin-stimulated glucose uptake, is the introduction of Ins 1,4,5-P_3 into the cell. Insulin-stimulated 2-deoxy-D-glucose transport was measured in permeabilized 3T3-L1 adipocytes following pre-incubation with Ins 1,4,5-P_3 (45 μg per dish of cells)

(Figure 3.1.5). Again, attenuation of the insulin-stimulated (10 nM for 20 min) response was not observed.

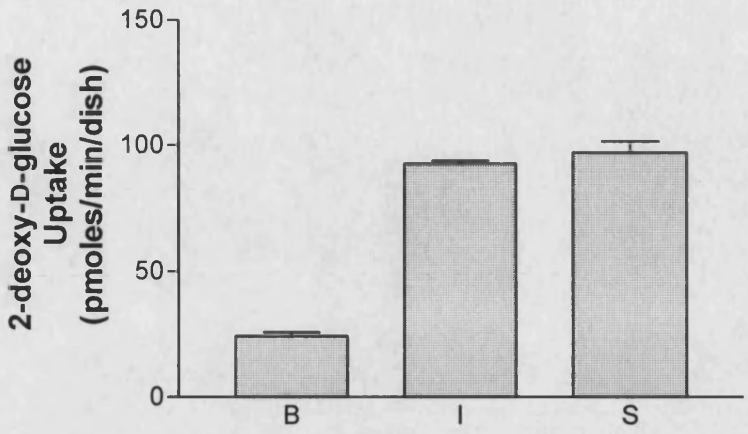

Figure 3.1.5. Insulin-stimulated 2-deoxy-D-Glucose Uptake in Permeabilized 3T3-L1 Adipocytes Following Incubation with Inositol 1,4,5-trisphosphate.

3T3-L1 adipocytes were treated as in Figure 3.1.4, except that the pre-incubation was with 45 μg inositol 1,4,5-trisphosphate per dish (**S**). Values are the means ± S.E.M. from two independent experiments done in duplicate (n = 4).

Thus, the pre-incubation of permeabilized 3T3-L1 adipocytes with either IRS-1 PH domain or Ins 1,4,5-P_3 does not appear to affect subsequent insulin-stimulated 2-deoxy-D-glucose uptake. The failure to see an effect was not likely to be due to an inadequacy of the cell permeabilization procedure, as the IRS-1 PH domain was able to attenuate insulin-stimulated IRS-1 phosphorylation in similarly permeabilized 3T3-L1 adipocytes (*Results and Discussion 3.1.3*). A possibility is that either compound was not sufficient in quantity to have an effect on the insulin-stimulated response. Though a submaximal stimulation with 10 nM insulin was used in the experiments, the use of even lower insulin doses may be beneficial. Also, although the binding of PI 4,5-P_2 and Ins 1,4,5-P_3 to the PH domain have been identified (Harlan *et al.*, 1994, and Lemmon *et al.*, 1995), the binding of these compounds to the IRS-1 PH domain has not been described. Thus, it is possible that Ins 1,4,5-P_3 may not interact with the IRS-1 PH domain *in vivo*.

Another approach to determine if the PH domain targets IRS-1/PI 3-K to the LDM was to measure the PI 3-K activity in that fraction from insulin-stimulated permeabilized 3T3-L1 adipocytes pre-incubated with IRS-1 PH domain (Figure 3.1.6). An insulin treatment at 10 nM for 10 min was determined to cause maximal recruitment of p85α to the microsomal fraction (Nave *et al.*, 1996a). This level of stimulation led to activity in the LDM which was the same regardless of whether the insulin-stimulated cells were pre-treated with IRS-1 PH domain or not.

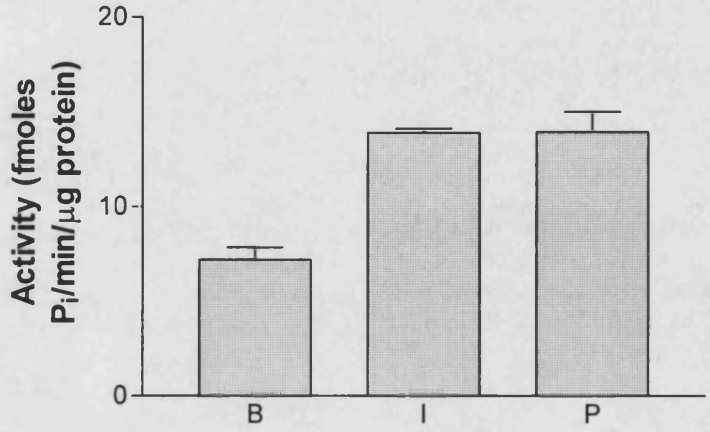

Figure 3.1.6. PI 3-K Activity in the LDM Fraction from Insulin-stimulated Permeabilized 3T3-L1 Adipocytes Following Incubation with IRS-1 PH Domain.

Each dish of permeabilized 3T3-L1 adipocytes was pre-incubated for 20 min before treatment without (**B**) or with (**I**) 10 nM insulin for 10 min (*Methods 2.3.2*); one group was pre-incubated with 17 μM IRS-1 PH domain prior to insulin stimulation (**P**). The cells were homogenized and subfractionated to obtain the LDM (*Methods 2.6.1*). Protein samples of 0.8 μg were assayed for PI 3-K activity (*Methods 2.5.1*). Values are the means from a single experiment done in duplicate. Error bars show Min and Max values.

Though the translocation of p85 to the microsomal membranes upon insulin stimulation of 3T3-L1 adipocytes has been identified, the mechanism involved was not investigated (Nave *et al.*, 1996a, and Ricort *et al.*, 1996). However, consistent with the role of IRS-1 in targeting PI 3-K to an intracellular membrane site is the appearance of tyrosine-phosphorylated IRS-1 in the LDM fraction upon stimulation of 3T3-L1 adipocytes with insulin, but not with PDGF (Ricort *et al.*, 1996). In this study however, the presence of exogenous IRS-1 PH domain did not attenuate insulin-

stimulated PI 3-K activity in the LDM fraction of permeabilized 3T3-L1 adipocytes. It is difficult to interpret the cause of this effect. First, it is not known if the quantity of IRS-1 PH domain was sufficient to affect p85 translocation. Second, and most importantly, it needs to be established that the IRS-1 PH domain can associate with the LDM. This could be achieved by introducing biotinylated IRS-1 PH domain or the IRS-1 PH domain as a GST fusion protein into permeabilized 3T3-L1 adipocytes prior to detection in subcellular fractions with streptavidin or a GST antibody. Further, p85 exists in the LDM of basal 3T3-L1 adipocytes, where tyrosine phosphorylated IRS-1 is absent (Ricort *et al.*, 1996). Thus, this observation argues against membrane-association via IRS-1, since p85 can only interact with IRS-1 in the tyrosine-phosphorylated state. Nevertheless, another possibility is that the PH domain targets IRS-1 to the LDM so that it can activate p85 already present there. If this idea is correct, exogenous IRS-1 PH domain should also inhibit this process.

Thus, using the methods described in this study, a role for the IRS-1 PH domain in enabling insulin-stimulated PI 3-K activity to occur in the LDM of 3T3-L1 adipocytes was not established. However, it is necessary to determine if the IRS-1 PH domain is able to interact with the LDM fraction at all, and if so, if it could compete for binding sites with IRS-1. Further, the nature of p85 is such that it has several N-terminal domains that are not involved in the interaction with p110 (Kapeller and Cantley, 1994). These regions could be important for membrane-association.

3.1.3 Attenuation of Insulin-stimulated Tyrosine Phosphorylation of IRS-1

Another proposed role for the PH domain is to target IRS-1 to the plasma membrane. This is based on two observations. First, an interaction between a PH domain and PI 4,5-P_2 has been described (Harlan *et al.*, 1994). Second, deletion of the PLC δ_1 PH domain prevents the protein from associating with the plasma membrane (Paterson *et al.*, 1995). Further, studies by other groups indicate that the PH domain of IRS-1 is important for its phosphorylation by the insulin receptor (Myers Jr. *et al*, 1995, and

Voliovitch, *et al.*, 1995). Thus, these findings have important implications for insulin-regulated glucose uptake. If IRS-1 is unable to localize at the plasma membrane near the insulin receptor due to the absence or disruption of its PH domain, then this defect may affect insulin-stimulated glucose transport. However, it has been shown earlier in this study (*Results and Discussion 3.1.2*) that the presence of exogenous IRS-1 PH domain was unable to perturb insulin-stimulated glucose uptake in permeabilized 3T3-L1 adipocytes. Thus, further experiments were undertaken to eliminate the possibility that the result was due to a fault with the IRS-1 PH domain protein. If the bacterially-expressed protein is found to be able to affect insulin-stimulated phosphorylation of IRS-1 in permeabilized 3T3-L1 adipocytes, then the result would indicate that the IRS-1 PH domain is functional.

By introducing excess IRS-1 PH domain into permeabilized 3T3-L1 adipocytes prior to insulin stimulation, one might expect to see a reduction in IRS-1 phosphorylation, as endogenous IRS-1 would compete with exogenous PH domain for binding sites at the plasma membrane. Initial experiments (Figure 3.1.7) in which permeabilized cells were pre-incubated with 3.5 μM IRS-1 PH domain prior to stimulation with 100 nM insulin for 10 min demonstrated no attenuation of IRS-1 tyrosine phosphorylation by the insulin receptor. However, by shortening the duration of insulin treatment, disruption of insulin-stimulated IRS-1 phosphorylation by the IRS-1 PH domain could be observed (Figure 3.1.8). Pre-treatment with 10 μM IRS-1 PH domain prior to stimulation with 100 nM insulin for 2 min led to a phosphorylated IRS-1 band with an intensity that was 43.1% of that from control insulin-stimulated cells (after subtraction of the value for the band from basal cells). A similar experiment was carried out, in which permeabilized cells were pre-incubated with 3.5 μM IRS-1 PH domain (Figure 3.1.9). Attenuation of IRS-1 phosphorylation was also seen, confirming that it was the duration of insulin treatment in the initial experiments that was responsible for the lack of observed effect.

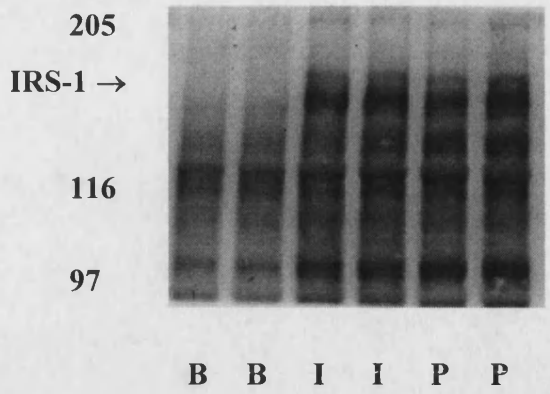

Figure 3.1.7. Insulin-stimulated Tyrosine Phosphorylation of IRS-1 Following the Introduction of IRS-1 PH Domain into Permeabilized 3T3-L1 Adipocytes.

Each dish of 3T3-L1 adipocytes was permeabilized and pre-incubated for 15 min before a further 10 min incubation without (**B**) or with (**I**) 100 nM insulin (*Methods 2.3.2*); one group was pre-incubated with 3.5 μM IRS-1 PH domain prior to insulin stimulation (**P**). Each dish of cells was immediately solubilized in 200 μl boiling-hot sample buffer (with 1 mM Na_3VO_4) before heating at 100 °C for 5 min and sonication. Samples were resolved on a 7% SDS-PAGE gel, transferred to nitrocellulose and immunblotted with anti-phosphotyrosine (*Methods 2.7*). Markers show molecular weights in kDa.

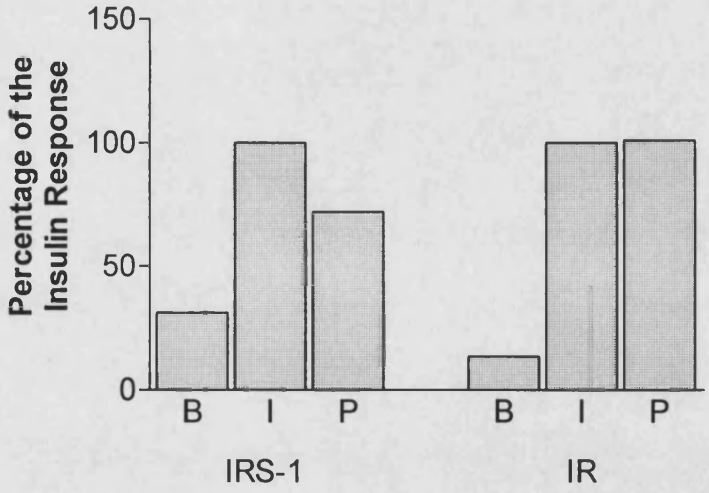

Figure 3.1.9. Attenuation of Insulin-stimulated Tyrosine Phosphorylation of IRS-1 Following the Introduction of 3.5 μM IRS-1 PH Domain into Permeabilized 3T3-L1 Adipocytes.

3T3-L1 adipocytes were treated as in Figure 3.1.8, except that pre-incubation was for 20 min with 3.5 μM IRS-1 PH domain before stimulation with 100 nM insulin for 2 min. A densitometric scan was made of the tyrosine-phosphorylated **IRS-1** and insulin receptor (**IR**) bands.

(a)

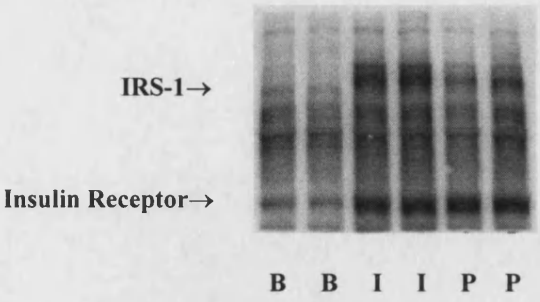

(b)

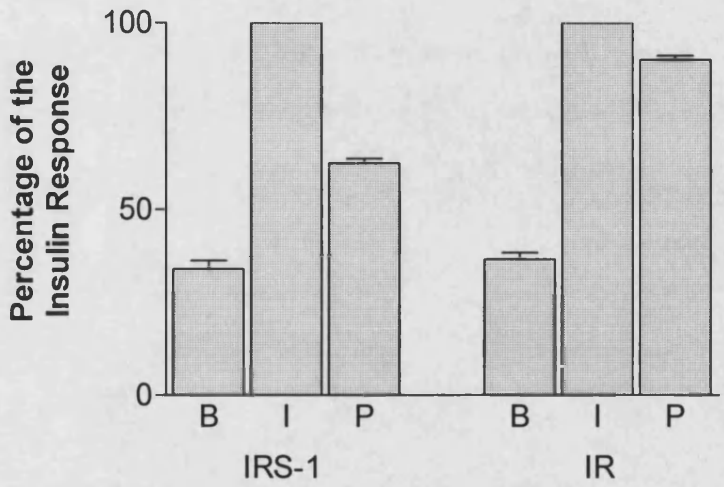

Figure 3.1.8. Attenuation of Insulin-stimulated Tyrosine Phosphorylation of IRS-1 Following the Introduction of IRS-1 PH Domain into Permeabilized 3T3-L1 Adipocytes.

3T3-L1 adipocytes were treated as in Figure 3.1.7, except that the pre-incubation was for 20 min with 10 μM IRS-1 PH domain before stimulation with 100 nM insulin for 2 min. (**a**) Immunoblot with anti-phosophotyrosine. (**b**) Densitometric scan of tyrosine-phosphorylated bands for **IRS-1** and the insulin receptor (**IR**). Values are the means from two independent experiments. Error bars show Min and Max values.

As the IRS-1 PH domain is able to affect phosphorylation of IRS-1 by the insulin receptor, then this may perturb downstream events in this signalling pathway. PI 3-K is activated upon binding to phosphorylated IRS-1, so its activity on

immunoprecipitated IRS-1 was measured following insulin stimulation of permeabilized 3T3-L1 adipocytes pre-treated with IRS-1 PH domain (Figure 3.1.10): however, no reduction in activity was observed. The activation of PI 3-K leads ultimately to an increase in glucose uptake, so this was also measured under the same conditions that affect insulin-stimulated phosphorylation of IRS-1 (Figure 3.1.11): again, no reduction in 2-deoxy-D-glucose uptake was seen.

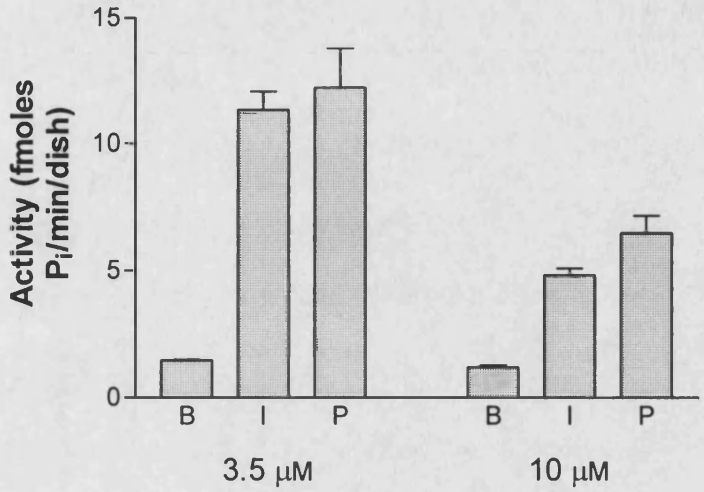

Figure 3.1.10. PI 3-K Activity on IRS-1 Immunoprecipitates Following Insulin Stimulation of Permeabilized 3T3-L1 Adipocytes Pre-incubated with IRS-1 PH Domain.

3T3-L1 adipocytes were treated as in Figure 3.1.8. IRS-1 was immunoprecipitated and assayed for PI 3-K activity as in *Methods 2.5.1*. Values are the means from single experiments (one with **3.5** μM and the other with **10** μM PH domain) done in duplicate. Error bars show Min and Max values.

Earlier studies by Myers Jr. *et al.* (1995) and Voliovitch *et al.* (1995) had suggested a role for the PH domain in coupling IRS-1 to the insulin receptor. In this study, the presence of exogenous IRS-1 PH domain in permeabilized 3T3-L1 adipocytes was sufficient to attenuate insulin-stimulated tyrosine phosphorylation of IRS-1, but only at shorter insulin stimulation times. However, a control protein should have also been tested for its ability to affect receptor-mediated IRS-1 phosphorylation: this could be a protein with a similar molecular weight to the IRS-1 PH domain, or a PH domain mutant. Nevertheless, the results are consistent with Myers Jr. *et al.* (1995), who

demonstrated that the absence of a PH domain impaired insulin-stimulated phosphorylation of IRS-1, but not if the insulin receptor was overexpressed. Thus, both investigations indicate a role, though not essential, of the PH domain in allowing IRS-1 phosphorylation by the insulin receptor. So far, the nature of the interaction of the IRS-1 PH domain with the insulin receptor has not been identified, though it does not appear to involve direct binding to the receptor (Myers Jr. *et al.*, 1995). In further investigations, it would be interesting to repeat the experiments again, but in a cell-free system. Thus, the purified insulin receptor could be reconstituted into a varied lipid environment before determining the phosphorylation of recombinant IRS-1 in the absence or presence of IRS-1 PH domain. Thus, it may suggest a role for certain phospholipids in this process. Further, it may help to assess whether an intermediate protein is required for the interaction of IRS-1 with the insulin receptor.

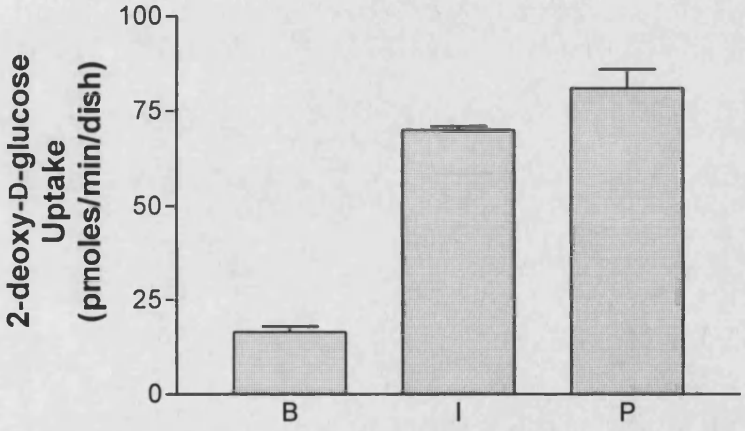

Figure 3.1.11. Uptake of 2-deoxy-D-Glucose Following Insulin Stimulation of Permeabilized 3T3-L1 Adipocytes Pre-incubated with IRS-1 PH Domain.

3T3-L1 adipocytes were treated as in Figure 3.1.8. Uptake of 2-deoxy-D-glucose was measured as in *Methods 2.4.2*. Values are the means from a single experiment done in duplicate. Error bars show Min and Max values.

However, under the same conditions that led to impaired insulin-stimulated IRS-1 phosphorylation, there was no effect on the insulin-stimulation of PI 3-K activity in IRS-1 immunoprecipitates or of 2-deoxy-D-glucose uptake. In contrast, Myers Jr. *et al.* (1995) found that the deletion of the IRS-1 PH domain led to complete inhibition of insulin-stimulated PI 3-K activity in IRS-1 immunoprecipitates. However, in their

cell system, insulin-stimulated IRS-1 phosphorylation was virtually blocked. Thus, a possible explanation for the failure in this study to observe inhibition by the IRS-1 PH domain of insulin-stimulated events downstream of IRS-1 phosphorylation could be that, under normal conditions, only a fraction of phosphorylated IRS-1 is required for activation of downstream processes. Thus, partial inhibition of insulin-stimulated IRS-1 phosphorylation would not be sufficient to have an effect on downstream signalling. Also, in measurements of 2-deoxy-D-glucose uptake following insulin stimulation in the presence of exogenous IRS-1 PH domain, the 5 min assay time may see the full tyrosine phosphorylation of IRS-1 occurring. Thus, this may also explain the failure to see attenuation of insulin-stimulated transport activity.

Though the methods described in this study were unable to completely block insulin-stimulated tyrosine phosphorylation of IRS-1 and resultant downstream processes, they do however point to a role for the PH domain in coupling IRS-1 to its receptor. In view of the recognition of a role for the IRS-1 PTB domain in coupling IRS-1 to the insulin receptor (Yenush *et al.*, 1996), it would be interesting to determine insulin-stimulated IRS-1 phosphorylation following the introduction of both the PH and PTB domains into permeabilized 3T3-L1 adipocytes: it is possible that both domains may be more effective in inhibiting this process than the PH domain alone.

3.2 Development of an Assay for PKB

Before studies could be undertaken to investigate the role of PKB in insulin-regulated glucose uptake, an assay for the kinase had to be developed. The following experiments describe how the eventual method (*Methods 2.5.2*) was arrived at. Initially, the possibility of measuring PKB activity in plasma membrane-free cell extracts from 3T3-L1 adipocytes was investigated (Figure 3.2.1), using Crosstide as the enzyme substrate, since the peptide is from a sequence in GSK-3 that is phosphorylated by PKB *in vitro* (Cross *et al.*, 1995).

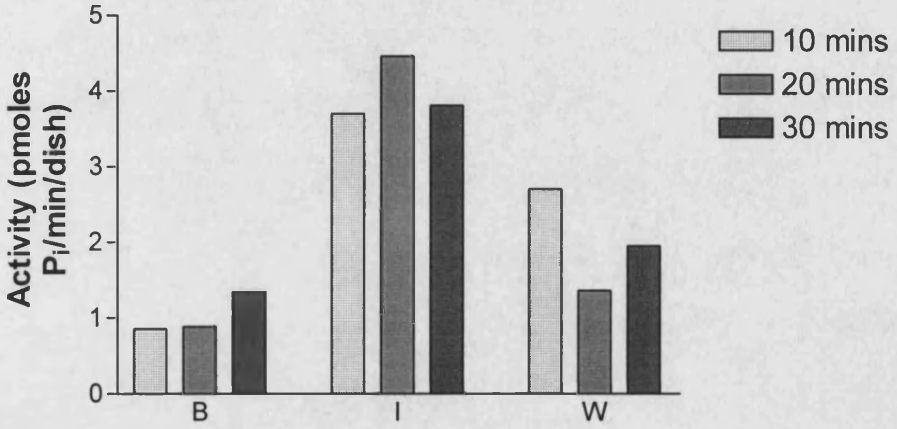

Figure 3.2.1. Measurement of Crosstide-phosphorylating activity in Post-Crude-Plasma-Membrane Fractions from 3T3-L1 Adipocytes.

3T3-L1 adipocytes were insulin-stimulated as in *Methods 2.3.1*, except that a 30 min pre-incubation in 1 ml KRH buffer was included before a further 10 min incubation without (**B**) or with (**I**) 100 nM insulin; one pre-incubation included 1 μM wortmannin before insulin treatment (**W**). Cells were homogenized and the crude plasma membrane fraction removed (*Methods 2.6.1*). Kinase activity in 10 μl aliquots of cell extract was measured as in *Methods 2.5.2*, using 25 μg Crosstide per assay. Samples were incubated for **10**, **20** or **30 min**, after which 10 μl aliquots were spotted onto phosphocellulose. Background counts were determined from an aliquot of radiolabelled ATP with activity equivalent to that in 10 μl of reaction mixture (containing cell extract).

Insulin stimulation (100 nM for 10 min) was found to raise kinase activity by about 4-fold over basal levels. Pre-treatment of cells with 1 μM wortmannin - to block activation of PKB by upstream PI 3-K activation (Kohn *et al.*, 1995) - prior to insulin

treatment did not completely prevent the increase in kinase activity. This observation indicates that kinases other than PKB in the 3T3-L1 adipocyte homogenates may have also been catalyzing the phosphorylation of Crosstide. Taking into consideration that the insulin-stimulated response was low, it was decided that PKB activity should be measured in PKB immunoprecipitates.

Using anti-Rac-CT to immunoprecipitate PKB from cell lysate, kinase activity from basal and insulin-stimulated 3T3-L1 adipocytes was measured. However, phosphorylated Crosstide was not detected in the reaction mixture supernatant after incubation with the immunoprecipitated PKB (Figure 3.2.2).

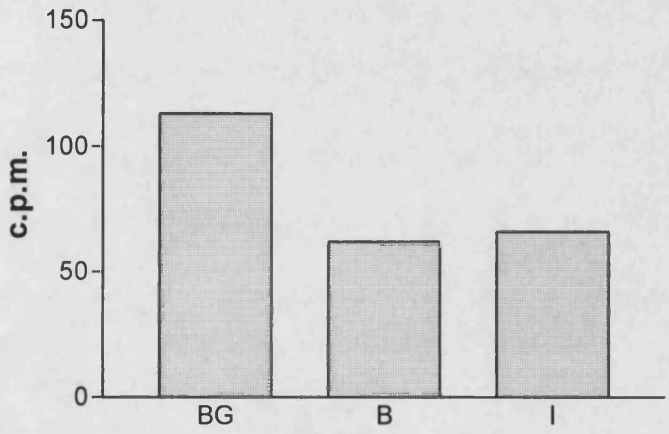

Figure 3.2.2. Crosstide-phosphorylating Activity in Rac-CT Immunoprecipitates from Basal and Insulin-stimulated 3T3-L1 Adipocytes.

3T3-L1 adipocytes prepared as in *Methods 2.3.1* were treated without (**B**) or with (**I**) 100 nM insulin for 20 min. PKB was immunoprecipitated from each dish (5 μg anti-Rac-CT conjugated to 50 μl protein A sepharose) and activity assayed as in *Methods 2.5.2*, using 25 μg Crosstide per assay in 30 min incubations. Aliquots of 10 μl of reaction mixture supernatant were spotted onto phosphocellulose. Background (**BG**) counts were determined from 50 μl protein A sepharose that had been treated in the same way as the immunoprecipitates.

To investigate the possibility that the Crosstide substrate may have been binding to or become trapped in the immunoprecipitates, another assay was carried out using protamine sulphate, a non-physiological protein substrate (Jones *et al.*, 1991) (Figure

3.2.3). It was found that phosphorylated protein - not present in the supernatant - could be released from the immunoprecipitates with electrophoresis sample buffer.

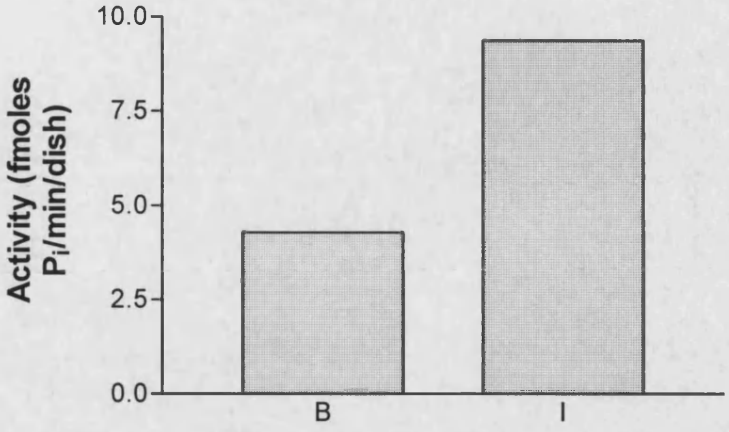

Figure 3.2.3. Phosphorylated Protamine Sulphate Binds to Rac-CT Immuno-precipitates.

3T3-L1 adipocytes prepared as in *Methods 2.3.1* were treated without (**B**) or with (**I**) 100 nM insulin for 20 min. PKB was immunoprecipitated from each dish (2.5 µg anti-Rac-CT conjugated to 25 µl protein A sepharose) and activity assayed as in *Methods 2.5.2*, using 25 µg protamine sulphate per assay in 30 min incubations. Reaction mixture supernatant was removed and protein was eluted from the beads with 40 µl 2× sample buffer before separation on a 13% SDS-PAGE gel (*Methods 2.7.2*). Radioactive bands were then cut out and counted. Background counts were determined from an empty lane on the gel and subtracted from the other counts.

Thus, it was concluded that a way to overcome the problem of Crosstide binding to the Rac-CT immunoprecipitates might be to use a detergent solution to elute the peptide, which could then be spotted onto phosphocellulose. To determine if the presence of SDS affects the binding of phosphorylated Crosstide to phosphocellulose, kinase activity was measured again in plasma membrane-free cell extract from 3T3-L1 adipocytes. Aliquots from the reaction mixture were then either spotted directly onto phosphocellulose, or mixed with SDS solution first before spotting (Figure 3.2.4). The counts detected on phosphocellulose were similar regardless of whether the aliquots added contained SDS or not.

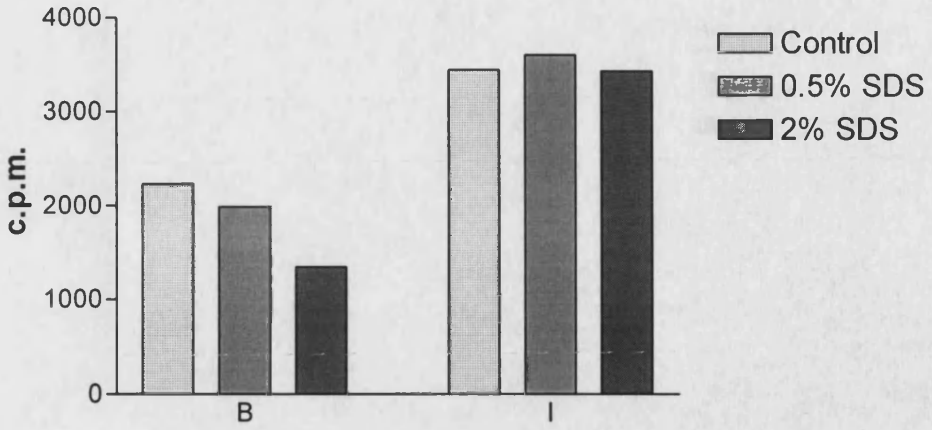

Figure 3.2.4. Binding of Phosphorylated Crosstide to Phosphocellulose in the Absence and Presence of SDS.

3T3-L1 adipocytes were treated without (**B**) or with (**I**) insulin, homogenized, fractionated and assayed for kinase activity as in Figure 3.2.1. At the end of a 30 min incubation, 10 µl reaction mixture was mixed with 10 µl **0.5%** (w/v) or **2%** (w/v) **SDS** before spotting onto phosphocellulose. For the **control**, 10 µl reaction mixture (with cell extract) was spotted directly onto phosphocellulose.

Another measurement of kinase activity in immunoprecipitates of PKB from 3T3-L1 adipocytes was made using anti-Akt1(C-20) (the Rac-CT antibody was discontinued by the supplier) to immunoprecipitate the kinase (Figure 3.2.5). This time, at the end of the assay, aliquots of the supernatant were spotted onto phosphocellulose separately from aliquots of 2% (w/v) SDS that had been mixed with the beads. Unexpectedly, little or no phosphorylated Crosstide was detected on the immunoprecipitates, perhaps because a different antibody was used, or because protein G sepharose was used instead of protein A. PKB activity was found to be 5-6 times higher in insulin-stimulated cells than in basal cells.

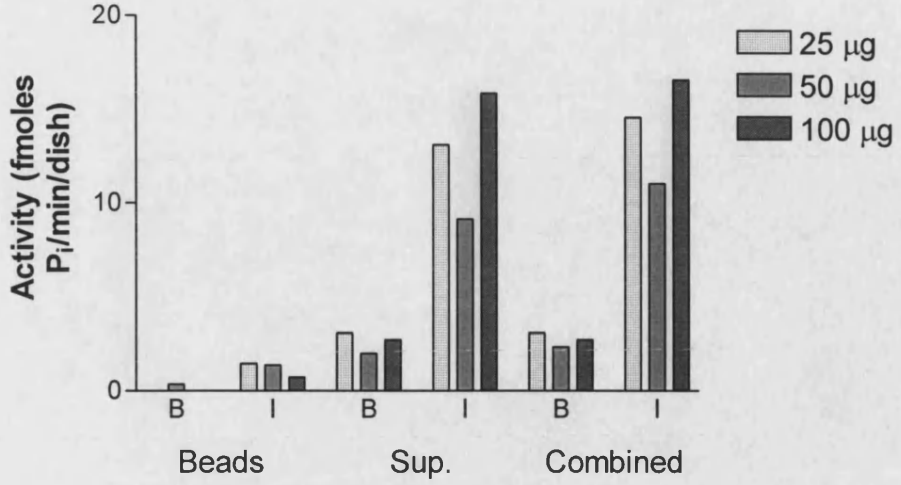

Figure 3.2.5. Crosstide-phosphorylating Activity in Akt1(C-20) Immunoprecipitates from 3T3-L1 Adipocytes.

3T3-L1 adipocytes prepared as in *Methods 2.3.1* were treated without (**B**) or with (**I**) 100 nM insulin for 20 min. PKB was immunoprecipitated from each dish (2.5 µg anti-Akt1(C-20) conjugated to 25 µl protein G sepharose) and assayed for kinase activity as in *Methods 2.5.2*, using either **25**, **50** or **100** µg Crosstide per assay in 30 min incubations. Supernatant was removed and 10 µl spotted onto phosphocellulose (**Sup.**); beads were mixed with 40 µl 2% (w/v) SDS for 10 min before 10 µl was spotted (**Beads**). Counts from both samples were combined to give total activity (**Combined**). For the background, 25 µl protein G sepharose was treated in the same way as the immunoprecipitates.

In order to determine the time range where incorporation of phosphate into Crosstide is linear, subsequent measurements of PKB activity in immunoprecipitates from 3T3-L1 adipocytes were carried out in which different incubation times were studied. However, an insulin-stimulated rise in PKB activity could no longer be observed (data not shown). In order to assess if there was a problem with the stock of Crosstide, an assay of PKB activity in rat adipocytes was carried out using either the peptide or protamine sulphate as the enzyme substrate (Figure 3.2.6). An increase in PKB activity upon insulin stimulation was observed if the protein was used as the substrate in the assay instead of the peptide. Thus, protamine sulphate was used in all subsequent assays for PKB.

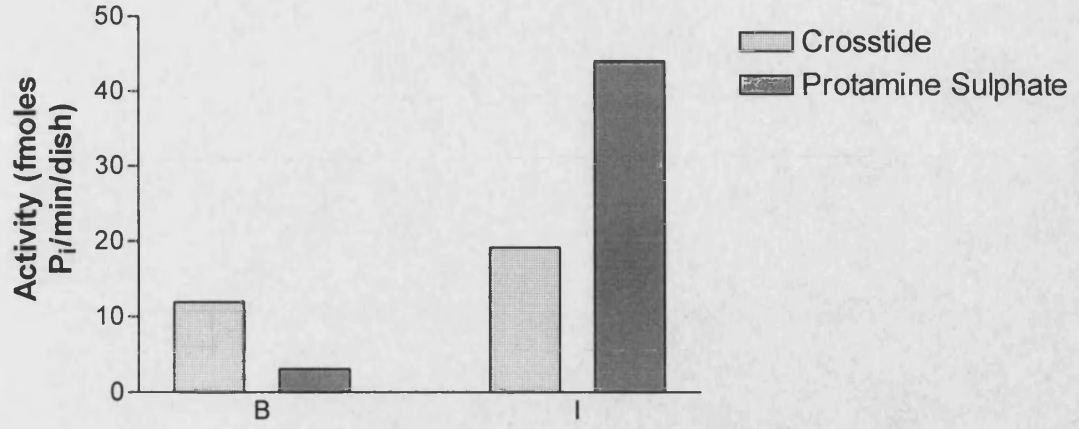

Figure 3.2.6. Comparison between Crosstide and Protamine Sulphate as the Substrate for Measurement of PKB Activity in Rat Adipocytes.

Freshly-isolated rat adipocytes prepared as in *Methods 2.2.2* were treated without (**B**) or with (**I**) 20 nM insulin for 20 min, before immunoprecipitation of PKB (from 0.5 ml of 40% (v/v) cells) and measurement of kinase activity as in *Methods 2.5.2*, using either 25 μg **Crosstide** or 25 μg **Protamine Sulphate** per assay in 20 min incubations. Aliquots of 10 μl of supernatant were spotted onto phosphocellulose. For the background, 10μl protein G sepharose was treated as for the immunoprecipitates, with either Crosstide or protamine sulphate in the reaction mixture.

As protamine sulphate was to be used for all further assays, it was necessary to assess its characteristics as a PKB substrate. Measurements of PKB activity in 3T3-L1 adipocytes were carried out using different incubation times in the assay, in order to determine if phosphorylation of protamine sulphate was linear over 20 min (Figure 3.2.7b); in the same experiment, it was determined whether or not the phosphorylated protein binds to the immunoprecipitates (Figure 3.2.7a). As the rate of phosphorylation was linear for assay times of 10, 15 and 20 min, it was decided that a reaction time of 20 min would be used in all further PKB assays. As phosphorylated protamine sulphate was detected on the immunoprecipitates, various ways of eluting and spotting the phosphorylated protein were investigated (Figure 3.2.8). The method of mixing the removed supernatant and eluted protein before spotting onto phosphocellulose gave similar levels of PKB activity to that determined using the previous method of spotting the two components separately, and was thus used in subsequent assays.

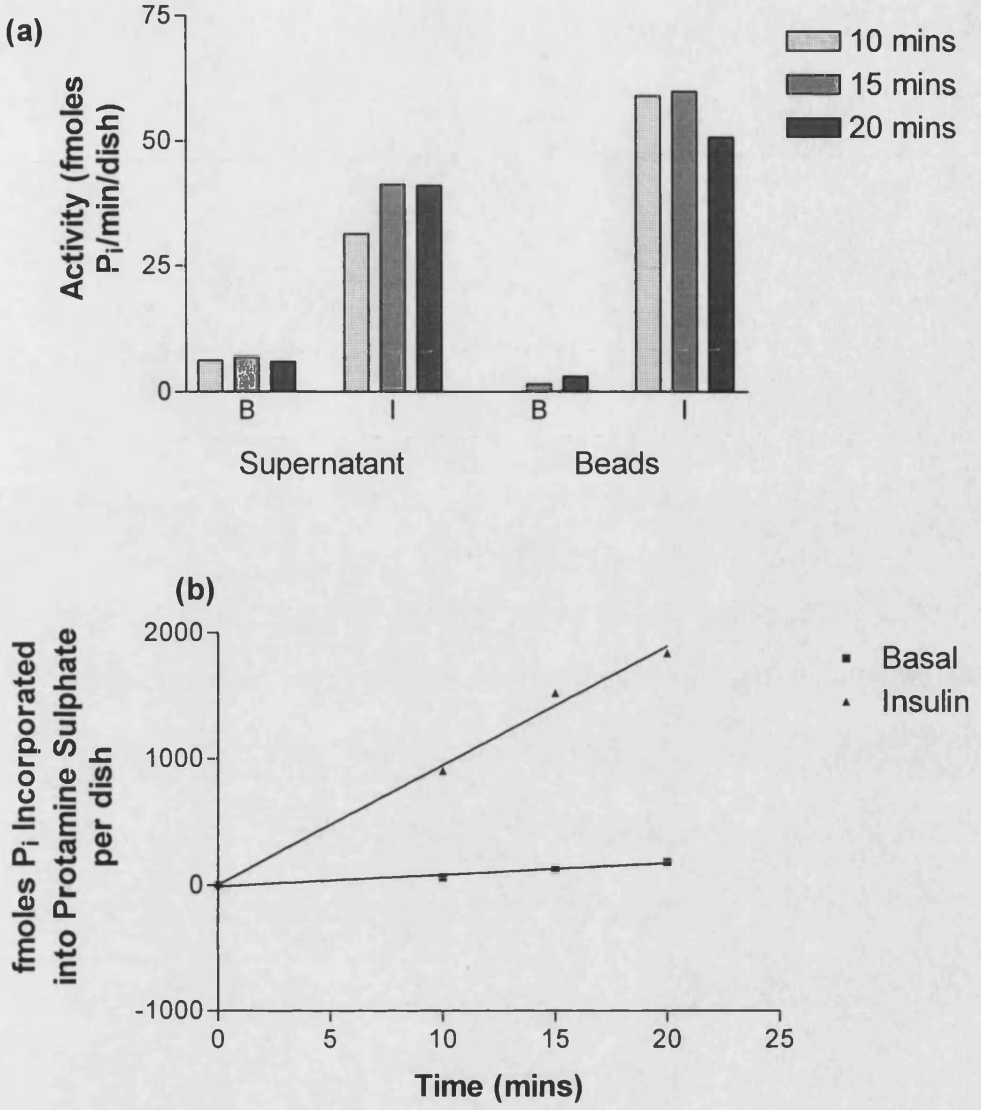

Figure 3.2.7. Measurement of PKB Activity with Protamine Sulphate as Substrate in 3T3-L1 Adipocytes Using Different Incubation Times in the Assay.

3T3-L1 adipocytes prepared as in *Methods 2.3.1* were treated without (**B** or **Basal**) or with (**I** or **Insulin**) 100 nM insulin for 20 min, before immunoprecipitation of PKB and measurement of kinase activity as in *Methods 2.5.2*, using 25 µg protamine sulphate per assay in **10**, **15** or **20 min** incubations. At the end of the assay, 10 µl of removed supernatant was spotted onto phosphocellulose, as was 10 µl of 40 µl 2% (w/v) SDS that had been mixed with the beads for 10 min. **(a)** Phosphorylated protamine sulphate found on the **Beads** and in the **Supernatant** are plotted separately. **(b)** Phosphorylated protamine sulphate from the beads and supernatant are combined to give total phosphorylated protein.

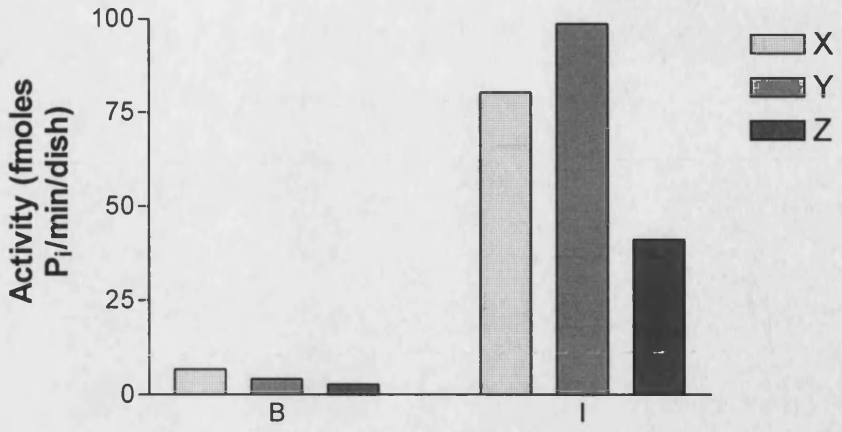

Figure 3.2.8. Different Methods of Eluting and Spotting Phosphorylated Protamine Sulphate at the End of a PKB Assay.

3T3-L1 adipocytes prepared as in *Methods 2.3.1* were treated without (**B**) or with (**I**) 100 nM insulin for 20 min, before immunoprecipitation of PKB and measurement of kinase activity as in *Methods 2.5.2*. Samples were assayed for 20 min, before: (**X**) spotting 10 µl removed supernatant separately from 10 µl of 40 µl 2% (w/v) SDS that had been mixed with the beads for 10 min; (**Y**) spotting 20 µl from a combined solution of 50 µl removed supernatant and 40 µl 2% (w/v) SDS that had been mixed with the beads for 10 min; (**Z**) spotting 20 µl of a combined solution where 40 µl 2% (w/v) SDS had been mixed with beads and supernatant for 10 min.

The appropriate amount of Akt1(C-20) antibody required to immunoprecipitate PKB from a dish of 3T3-L1 adipocytes was determined. Cell lysates that had been subjected to immunoprecipitation with different quantities of the antibody were subsequently immunoblotted with anti-Rac-CT. Thus, any non-immunoprecipitated PKB could be detected (Figure 3.2.9). It was found that at least 1 µg antibody was able to remove essentially all of the PKB from a dish of 3T3-L1 adipocytes.

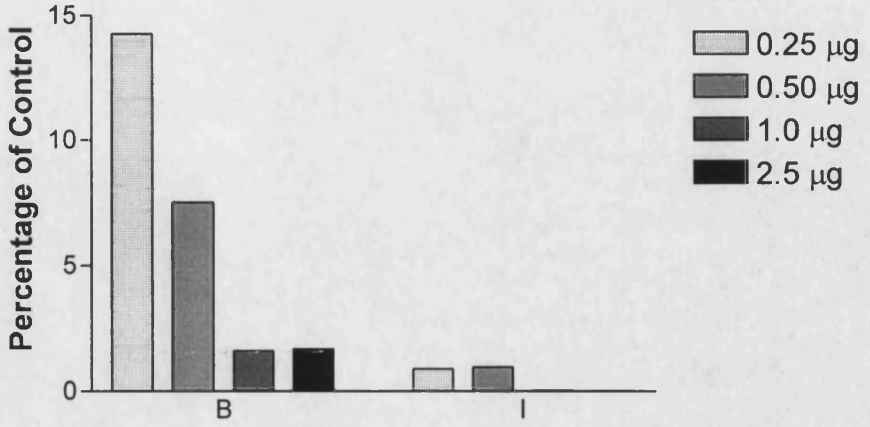

Figure 3.2.9. Western Blotting with Anti-Rac-CT of Cell Lysate from 3T3-L1 Adipocytes that was Subjected to Immunoprecipitation with Different Quantities of anti-Akt1(C-20).

Basal (**B**) and insulin-stimulated (**I**) 3T3-L1 adipocytes were prepared, lysed and immunoprecipitated (*Methods 2.3.1* and *2.5.2*). Immunoprecipitation was with **0.25**, **0.5**, **1** or **2.5** µg Akt1(C-20) antibody conjugated to 25 µl protein G sepharose. Samples of 25 µl cell lysate were then boiled with 25 µl 2× sample buffer. Samples were resolved on a 10% SDS-PAGE gel, transferred and immunoblotted (*Methods 2.7*). The control was cell lysate not subjected to immunoprecipitation of PKB. Bands were analyzed by densitometry and expressed as a percentage of the control band.

3.3 Studies with PKB in 3T3-L1 and Rat Adipocytes

Several experiments were undertaken in order to provide circumstantial evidence for or against the involvement of PKB in insulin-stimulated glucose uptake. First, the insulin stimulation of PKB activity in 3T3-L1 adipocytes was measured as a function of dose and time. The insulin-stimulated response could then be compared with that for glucose transport. Second, the effects of wortmannin on insulin-activated PKB and insulin-stimulated glucose uptake in 3T3-L1 adipocytes were compared, since both processes appear to be regulated by PI 3-K (Kohn *et al.*, 1995, and Clarke *et al.*, 1994). If PKB stimulates glucose transport, then wortmannin should reduce the activity of the former more rapidly than that of the latter. Further, PP2A is a putative inactivator of PKB; the phosphatase can be inhibited by okadaic acid (Andjelkovic *et al.*, 1996). Thus, the effects of okadaic acid on wortmannin inhibition of insulin-stimulated activities for PKB and glucose transport were also compared. Third, measurements of PKB activity in subcellular fractions of adipocytes were made in order to determine the location of PKB action. The detection of insulin-stimulated activity in membrane fractions would support a role for the kinase in regulating GLUT4 trafficking. Fourth, the putative regulation of glucose uptake by PKB was investigated by using Crosstide as a competitive inhibitor of PKB in permeabilized 3T3-L1 adipocytes. Inhibition of insulin-stimulated glucose uptake by this peptide would suggest the involvement of PKB in this process.

3.3.1 Insulin Stimulation of PKB Activity and Glucose Uptake in 3T3-L1 Adipocytes

The stimulation of endogenous PKB activity by insulin has already been demonstrated in L6 myotubes (Cross *et al.*, 1995), in skeletal muscle and adipose tissue (Cross *et al.*, 1997), and in 3T3-L1 adipocytes (Tanti *et al.*, 1997). PKB activity in 3T3-L1 adipocytes under basal and insulin-stimulated conditions was further characterized in the study described here. Cells were stimulated for 20 min with a range of insulin concentrations (from 1 pM to 1 μM) prior to measurement of PKB activity (Figure

3.3.1a). A sigmoidal dose-response curve was obtained: activity began to rise above insulin doses of 100 pM before reaching a plateau at doses above 1 μM. The EC_{50} (the dose that gives the response between the top and bottom plateau) was 21.8 nM insulin.

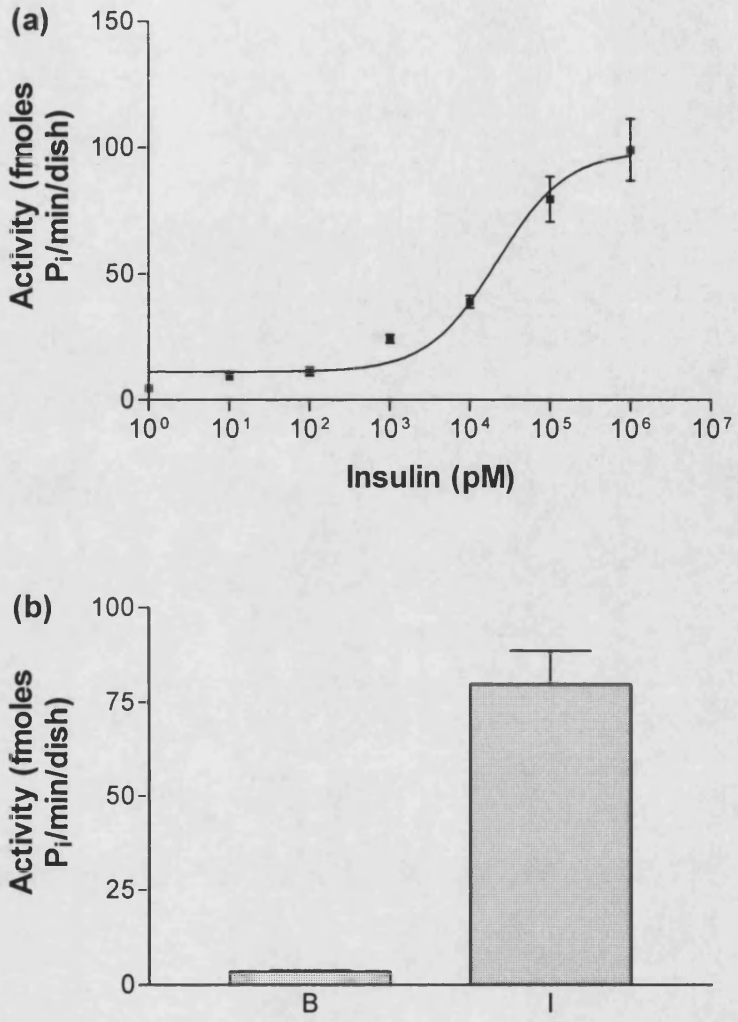

Figure 3.3.1. PKB Activity in 3T3-L1 Adipocytes Following Insulin Stimulation with Different Doses.

(**a**) 3T3-L1 adipocytes prepared as in *Methods 2.3.1* were stimulated for 20 min with 0.001, 0.01, 0.1, 1, 10, 100 and 1000 nM insulin. PKB was immunoprecipitated and assayed for activity as in *Methods 2.5.2*. (**b**) PKB activity in 3T3-L1 adipocytes stimulated without (**B**) or with (**I**) 100 nM insulin for 20 min. Values are the means ± S.E.M. from three independent experiments.

The PKB activity in 3T3-L1 adipocytes following 100 nM insulin stimulation was nearly 23-fold over that in basal cells (Figure 3.3.1b). This response is greater than that observed by other groups. Cross *et al.* (1997) found a maximal insulin-stimulated rise in PKB activity of 14-fold in freshly-isolated rat adipocytes, whereas Tanti *et al.* (1997) determined an 8-fold increase in 3T3-L1 adipocytes following 100 nM insulin stimulation for 5 min. It is difficult to determine whether this discrepancy was due to low basal activity and/or high insulin-stimulated activity in this thesis, as the other groups have only described PKB activity as a percentage of the maximum. A possible reason may be that protamine sulphate was used as the substrate instead of Crosstide, which was preferred by the other groups. However, it has been shown earlier in this thesis (*Results and Discussion 3.2*) that the phosphorylation of protamine sulphate by immunoprecipitated PKB from basal and insulin-stimulated 3T3-L1 adipocytes is linear over a 20 min assay period. A more likely reason is that, in this thesis, PKB immunoprecipitates were treated with detergent at the end of an assay in order to remove any non-specifically bound phosphorylated substrate. As shown earlier (Figure 3.2.7a), phosphorylated protamine sulphate is distributed similarly between the supernatant and PKB immunoprecipitates from insulin-stimulated cells. However, for PKB immunoprecipitates from basal cells, the phosphorylated substrate is located mainly in the supernatant. Thus, the detergent extracts would have a greater effect on measured insulin-stimulated activity than on measured basal activity, giving a greater basal/insulin difference. Species difference could be another possible explanation for why the fold-increase for insulin-stimulated PKB activity was determined to be greater than that found by Cross *et al.* (1997). Thus, they measured PKB activity in freshly-isolated rat adipocytes, which may give a different response to 3T3-L1 adipocytes.

To determine the time-course of activation of PKB by insulin in 3T3-L1 adipocytes, cells were stimulated with 100 nM insulin for different times, from 2 min to 1 h (Figure 3.3.2). PKB activity was similar whether the cells were stimulated for 2 min or for 1 h. Thus, activation of PKB by insulin in 3T3-L1 adipocytes is rapid and is maintained despite prolonged acute stimulation. This time-course data for insulin stimulation of PKB activity is consistent with Cross *et al.* (1997). In freshly-isolated

rat adipocytes, they found that half-maximal activity occurred at 2 min, with maximal activity at 5 min; activity was maintained for at least 1 h. The rapid and sustained rise in PKB activity following insulin stimulation is consistent with its putative role in insulin-stimulated glucose uptake, as stimulation of 2-deoxy-D-glucose uptake in 3T3-L1 adipocytes is not maximal until after 10-15 min treatment with 100 nM insulin (Fingar and Birnbaum, 1994b). Thus, in 3T3-L1 adipocytes, insulin stimulation maximally activates PKB before there is a maximal level of glucose transport.

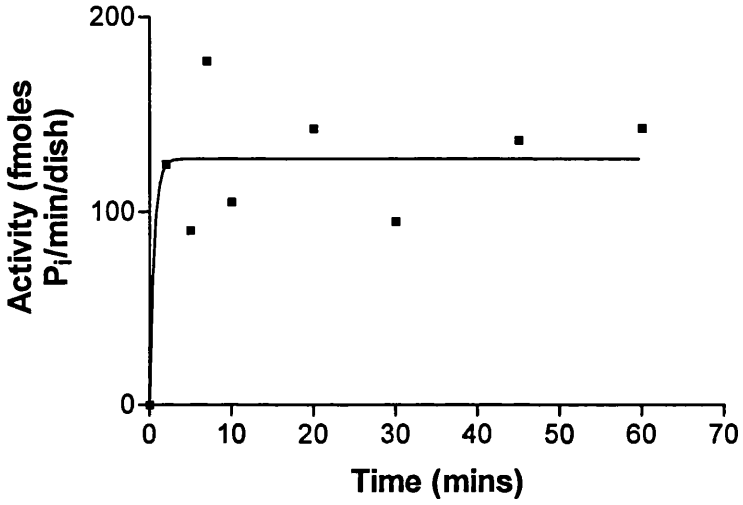

Figure 3.3.2. PKB Activity in 3T3-L1 Adipocytes Following Stimulation with Insulin for Different Lengths of Time.

3T3-L1 adipocytes prepared as in *Methods 2.3.1* were stimulated with 100 nM insulin for 2 min to 1 h. PKB was immunoprecipitated and assayed for activity as in *Methods 2.5.2*. Values are from a single experiment.

To compare the insulin stimulation of glucose uptake with that of PKB activity in 3T3-L1 adipocytes, measurements of 2-deoxy-D-glucose uptake were made at the insulin concentrations that were used in Figure 3.3.1a (Figure 3.3.3a). The sigmoidal dose-response curve observed was to the left of that for insulin-stimulated PKB activity (Figure 3.3.3b). Uptake of 2-deoxy-D-glucose began to increase at doses above 10 pM before reaching a plateau above doses of 100 nM. The EC_{50} was 1.19 nM insulin. Also, while 100 nM insulin stimulation for 20 min produced a maximal response in terms of glucose uptake, the same could not be said for PKB activity.

Thus, glucose transport is more sensitive to insulin stimulation than PKB activity in 3T3-L1 adipocytes.

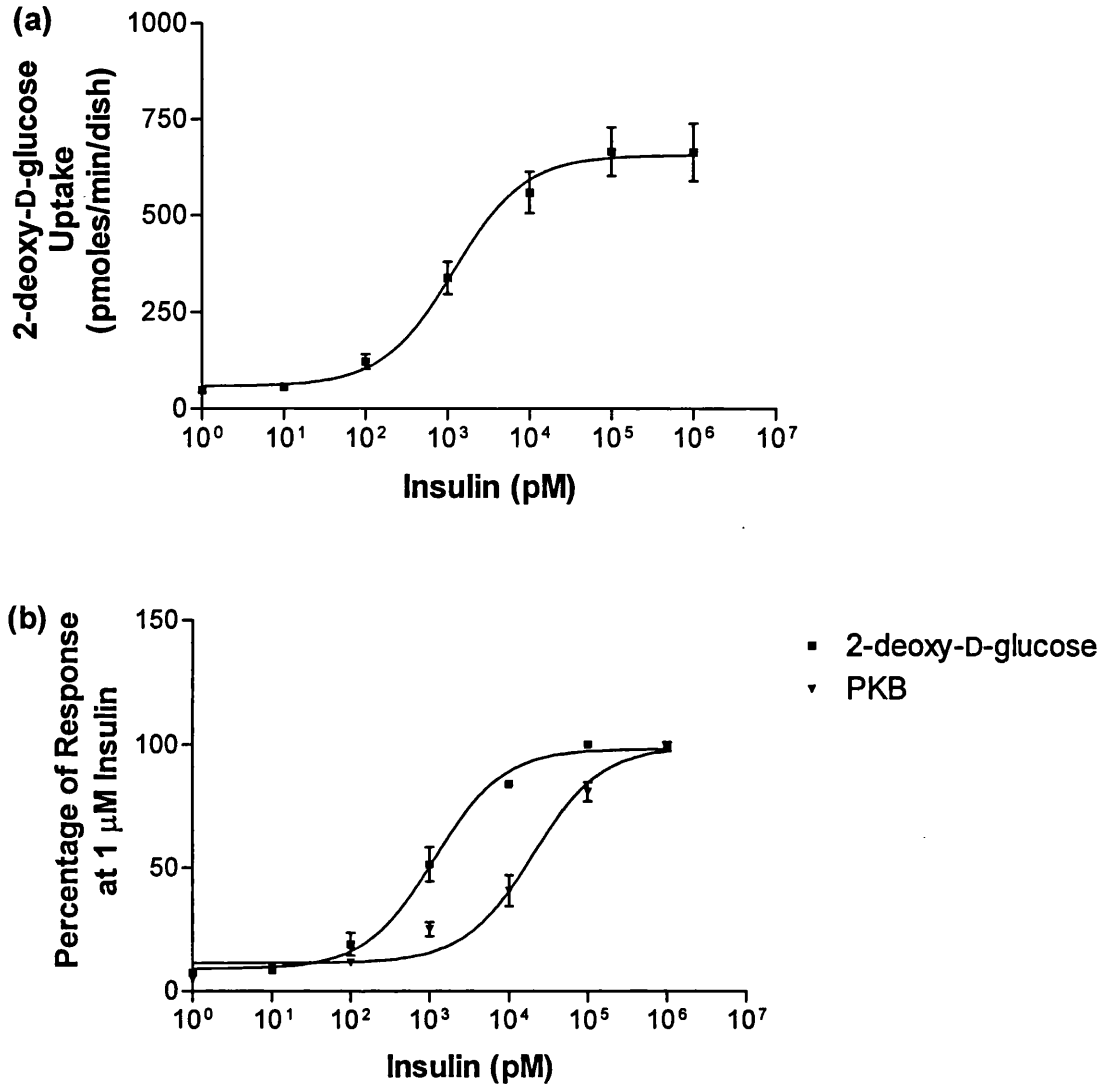

Figure 3.3.3. Uptake of 2-deoxy-D-glucose in 3T3-L1 Adipocytes Following Insulin Stimulation with Different Doses.

3T3-L1 adipocytes prepared as in *Methods 2.3.1* were stimulated for 20 min with 0.001, 0.01, 0.1, 1, 10, 100 and 1000 nM insulin. **(a)** Uptake of 2-deoxy-D-glucose was measured as in *Methods 2.4.1.* Values are the means ± S.E.M. from three independent experiments. **(b)** Data from Figures 3.3.1a **(PKB)** and 3.3.3a **(2-deoxy-D-glucose)** are expressed as a percentage of the response at 1 μM insulin stimulation.

Similarly, the dose-response curve for insulin-stimulated insulin receptor β-subunit phosphorylation in 3T3-L1 adipocytes is also to the right of that for insulin-stimulated glucose uptake (Kohanski *et al.*, 1986). They determined an EC_{50} value of 8 nM for the former, which is less than that for insulin stimulation of PKB activity (21.8 nM). Kohanski *et al.* (1986) also determined an EC_{50} of 2 nM for insulin-stimulated glucose transport, which is similar to that determined here (1.19 nM). The greater sensitivity of glucose transport to insulin stimulation than β-subunit phosphorylation or activation of PKB may be a result of amplification of the signal from the insulin receptor.

3.3.2 Inhibition of Insulin Stimulation of PKB Activity and Glucose Uptake in 3T3-L1 Adipocytes

The pre-treatment of CHO cells overexpressing the insulin receptor with wortmannin (which blocks PI 3-K activity) inhibits insulin activation of PKB (Kohn *et al.*, 1995). Experiments were undertaken to determine if this was also the case in 3T3-L1 adipocytes. Thus, cells were stimulated with 100 nM insulin for 20 min to activate PKB, before treatment with 1 μM wortmannin for different lengths of time; measurements of PKB activity were subsequently made (Figure 3.3.4a). This insulin and wortmannin treatment regime was the same as that used to demonstrate maximal inhibition of insulin-stimulated PI 3-K activity by wortmannin in 3T3-L1 adipocytes (Yang *et al.*, 1996). PKB activity declined rapidly following wortmannin treatment with a half-time of 52.8 s, before reaching a plateau of 4.35 fmoles P_i/min/dish. Thus, the addition of wortmannin to insulin-stimulated 3T3-L1 adipocytes causes a rapid decline in PKB activity to basal levels. As wortmannin does not inhibit PKB *in vitro* (Kohn *et al.*, 1995), then this result suggests that insulin stimulation of PKB activity occurs via PI 3-K only, without contributions from convergent signalling pathways. Further evidence for PI 3-K regulation of PKB in 3T3-L1 adipocytes could be provided by the use of the other PI 3-K inhibitor, LY294002. Alternatively, a dominant negative form of PI 3-K could be expressed in 3T3-L1 adipocytes. The virtual inhibition of insulin-stimulated PKB activity by wortmannin is consistent with

previous studies in CHO cells co-expressing the insulin receptor and PKBα (Kohn *et al.*, 1995) and in L6 myotubes (Cross *et al.*, 1995). In these studies, the addition of wortmannin prior to insulin stimulation blocked the rise in PKB activity.

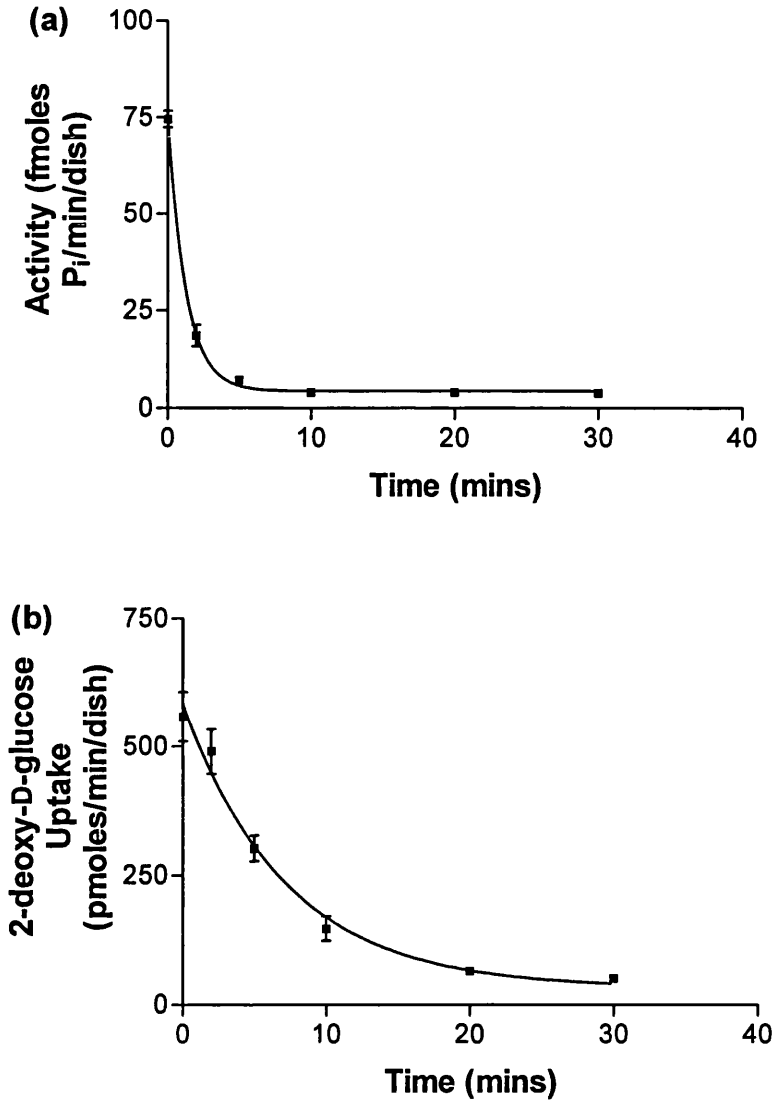

Figure 3.3.4. Inhibition of Insulin-stimulated PKB Activity and 2-deoxy-D-glucose Uptake by Wortmannin in 3T3-L1 Adipocytes.

3T3-L1 adipocytes prepared as in *Methods 2.3.1* were stimulated with 100 nM insulin for 20 min before 1 μM wortmannin was added for a further 2 to 30 min. **(a)** PKB was immunoprecipitated and assayed for activity as in *Methods 2.5.2.* **(b)** Uptake of 2-deoxy-D-glucose was measured as in *Methods 2.4.1*, using assay times of 2 min. Values are the means ± S.E.M. from three independent experiments.

As a comparison, the inhibition of insulin-stimulated glucose uptake in 3T3-L1 adipocytes by wortmannin was also determined (Figure 3.3.4b). Cells were stimulated with 100 nM insulin for 20 min prior to 1 μM wortmannin treatment and measurement of 2-deoxy-D-glucose uptake. Transport of 2-deoxy-D-glucose declined less rapidly than PKB activity following wortmannin treatment, with a half-time of 5 min. Transport did not begin to plateau at the lower level until after 30 min treatment with wortmannin, whereas for PKB activity, the plateau occurred after 10 min. Thus, insulin-activated PKB activity is more sensitive to wortmannin inhibition than insulin-stimulated glucose uptake in 3T3-L1 adipocytes. Further, the data from Figure 3.3.4 is consistent with the idea that PKB is an upstream regulator of glucose transport, since the virtual inactivation of PKB occurs more quickly than the reduction in transport activity to basal levels.

PP2A can dephosphorylate and inactivate immunoprecipitated PKB from vanadate-stimulated Swiss 3T3 cells (Andjelkovic *et al.*, 1996). As stimulated kinase activity is reduced by 92%, this suggests PP2A may inactivate PKB *in vivo*. Further, the presence of okadaic acid during PP2A treatment prevents inhibition of kinase activity in PKB immunoprecipitates. Thus, studies were carried out in 3T3-L1 adipocytes to determine if okadaic acid could affect the inhibition of insulin-stimulated PKB activity by wortmannin (Figure 3.3.5a). During treatment with 100 nM insulin for 20 min, 1 μM okadaic acid was also present. Cells were then further incubated with 1 μM wortmannin before measurement of PKB activity. Following the addition of the PI 3-K inhibitor, PKB activity declined with a half-time of 224.8 s before reaching a plateau of 12.19 fmoles P_i/min/dish. It was shown above (*Results and Discussion 3.3.2*) that the inhibition of insulin-stimulated PKB activity by wortmannin occurs with a half-time of 52.8 s before reaching a plateau of 4.35 fmoles P_i/min/dish (Figure 3.3.4a). Thus, okadaic acid treatment reduces the rate at which wortmannin treatment leads to inhibition of insulin-stimulated PKB activity. Also, okadaic acid reduces the extent of wortmannin inhibition of insulin activation of PKB. These two observations indicate that okadaic acid can partially counteract the block of insulin activation of PKB by wortmannin in 3T3-L1 adipocytes. Thus, the results suggest that PP2A has only a partial role to play in the dephosphorylation and subsequent inactivation of

PKB. If it is the major inactivator of PKB, as suggested by *in vitro* studies (Andjelkovic *et al.*, 1996), then okadaic acid should have prevented the huge reduction in activity upon wortmannin inhibition.

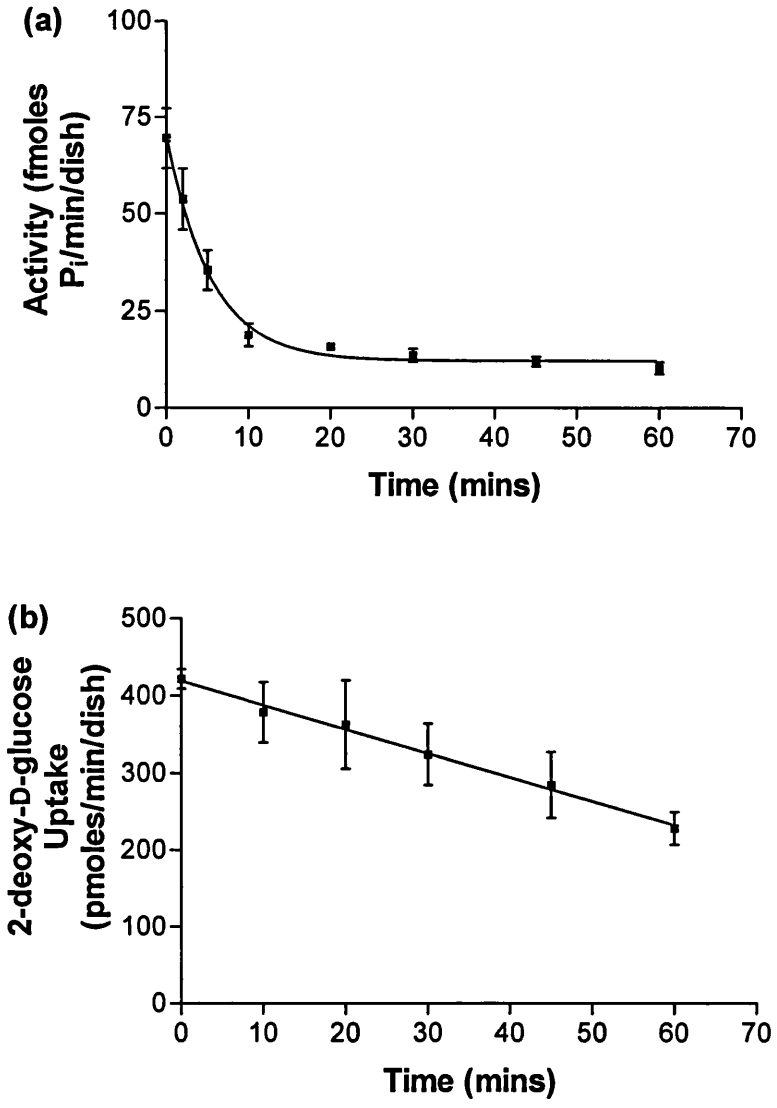

Figure 3.3.5. Inhibition of PKB Activity and 2-deoxy-D-glucose Uptake by Wortmannin in 3T3-L1 Adipocytes Following Treatment with Insulin and Okadaic Acid.

3T3-L1 adipocytes prepared as in *Methods 2.3.1* were treated with 100 nM insulin and 1 μM okadaic acid for 20 min before 1 μM wortmannin was added for a further 2 to 60 min. **(a)** PKB was immunoprecipitated and assayed for activity as in *Methods 2.5.2*. **(b)** Uptake of 2-deoxy-D-glucose was measured as in *Methods 2.4.1*, using assay times of 2 min. Values are the means ± S.E.M. from three independent experiments.

Earlier studies in 3T3-L1 adipocytes had shown that pre-treatment with 1 μM okadaic acid attenuates insulin-stimulated PI 3-K activity in anti-phosphotyrosine immunoprecipitates by 65% (Jullien *et al.*, 1993). However, their results are inconsistent with the study described here. The activity of downstream PKB in insulin-stimulated 3T3-L1 adipocytes is 74.6 ± 2.13 fmoles P_i/min/dish, whereas it is 69.5 ± 7.81 fmoles P_i/min/dish in the presence of okadaic acid (Figures 3.3.4a and 3.3.5a). The two values are not significantly different ($P > 0.05$). Thus, okadaic acid treatment appears to have no effect on insulin stimulation of PKB activity (though it may activate PKB in the absence of insulin stimulation - compare the plateau in Figure 3.3.4a with that in Figure 3.3.5a). The reason for the discrepancy is not clear. A possibility is that Jullien *et al.* (1993) treated their cells with okadaic acid before stimulating with insulin, whereas in the study described here, both compounds were added at the same time to the dishes of cells. Thus, the inhibitory effects of okadaic acid on the insulin stimulation of PI 3-K may be reduced in the latter method.

If PKB does regulate glucose transport, then okadaic acid should also partially block the wortmannin inhibition of insulin-stimulated glucose uptake. Thus, 3T3-L1 adipocytes were treated with 100 nM insulin and 1 μM okadaic acid for 20 min, before 1 μM wortmannin was added for various lengths of time prior to measurement of 2-deoxy-D-glucose uptake (Figure 3.3.5b). Compared with cells that were insulin-stimulated in the absence of okadaic acid (Figure 3.3.4b), the decline in 2-deoxy-D-glucose uptake following wortmannin treatment was slower and linear over the time-points up to 60 min. Even after 60 min incubation with wortmannin, the transport rate was greater than 200 pmoles/min/dish (Figure 3.3.5b), compared with 33 pmoles/min/dish at 30 min in cells which were untreated with okadaic acid (Figure 3.3.4b).

From the data in Figures 3.3.4a and 3.3.5a, it can be calculated that okadaic acid increases the half-time for wortmannin inhibition of insulin-stimulated PKB activity by a factor of 4.26. If okadaic acid affects the half-time for wortmannin inhibition of insulin-stimulated glucose uptake by the same factor, then its value should be 21.3 min. However, the results show that the half-time is greater than 60 min (Figure

3.3.5b). Thus, the ability of okadaic acid to attenuate the wortmannin inhibition of insulin-stimulated glucose uptake may not be solely due to action at the level of PKB. A possibility is that okadaic acid may also act at another target to counteract wortmannin inhibition of insulin-stimulated glucose uptake. In future experiments, it would be interesting to determine the rate of loss of ATB-BMPA-labelled cell surface GLUT4 following the addition of wortmannin to adipocytes insulin-stimulated in the presence of okadaic acid. This would allow an estimation of the rates of endocytosis and exocytosis of GLUT4 (Yang and Holman, 1993): these values could then be compared with those for 3T3-L1 adipocytes expressing constitutively active PKB.

3.3.3 Insulin Stimulation of PKB Activity in Subcellular Fractions of Adipocytes

The addition of a *src* myristoylation sequence to the N-terminus of PKB lacking its PH domain has been shown to cause constitutive activation of the kinase when this is expressed in 3T3-L1 cells (Kohn *et al.*, 1996b). This indicates that the site of activation and action of insulin-activated PKB in the cell may be at a membrane location, since the myristoylation sequence enables a protein to attach to a membrane. In order to determine the effect of insulin on the subcellular location of PKB activity, 3T3-L1 adipocytes were subfractionated into cytoplasmic, PM and LDM fractions prior to measurement of kinase activity. PKB activity was found to be present in all three fractions (Figure 3.3.6a). An insulin-stimulated increase in activity occurred only in the cytoplasmic fraction, where a 3-fold response was observed. A similar result was obtained when the experiment was repeated using freshly-isolated rat adipocytes, instead of 3T3-L1 adipocytes (Figure 3.3.6b).

The insulin-stimulated increase in cytosolic PKB activity does not appear to be due to translocation from either the plasma membrane or the LDM fractions, as activity in those compartments are similar in the basal and insulin-stimulated states. A possibility is that cytosolic PKB is activated at a membrane site, but then returns to

the cytoplasm. Thus, determination of PKB activity in subcellular fractions at different insulin stimulation times may show this.

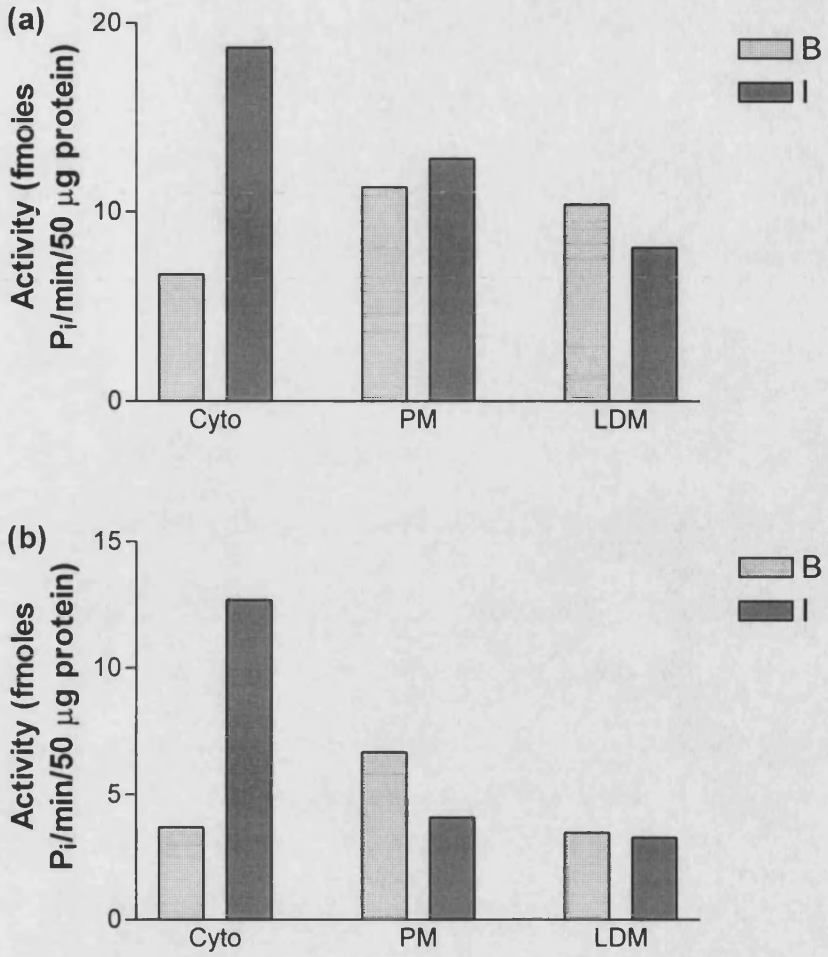

Figure 3.3.6. PKB Activity in Subcellular Fractions of 3T3-L1 and Rat Adipocytes.

3T3-L1 adipocytes (**a**) and freshly-isolated rat adipocytes (**b**) prepared as in *Methods 2.3.1* and *2.2.2* were treated without (**B**) or with (**I**) insulin for 20 min (100 nM for the former and 20 nM for the latter) . Cells were homogenized and subfractionated into cytoplasmic (**C**), plasma membrane (**PM**) and low density microsome (**LDM**) fractions as in *Methods 2.6.* Aliquots of 50 μg protein were subjected to PKB immunoprecipitation (2 μg anti-Akt1(C-20) conjugated to 10 μl protein G sepharose in 1 ml lysis buffer) and assayed for activity as in *Methods 2.5.2.* Values are from a single experiment in each case.

The increase in activity of cytosolic PKB is consistent with its role as a regulator of the cytosolic proteins GSK-3 (Cross *et al.*, 1995) and $pp70^{S6k}$ (Burgering and Coffer, 1995), but not with its role as a regulator of GLUT4 translocation, since insulin-

stimulated PI 3-K appears to act at an intracellular membrane compartment (Nave *et al.*, 1996a, and Ricort *et al.*, 1996). A possibility may be that, instead of acting at an intracellular compartment to initiate GLUT4 exocytosis, PKB may regulate signalling molecules involved in the fusion of GLUT4 vesicles with the plasma membrane.

3.3.4 Insulin Stimulation of Glucose Uptake in Permeabilized 3T3-L1 Adipocytes Pre-treated with Crosstide

Crosstide is a peptide that corresponds to a sequence from GSK-3 that is phosphorylated by PKB upon insulin stimulation of L6 myotubes (Cross *et al.*, 1995). If this peptide is present inside a cell, it may compete with endogenous substrates for phosphorylation by PKB, thereby attenuating the cellular responses regulated by the kinase. Thus, Crosstide was introduced into permeabilized 3T3-L1 adipocytes to determine if it would perturb insulin-stimulated glucose uptake. Permeabilized cells were pre-incubated with Crosstide (50 μg per dish) for 15 min prior to stimulation with 100 nM insulin for 20 min and subsequent measurement of 2-deoxy-D-glucose uptake (Figure 3.3.7). However, insulin-stimulated transport was the same regardless of whether the cells were pre-incubated with Crosstide or not. Increasing the amount of Crosstide per dish to 100 μg and reducing the insulin stimulation time to 5 min had no effect.

Thus, the use of Crosstide as a competitive inhibitor of PKB (at concentrations greater than 80 μM) does not appear to perturb submaximal insulin stimulation (100 nM for 5 min) of 2-deoxy-D-glucose uptake in 3T3-L1 adipocytes. A problem with interpreting this result is that it is not known whether PKB activity towards endogenous substrates was sufficiently blocked. As a control, the phosphorylation of endogenous GSK-3 or the activation of $pp70^{S6k}$ could be measured in response to insulin stimulation in the presence of Crosstide: attenuation of these PKB-regulated events would indicate competitive inhibition of PKB. These experiments were performed before it was discovered that it was no longer possible to assay PKB activity in immunoprecipitates with Crosstide as the substrate (*Results and Discussion 3.2*). Thus, the possibility that

there is a fault with the Crosstide peptide can be ruled out. An alternative method to inhibition of PKB activity in 3T3-L1 adipocytes might be to block its activation. Two residues in PKBα (ser-473 and thr-308) are phosphorylated in response to insulin stimulation (Alessi *et al.*, 1996). Thus, the introduction into 3T3-L1 adipocytes of two peptides corresponding to these phosphorylation sites of PKB may block insulin-activation of this kinase.

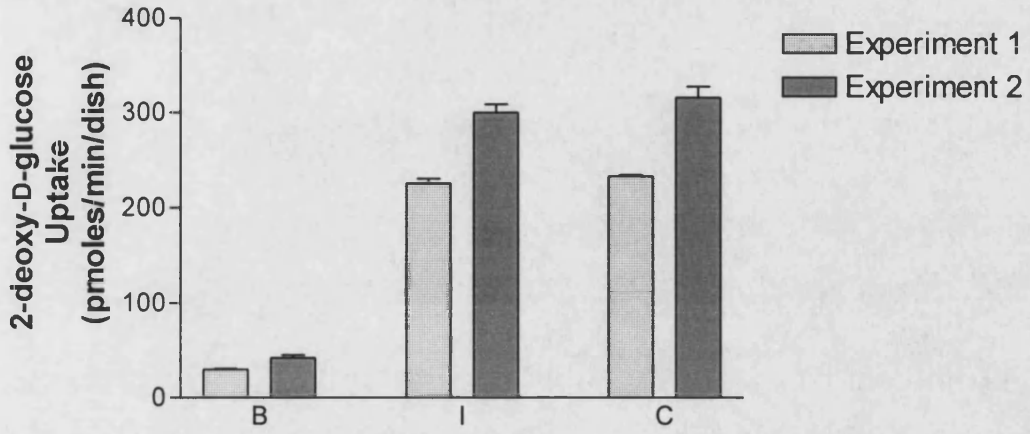

Figure 3.3.7. Introduction of Crosstide into Permeabilized 3T3-L1 Adipocytes prior to Measurement of Basal and Insulin-stimulated 2-deoxy-D-glucose Uptake.
Permeabilized 3T3-L1 adipocytes prepared as in *Methods 2.3.2* were pre-incubated for 15 min prior to treatment without (**B**) or with (**I**) 100 nM insulin; one group of cells were pre-incubated with Crosstide prior to insulin stimulation (**C**). Uptake of 2-deoxy-D-glucose was measured as in *Methods 2.4.2*. (**Experiment 1**) Pre-incubation with 50 μg Crosstide per dish and insulin stimulation for 20 min. (**Experiment 2**) Pre-incubation with 100 μg Crosstide per dish and insulin stimulation for 5 min. Values are the means from a single duplicate experiment. Error bars show Min and Max values.

3.4 Studies with 3T3-L1 Adipocytes Expressing a Constitutively Active Form of PKB

The expression of a constitutively active form of PKB in 3T3-L1 adipocytes has previously been shown to raise basal glucose uptake (Kohn *et al.*, 1996b). The ATB-BMPA photolabel was used to determine the effect of this constitutively active kinase on cell surface levels of GLUT1 and GLUT4. Thus, an assessment of the relative contributions of both transporter isoforms to the elevated glucose transport activity could be made.

3T3-L1 adipocytes expressing constitutively active PKB were supplied by Professor R.A. Roth. Fibroblasts were infected with a murine retrovirus encoding a variant of PKB known as myrAkt Δ4-129, which has the PH domain (amino acids 4-129) deleted and a *src* myristoylation sequence added onto the N-terminus. Control cells express wild-type PKB (wtAkt). Both PKB constructs have a hemagglutinin epitope tag at the C-terminus. Previous studies (Kohn *et al.*, 1996b) have shown that constitutively active PKB causes an increase in glucose uptake in basal cells by elevating GLUT1 expression and GLUT4 translocation. Total cellular GLUT1 was determined by Western blotting. GLUT4 translocation was measured by the group with two different methods. The first was a plasma membrane sheet assay. Cells grown on glass coverslips were sonicated to remove the cytoplasm. GLUT4 on the remaining plasma membrane was then detected by immunofluorescence microscopy. The second approach involved use of an anti-*myc* antibody binding assay. GLUT4 containing the c-*myc* epitope was detected on the cell surface with an anti-*myc* antibody. However, these techniques did not show a large increase in GLUT4 translocation upon insulin stimulation of control cells (these were 3T3-L1 adipocytes expressing either an empty vector or constitutively active PKB with a point mutation in the *src* myristoylation sequence). Also, cell surface GLUT1 was not quantitated. Thus, the ATB-BMPA photolabel was used to clarify matters.

To check that the 3T3-L1 adipocytes were expressing functional myrAkt Δ4-129, glucose transport was measured in the basal and insulin-stimulated state (Figure

3.4.1). For 3T3-L1 adipocytes expressing wtAkt (wtAkt cells), insulin stimulation increased 2-deoxy-D-glucose uptake by 21.6-fold over basal levels. For 3T3-L1 adipocytes expressing myrAkt Δ4-129 (myrAkt Δ4-129 cells), basal 2-deoxy-D-glucose transport was 38.9% of the insulin-stimulated value, and 9.6-fold greater than basal uptake in control wtAkt cells. These figures for the myrAkt Δ4-129 cells are different from those previously determined by Kohn *et al.* (1996b). They found that basal glucose uptake was 70% of the insulin-stimulated value, and 5-fold greater than in basal control 3T3-L1 adipocytes infected with an empty vector. Their method was slightly different, as they subtracted background counts (assessed by cytochalasin B binding) from all transport counts. However, this procedure would increase the basal/stimulated fold-increase determined in the study described here. Nevertheless, it is also shown here that the myrAkt Δ4-129 cells have an elevated level of basal glucose uptake.

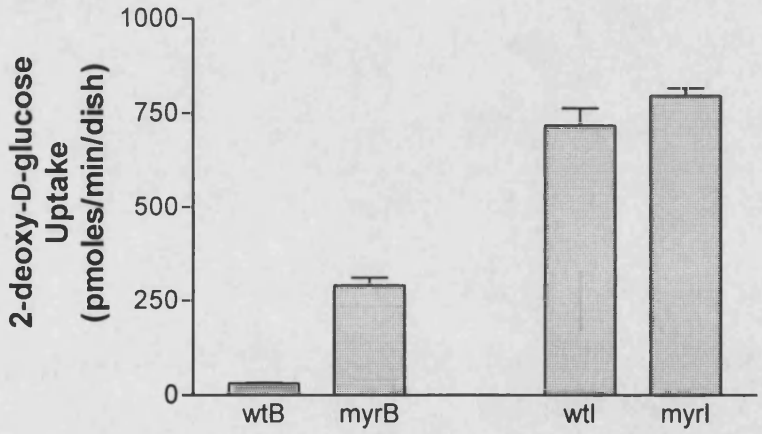

Figure 3.4.1. Uptake of 2-deoxy-D-glucose under Basal and Insulin-stimulated Conditions in 3T3-L1 Adipocytes Expressing wtAkt and myrAkt Δ4-129.

3T3-L1 adipocytes expressing wtAkt or myrAkt Δ4-129 were treated without (**wtB** and **myrB**, respectively) or with (**wtI** and **myrI**, respectively) 100 nM insulin for 20 min as in *Methods 2.3.1.* Uptake of 2-deoxy-D-glucose was measured as in *Methods 2.4.1.* Values are the means ± S.E.M. from four independent experiments, of which three were done in duplicate (n = 7).

Cell surface GLUT1 and GLUT4 in 3T3-L1 adipocytes expressing wtAkt and myrAkt Δ4-129 were quantitated by photolabelling with ATB-BMPA (Figures 3.4.2 and

3.4.3). For wtAkt cells, insulin treatment resulted in a 4.2-fold and a 10.5-fold increase in GLUT1 and GLUT4 respectively at the plasma membrane. These values are similar to those determined for non-transfected 3T3-L1 adipocytes (Calderhead *et al.*, 1990). In basal myrAkt Δ4-129 cells, cell surface GLUT1 was 6-fold greater than in basal wtAkt cells. Further, insulin stimulation of myrAkt Δ4-129 cells led to a 1.8-fold increase in GLUT1 at the cell surface. GLUT4 cell surface levels were similar in the insulin-stimulated state for both groups of cells. However, in the basal state, myrAkt Δ4-129 cells had 3.9-times more cell surface GLUT4 than wtAkt cells. Thus, the data reveals that the expression of constitutively active PKB in 3T3-L1 adipocytes leads to higher cell surface levels of GLUT1 and GLUT4 in the basal state. It also appears that total cellular GLUT1 (but not total cellular GLUT4) is increased, as determined by measurements of cell surface transporters in the insulin-stimulated state.

From the experiments described in this study, it is possible that the constitutively active PKB was not expressed to a similar level as that by Kohn *et al.* (1996b). This may explain the lower than expected basal glucose uptake in the myrAkt Δ4-129 cells (38.9% of the insulin-stimulated response, rather than 70%). Unfortunately, a hemagglutinin epitope antibody was not available at the time to allow immunoprecipitation of PKB, and thus a comparison of PKB activity between the two studies. However, an indicator of constitutive PKB activity is GLUT1 expression. Though total cellular GLUT1 was not quantitated in this study, a figure can be determined from the values obtained for cell surface GLUT1. It has been shown previously in 3T3-L1 adipocytes that half the total cellular transporters are present in the plasma membrane in the insulin-stimulated state (Yang and Holman, 1993). Assuming that this phenomenon also applies to 3T3-L1 adipocytes expressing wtAkt and myrAkt Δ4-129, then there is a 252% increase in GLUT1 expression in the latter compared with the former. This figure is greater than that of 55% determined by Kohn *et al.* (1996b) in their immunoblotting studies. Thus, in this regard, levels of constitutively active PKB appear to be comparable to those obtained by Kohn *et al.* (1996b).

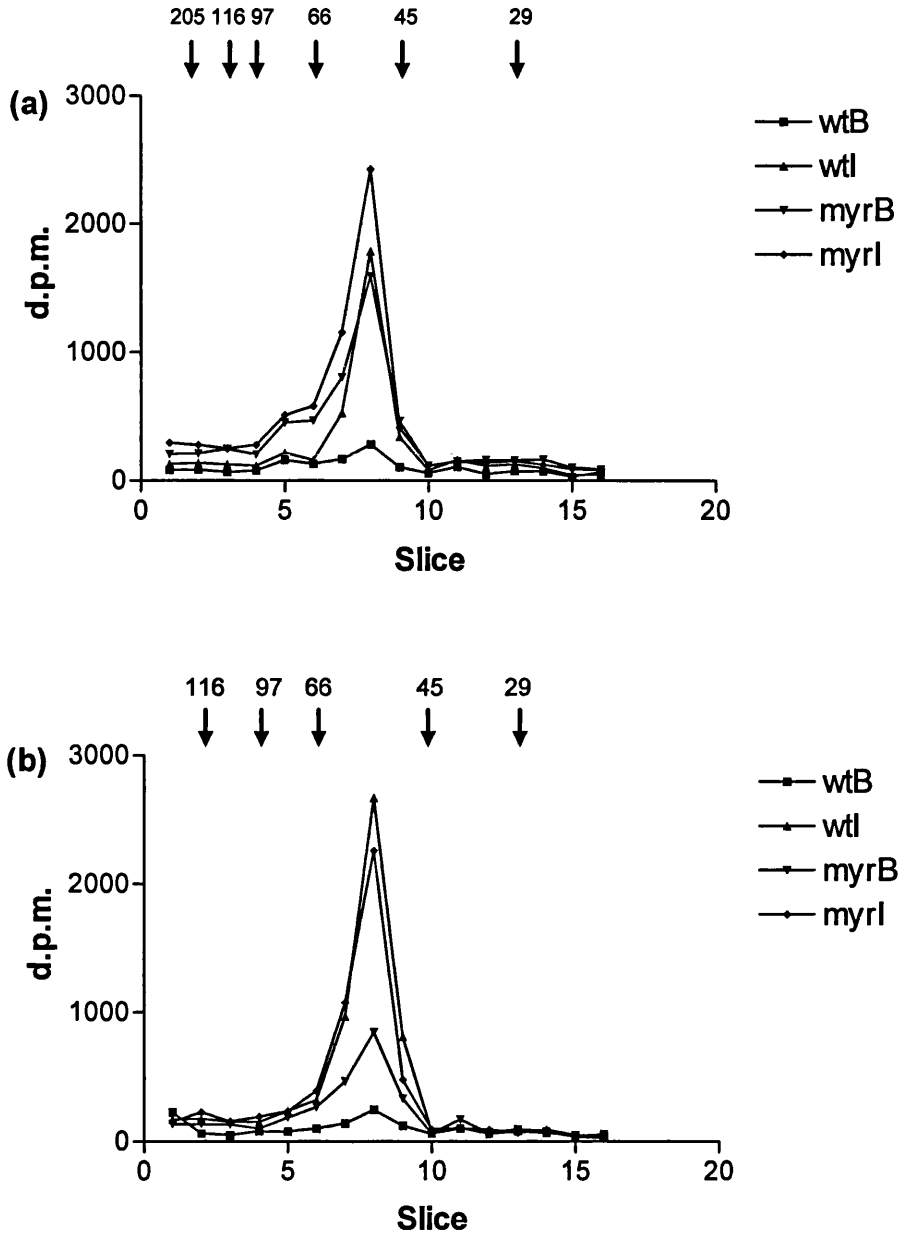

Figure 3.4.2. ATB-BMPA Photolabelling of Cell Surface GLUT1 and GLUT4 in Basal and Insulin-stimulated 3T3-L1 Adipocytes Expressing wtAkt and myrAkt Δ4-129.

3T3-L1 adipocytes expressing wtAkt or myrAkt Δ4-129 were treated without (**wtB** and **myrB**, respectively) or with (**wtI** and **myrI**, respectively) 100 nM insulin for 20 min, as in *Methods 2.3.1.* Cell surface transporters GLUT1 (**a**) and GLUT4 (**b**) were photolabelled with ATB-BMPA and processed, as in *Methods 2.4.3.* Molecular weight markers at the top of each graph have units of kDa. A typical experiment is shown.

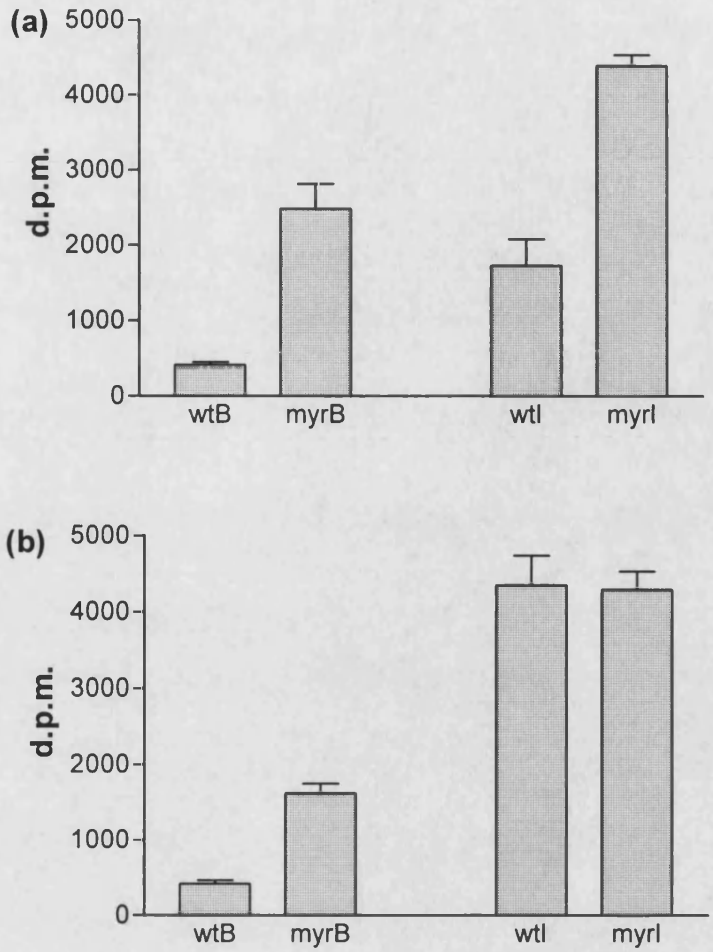

Figure 3.4.3. ATB-BMPA Photolabelling of Cell Surface GLUT1 and GLUT4 in Basal and Insulin-stimulated 3T3-L1 Adipocytes Expressing wtAkt and myrAkt Δ4-129.

3T3-L1 adipocytes expressing wtAkt or myrAkt Δ4-129 were treated without (**wtB** and **myrB**) or with (**wtI** and **myrI**) insulin before photolabelling of cell surface transporters with ATB-BMPA (as in Figure 3.4.2). Radioactivity counts associated with the transporters GLUT1 (**a**) and GLUT4 (**b**) were determined as in *Methods 2.4.3*. Values are the means ± S.E.M. from three (for GLUT1) and five (for GLUT4) independent experiments.

From the experiments described in this thesis, the basal level of cell surface GLUT4 in myrAkt Δ4-129 cells was 37% of that in the insulin-stimulated state. This figure is in contrast to Kohn *et al.* (1996b), who found maximal GLUT4 translocation in the basal state. The reason for this discrepancy does not appear to be due to reduced GLUT4 expression in the experiments described in this thesis, since insulin-stimulated levels of cell surface GLUT4 in 3T3-L1 adipocytes expressing wtAkt and myrAkt Δ4-129

were found to be similar. Further, the extent of GLUT4 translocation and 2-deoxy-D-glucose uptake in basal myrAkt Δ4-129 cells are similar (37% and 38.9% respectively of the insulin-stimulated response). These figures are consistent with the role of GLUT4 as the dominant isoform that contributes to glucose transport (Calderhead *et al.*, 1990). Thus, ATB-BMPA photolabelling has not underestimated cell surface levels of GLUT4. It is possible that Kohn *et al.* (1996b) may have overestimated the extent of GLUT4 translocation. First, ATB-BMPA photolabelling is a more quantitative method of determining levels of cell surface transporters. Second, though Kohn *et al.* (1996b) observed similar levels of cell surface GLUT4 in basal and insulin-stimulated myrAkt Δ4-129 cells, this does not correlate with their transport studies, where the basal response was 70% of the insulin-stimulated response. Nevertheless, taking glucose uptake as an indicator of GLUT4 translocation, the data from Kohn *et al.* (1996b) would indicate cell surface GLUT4 in basal myrAkt Δ4-129 cells that is around 70% of the insulin-stimulated response. Thus, Kohn *et al.* (1996b) would still observe greater GLUT4 translocation in basal myrAkt Δ4-129 cells than in the study described here. The reason for this discrepancy is unclear, especially as the expression of GLUT1 in myrAkt Δ4-129 cells reported here is comparable, if not greater, than that observed by Kohn *et al.* (1996b). In any case, constitutively active PKB does not appear to cause maximal GLUT4 translocation.

The ATB-BMPA photolabelling studies show that increased GLUT1 expression in myrAkt Δ4-129 cells is associated with an increase in cell surface levels in the basal and insulin-stimulated states. Though insulin-stimulated cell surface levels of GLUT1 are 2.5-fold greater in myrAkt Δ4-129 cells than in wtAkt cells, a similar difference was not observed in terms of 2-deoxy-D-glucose uptake. Thus, insulin-stimulated 2-deoxy-D-glucose transport in wtAkt cells was 88% of that in myrAkt Δ4-129 cells. Taken together with the observation that insulin-stimulated cell surface levels of GLUT4 were unchanged by the expression of myrAkt Δ4-129, it appears that increased GLUT1 expression does not contribute to the elevated glucose uptake in basal myrAkt Δ4-129 cells.

To determine the mechanism of action of PKB in the elevation of cell surface GLUT4, it would be interesting to examine the recycling of GLUT4. Basal myrAkt Δ4-129 cells would be labelled with ATB-BMPA and incubated for different lengths of time, such that labelled transporters are internalized. Then, the plasma membrane can subsequently be isolated, so that cell surface GLUT4 can be quantitated. Thus, the rate of internalization of GLUT4 can be determined, and rates of endocytosis and exocytosis estimated (Yang and Holman, 1993). This would allow an assessment of the relative contributions of both constants to GLUT4 translocation.

The low translocation of GLUT4 in basal myrAkt Δ4-129 cells compared with that in insulin-stimulated cells may represent a mechanism downstream of PKB that down-regulates cell surface GLUT4 in response to continuous stimulation. Thus, it is necessary to examine the effects of acute stimulation of PKB activity, as this would be a closer representation of normal physiological conditions. A possibility is treatment of 3T3-L1 adipocytes with PI 3,4-P_2. However, it does not fully activate PKB *in vitro* (Frech *et al.*, 1997), though the scenario may be different *in vivo*, as PI 3,4-P_2 was found to increase PKB activity in NIH 3T3 cells comparably to PDGF stimulation (Franke *et al.*, 1997). The availability of a compound that specifically inhibits PKB would also be useful in determining its role in insulin-stimulated GLUT4 translocation. An alternative to stable expression of myrAkt Δ4-129 in 3T3-L1 adipocytes would be to transiently express wild-type and dominant negative PKB. This method of expression has already been used by Dudek *et al.* (1997) to implicate a role for PKB in apoptosis in neural cells.

In summary, the data shows that the expression of constitutively active PKB in 3T3-L1 adipocytes leads to an increase in basal glucose uptake, but not to maximal insulin-stimulated levels. Though there is an increase in GLUT1 expression, the cause of the elevated basal glucose uptake appears to be due mainly to increased cell surface GLUT4. Thus, constitutively active PKB appears to stimulate submaximal glucose transport activity via GLUT4 translocation.

3.5 Studies with PKB in 3T3-L1 and Rat Adipocytes Chronically Treated with Insulin

Chronic treatment of 3T3-L1 adipocytes with insulin (500 nM for 24 h) leads to down-regulation of cell surface GLUT4, though there is no change in total cellular GLUT4 (Kozka *et al.*, 1991). This transporter isoform can no longer be recruited to the plasma membrane when the cells are washed and restimulated with insulin. Further, there is no change in the binding of insulin to its receptor following chronic treatment with insulin. Thus, the observed insulin resistance implies a defect in the insulin signalling pathway. The identification of the component(s) involved may help in understanding the mechanism underlying insulin-stimulated GLUT4 translocation. Down-regulation of PKB activity following chronic treatment of adipocytes with insulin would support the idea that the kinase is involved in this process.

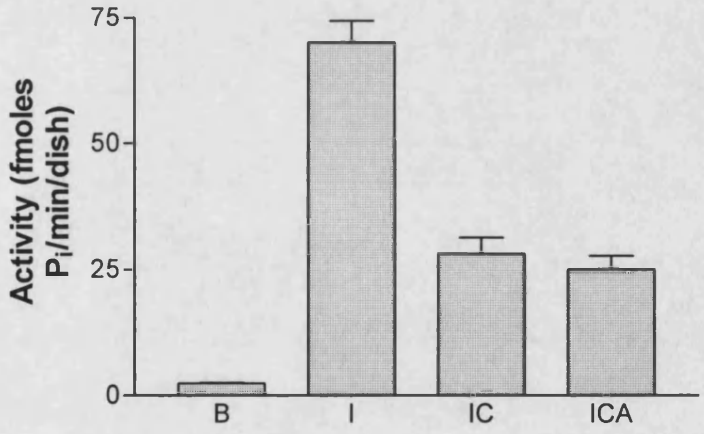

Figure 3.5.1. PKB Activity Following Chronic Treatment of 3T3-L1 Adipocytes with Insulin.

3T3-L1 adipocytes were either: acutely treated without (**B**) or with (**I**) 100 nM insulin for 20 min (*Methods 2.3.1*); chronically treated with 500 nM insulin for 24 h (**IC**) (*Methods 2.3.3*); chronically treated with 500 nM insulin for 24 h and incubated in KRM for 1 h prior to 100 nM insulin stimulation for 20 min (**ICA**) (*Methods 2.3.4*). PKB was immunoprecipitated and assayed for activity as in *Methods 2.5.2*. Values are the means ± S.E.M. from two independent experiments done in duplicate (n = 4).

In this thesis, experiments were undertaken in 3T3-L1 adipocytes to determine if insulin resistance induced by chronic treatment with insulin was associated with a down-regulation of PKB activity (Figure 3.5.1). A 24 h treatment with 500 nM insulin led to PKB activity that was 40.1% of that in cells acutely stimulated with 100 nM insulin for 20 min. When 3T3-L1 adipocytes chronically treated with insulin were incubated in Krebs-Ringers-MES buffer to remove bound insulin before an acute insulin stimulation was given, no further increase in PKB activity was observed. Thus, chronic treatment of 3T3-L1 adipocytes with insulin appears to down-regulate PKB activity. Further, PKB activity is resistant to restimulation.

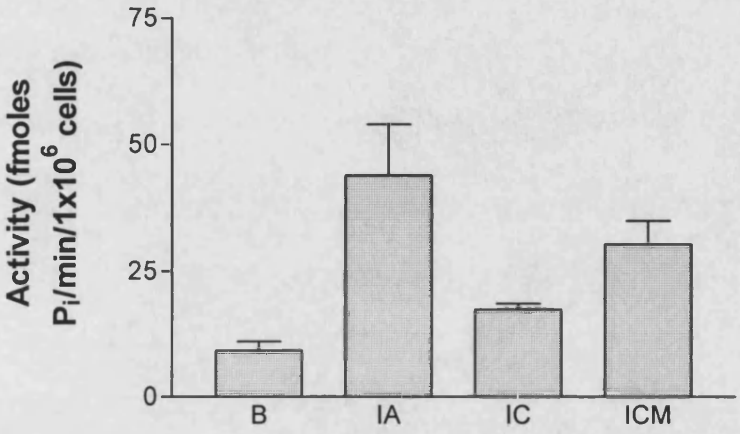

Figure 3.5.2. PKB Activity in Rat Adipocytes Maintained in Culture in the Presence of Insulin with or without Metformin.

Freshly-isolated rat adipocytes were either cultured for 24 h before acute treatment without (**B**) or with (**I**) 20 nM insulin for 30 min, or they were chronically treated with 500 nM insulin in a 24 h culture without (**IC**) or with (**ICM**) 1 mM metformin (*Methods 2.2.2* and *2.3.5*). PKB was immunoprecipitated from 0.5 ml 40% (v/v) cells and assayed for activity as in *Methods 2.5.2*. Values are the means ± S.E.M. from four independent experiments. $P < 0.05$ for **B** vs. **IA**, **IA** vs. **IC**, and **IC** vs. **ICM**; $P > 0.05$ (ns) for **IA** vs. **ICM**.

For rat adipocytes maintained in a 24 h culture with 500 nM insulin, the presence of 1 mM metformin prevents down-regulation of cell surface GLUT4 (Kozka and Holman, 1993). Thus, experiments were undertaken to determine if metformin could also prevent the down-regulation of PKB activity following chronic treatment of rat adipocytes with insulin (Figure 3.5.2). Acute stimulation with 20 nM insulin of rat

adipocytes cultured under basal conditions produced a 4.7-fold increase in PKB activity over unstimulated basal levels. For rat adipocytes cultured with 500 nM insulin for 24 h, PKB activity was 40% of that in adipocytes cultured under basal conditions before acute stimulation with 20 nM insulin. The presence of 1 mM metformin during the 24 h culture with 500 nM insulin resulted in PKB activity that was not significantly different from that in rat adipocytes cultured under basal conditions before acute stimulation with 20 nM insulin ($P < 0.05$). Thus, metformin appears to block the down-regulation of PKB activity that is associated with chronic treatment of rat adipocytes with insulin.

Insulin stimulation of freshly-isolated rat adipocytes results in the migration of PKB to higher molecular weight regions on SDS-PAGE gels (Kohn *et al.*, 1995). This effect was investigated in rat adipocytes chronically treated with insulin and metformin (Figure 3.5.3).

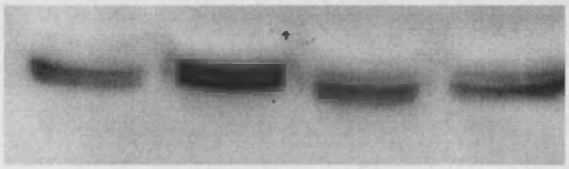

B **I** **IC** **ICM**

Figure 3.5.3. The Phosphorylation State of PKB in Rat Adipocytes Maintained in Culture in the Presence of Insulin with or without Metformin.

Rat adipocytes were prepared and treated as in Figure 3.5.2. Protein in cell lysates were resolved on 10% SDS-PAGE gels, transferred to nitrocellulose and immunoblotted with anti-Akt1(C-20) (*Methods 2.7*).

Acute stimulation with 20 nM insulin of rat adipocytes cultured under basal conditions produced multiple bands for PKB that were of higher molecular weight than those in cells cultured without insulin. The presence of 500 nM insulin during the 24 h culture of rat adipocytes prevented this migration, but did not if 1 mM metformin was also present during the chronic treatment. Thus, the results confirm that PKB activity is

down-regulated following chronic treatment of rat adipocytes with insulin, and that this down-regulation is prevented if metformin is present during the chronic treatment.

In the study described here, chronic treatment of 3T3-L1 adipocytes with insulin led to PKB activity that was less than half that seen with acute stimulation. In addition, the activity could not be further raised following a washing procedure and acute restimulation with insulin. No changes in the expression of PKB were detected in rat adipocytes chronically treated with insulin. Thus, chronic treatment with insulin down-regulates PKB activity without affecting expression, as well as rendering adipocytes resistant to restimulation of its activity. This observation is comparable to the effects of prolonged insulin stimulation on cell surface GLUT4 (Kozka *et al.*, 1991).

Chronic treatment of rat adipocytes with insulin decreases tyrosine phosphorylation of the insulin receptor by 70% compared with an acute insulin stimulation (Pryor *et al.*, 1997). Also, some groups have observed a reduction in IRS-1 expression with prolonged insulin treatment of 3T3-L1 adipocytes (Rice *et al.*, 1993, and Ricort *et al.*, 1995), though others have not for rat adipocytes (Pryor *et al.*, 1997). Thus, down-regulation of PKB activity due to chronic treatment of adipocytes with insulin is likely to be a consequence of the perturbation of these upstream components of the insulin signalling pathway. Consistent with this idea is the absence of reduced PKB expression with prolonged insulin stimulation: instead, PKB is present in a lower phosphorylated state. However, it cannot be ruled out that other factors may be directly down-regulating PKB activity, perhaps by covalent modification. To investigate this possibility, it would be necessary to be able to activate PKB via a mechanism independent of the insulin signalling pathway. One potential method would be treatment of adipocytes with PI 3,4-P_2, as this phospholipid has been shown to directly increase PKB activity in NIH 3T3 cells (Franke *et al.*, 1997). Another possibility would be to stimulate adipocytes with isoproterenol, as this drug has been shown to stimulate PKB activity via a wortmannin-insensitive pathway in rat adipocytes (Moule *et al.*, 1997). Thus, if either or both compounds are able to stimulate PKB activity in adipocytes chronically treated with insulin, then it would

indicate that PKB has not been directly down-regulated (that is, it has not been rendered inactivatable by prolonged insulin stimulation).

In the study described here, the inclusion of metformin during chronic treatment of rat adipocytes with insulin alleviated the down-regulation of PKB activity. Thus, as for cell surface GLUT4 (Kozka and Holman, 1993), metformin counteracts the effects of prolonged insulin treatment. Though the mechanism of action of metformin is unknown, Pryor *et al.* (1997) have shown that the reduction of the tyrosine phosphorylation of the insulin receptor of rat adipocytes chronically treated with insulin is prevented by concomitant metformin treatment. Thus, action at the level of the insulin receptor may explain the counteractive effect of metformin on the down-regulation of PKB. Consistent with this idea is the unchanged expression of PKB when rat adipocytes are chronically treated with insulin and metformin. Instead, PKB remains in a higher phosphorylated state, similar to that seen with acute stimulation of adipocytes with insulin. However, the action of metformin at other points in the insulin signalling pathway cannot be ruled out. To examine this possibility, two further experiments could be undertaken. The first would be to incubate immunoprecipitated PKB from basal cells (or from cells chronically treated with insulin) with metformin to determine if it directly activates the kinase. The second would be as for the first suggestion, but in the presence of cell lysate minus the insulin receptor, as metformin may act indirectly via a cytosolic factor on PKB activity.

In summary, the defects in the insulin signalling pathway following chronic treatment of adipocytes with insulin include down-regulation of PKB activity. Thus, the involvement of the kinase in the regulation of glucose transport cannot be ruled out. However, further studies are required to determine if the down-regulation of PKB activity is merely a secondary effect due to perturbation of the insulin receptor and IRS-1.

4.0 CONCLUSIONS

The aim of this study was to investigate the role of two components of the insulin signalling pathway in the regulation of glucose uptake: the IRS-1 PH domain and PKB. The IRS-1 PH domain does not appear to be required for IRS-1-mediated activation of PI 3-K, an enzyme implicated to be involved in insulin-stimulated glucose uptake. Thus, the role of the PH domain for the normal functioning of IRS-1 needs to be established, and in particular, its role in relation to insulin-regulated glucose uptake. PKB is an insulin-activated kinase that is downstream of PI 3-K. Thus, PKB may be a link between insulin stimulation of PI 3-K activity and the subsequent elevation of glucose transport activity.

Previous studies have indicated that the PH domain acts as a membrane-targeting signal. First, the PH domain can bind to $G\beta\gamma$ and PI 4,5-P_2 (Touhara *et al.*, 1994, and Harlan *et al.*, 1994): both are membrane-localized. Second, the deletion of the PLC δ_1 PH domain abolishes the ability of the enzyme to associate with the plasma membrane (Paterson *et al.*, 1995). Thus, it is possible that the PH domain may perform the same function for IRS-1. From this thesis, indirect evidence is consistent with the PH domain targeting IRS-1 to the plasma membrane: the introduction of exogenous IRS-1 PH domain into permeabilized 3T3-L1 adipocytes partially blocks insulin-stimulated IRS-1 phosphorylation. The additional requirement of the PTB domain for the targeting of IRS-1 to the insulin receptor (Yenush *et al.*, 1996) may explain why total inhibition of IRS-1 phosphorylation was not observed. However, it needs to be demonstrated that the IRS-1 PH domain can directly associate with the plasma membrane. Further, if there is an interaction between the two, it needs to be determined if the PH domain binds via a protein or a lipid. In the study described in this thesis, the lack of success in identifying an IRS-1 PH domain-binding protein does not eliminate the possibility that such a molecule exists, given that other groups have found protein-protein interactions involving the PH domain of other proteins (Touhara *et al.*, 1994, and Konishi *et al.*, 1995). However, the ability of phospholipids to bind the IRS-1 PH domain needs to be explored, given that other

groups have observed such interactions with other PH domains (Harlan *et al.*, 1994, and Lemmon *et al.*, 1995).

Since the PH domain appears to target IRS-1 to the plasma membrane, it is entirely possible that it may target the same protein to the LDM fraction of 3T3-L1 adipocytes. Support for this idea is provided by observations that tyrosine-phosphorylated IRS-1 appears in this membrane fraction following insulin stimulation of 3T3-L1 adipocytes (Ricort *et al.*, 1996). However, indirect evidence from this thesis suggest otherwise. Thus, in permeabilized 3T3-L1 adipocytes, exogenous IRS-1 PH domain does not block insulin-stimulated glucose transport or PI 3-K activity in the LDM. However, and importantly, it needs to be shown that the IRS-1 PH domain can interact with the LDM.

To demonstrate a role for PKB in insulin-stimulated glucose uptake, it would be preferable to use a specific inhibitor and activator of the enzyme. The availability of these compounds would help determine if PKB is both essential and sufficient for insulin stimulation of GLUT4 translocation. The phospholipid PI 3,4-P_2 has been shown to stimulate PKB activity *in vivo* in NIH 3T3 cells (Franke *et al.*, 1997). However, this compound may also activate other PH domain-containing proteins, so it may not be an appropriate choice of PKB activator. In this thesis, the use of Crosstide as a competitive inhibitor of insulin-stimulated PKB action in permeabilized 3T3-L1 adipocytes was not successful. However, the subsequent response that was measured was glucose uptake. It needs to be determined if Crosstide can affect insulin-stimulated cellular events that have been established as downstream of PKB, such as the activation of $pp70^{S6k}$ and the inactivation of GSK-3. Thus, due to the unavailability of activators and inhibitors of PKB, alternative experiments have to be undertaken instead.

From the experiments described in this thesis, circumstantial evidence is consistent with the idea that PKB is involved in insulin-stimulated glucose uptake in 3T3-L1 adipocytes. First, maximum insulin activation of PKB activity precedes maximum insulin stimulation of glucose transport in 3T3-L1 adipocytes. Thus, PKB activity

reaches near-maximal levels following 2 min insulin stimulation, whereas glucose uptake is maximal after 10-15 min insulin stimulation (Fingar and Birnbaum, 1994b). Similarly, following wortmannin treatment of insulin-stimulated 3T3-L1 adipocytes, the inactivation of PKB occurs more rapidly than the decline of glucose transport. The half-times for the reduction of the insulin-stimulated response are 52.8 s for the former and 5 min for the latter. Further, okadaic acid can counteract wortmannin inhibition of insulin-stimulated PKB activity and glucose transport activity. However, the site of action of okadaic acid is not fully understood. Thus, okadaic acid may affect glucose transport at another site other than that at the level of PKB. Second, the dose-response curve for insulin-stimulated PKB activity is to the right of that for insulin-stimulated glucose uptake. This observation is consistent with the concept of amplification of the signal from an upstream component of the signalling pathway.

Further circumstantial evidence for a role for PKB in insulin-stimulated glucose transport was obtained using adipocytes made insulin-resistant by chronic treatment with insulin. PKB activity is down-regulated following this treatment and cannot be elevated following washing of the cells and restimulation with insulin. Further, the inclusion of metformin during chronic treatment with insulin prevents the down-regulation of PKB activity. Thus, the data indicate that PKB may be involved in the signalling pathway linking the insulin receptor to GLUT4 translocation. However, chronic treatment with insulin affects signalling at the level of the insulin receptor and IRS-1 (Pryor *et al.*, 1997, Rice *et al.*, 1993, and Ricort *et al.*, 1995). Thus, since multiple pathways emanating from the receptor are likely to be perturbed, other aspects of insulin action not involved in glucose transport may be affected.

A method of investigating the effects of PKB activity on glucose uptake and GLUT4 translocation has involved the expression of a constitutively active form of PKB in 3T3-L1 adipocytes (Kohn *et al.*, 1996b). In this thesis, it was observed that the expression of this form of PKB leads to an elevation of glucose transport activity that is 38.9% of that in the insulin-stimulated state. This value is less than the 70% determined by Kohn *et al.* (1996b). Even so, they did not observe maximal glucose uptake in basal 3T3-L1 adipocytes expressing constitutively active PKB. The

increased basal glucose uptake appears to be the result of increased GLUT4 translocation, rather than increased GLUT1 expression. First, the extent of GLUT4 translocation is similar to that of increased glucose transport activity. Second, compared with control cells, there is an increase in cell surface levels of GLUT1, but not of GLUT4, in the insulin-stimulated state. However, there is no corresponding increase in maximal insulin-stimulated glucose uptake. Thus, the data show that constitutively active PKB is capable of increasing glucose uptake via GLUT4 translocation, but not to maximal levels. A potential caveat with this method is that the long-term effects of elevated PKB activity are manifested. Thus, it would be preferable to observe the effects of acute activation of PKB.

PKB becomes constitutively active in 3T3-L1 adipocytes if it is membrane-localized via the addition of an N-terminal myristoylation signal sequence to a PH domain deletion mutant of the kinase (Kohn *et al.*, 1996b). However, from the experiments described in this thesis, insulin stimulation only increases endogenous PKB activity in the cytoplasmic fraction of 3T3-L1 adipocytes. Possibly, PKB is activated at a membrane site before it migrates to the cytoplasm. However, the site of action for endogenous PKB would be different to that for constitutively active PKB. Thus, for the 3T3-L1 adipocytes expressing the constitutively active kinase, the elevated basal glucose uptake may be occurring via a mechanism that does not operate under normal physiological conditions. However, it could be equally argued that the constitutively active form of PKB is unable to cause maximal GLUT4 translocation because it is not able to act in the cytosol like endogenous PKB. The expression of alternative constitutively active forms of PKB in 3T3-L1 adipocytes would help to clarify matters.

In summary, there is an argument for and against a role for PKB in insulin-stimulated glucose uptake in adipocytes. The argument for the case is as follows. First, maximal insulin stimulation of PKB activity occurs before that of glucose transport activity. Second, wortmannin inhibits insulin-stimulated PKB activity more rapidly than insulin-stimulated glucose uptake. Third, activation of PKB is less sensitive to insulin stimulation than elevation of glucose uptake. Fourth, PKB activity, like cell surface

GLUT4, can be down-regulated by chronic treatment of adipocytes with insulin. Fifth, constitutively active PKB can raise basal glucose uptake via GLUT4 translocation. The argument against the case is as follows. First, the evidence from all the experiments undertaken with non-transfected adipocytes is only circumstantial. Thus, the evidence does not demonstrate a direct link between PKB activity and glucose uptake. Second, constitutively active PKB does not appear to maximally increase the levels of GLUT4 at the plasma membrane, since insulin stimulation can cause further translocation of the transporter isoform. Finally, since the constitutively active form of PKB is membrane-localized, then it may not be acting in a similar manner to insulin-stimulated PKB. This observation can be used to argue for or against a role for PKB in insulin-stimulated glucose uptake.

5.0 REFERENCES

Alessi, D.R., Andjelkovic, M., Caudwell, B., Cron, P., Morrice, N., Cohen, P., and Hemmings, B.A. (1996). Mechanism of activation of protein kinase B by insulin and IGF-1. *EMBO J.* **15**(23): 6541-6551.

Alessi, D.R., James, S.R., Downes, C.P., Holmes, A.B., Gaffney, P.R.J., Reese, C.B., and Cohen, P. (1997). Characterization of a 3-phosphoinositide-dependent protein kinase which phosphorylates and activates protein kinase Bα. *Current Biol.* **7**: 261-269.

Andjelkovic, M., Jakubowicz, T., Cron, P., Ming, X.-F., Han, J.-W., and Hemmings, B.A. (1996). Activation and phosphorylation of a pleckstrin homology domain containing protein kinase (RAC-PK/PKB) promoted by serum and protein phosphatase inhibitors. *Proc. Natl. Acad. Sci. USA* **93**: 5699-5704.

Araki, E., Lipes, M.A., Patti, M.-E., Bruning, J.C., Haag III, B., Johnson, R.S., and Kahn, C.R. (1994). Alternative pathway of insulin signalling in mice with targeted disruption of the *IRS-1* gene. *Nature* **372**: 186-190.

Backer, J.M., Myer Jr., M.G., Shoelson, S.E., Chin, D.J., Sun, X.-J., Miralpeix, M., Hu, P., Margolis, B., Skolnik, E.Y., Schlessinger, J., and White, M.F. (1992). Phosphatidylinositol 3'-kinase is activated by association with IRS-1 during insulin stimulation. *EMBO J.* **11**(9): 3469-3479.

Backer, J.M., Wjasow, C., and Zhang, Y. (1997). *In vitro* binding and phosphorylation of insulin receptor substrate 1 by the insulin receptor. *Eur. J. Biochem.* **245**: 91-96.

Baltensperger, K., Kozma, L.M., Cherniack, A.D., Klarlund, J.K., Chawla, A., Banerjee, U., and Czech, M.P. (1993). Binding of the Ras activator Son of sevenless to insulin receptor substrate-1 signaling complexes. *Science* **260**: 1950-1952.

Baltensperger, K., Kozma, L.M., Jaspers, S.R., and Czech, M.P. (1994). Regulation by insulin of phosphatidylinositol 3'-kinase bound to α- and β-isoforms of p85 regulatory subunit. *J. Biol. Chem.* **269**(46): 28937-28946.

Bandyopadhyay, G., Standaert, M.L., Zhao, L., Yu, B., Avignon, A., Galloway, L., Karnam, P., Moscat, J., and Farese, R.V. (1997). Activation of protein kinase C (α, β, and ζ) by insulin in 3T3/L1 cells. *J. Biol. Chem.* **272**(4): 2551-2558.

Bellacosa, A., Testa, J.R., Staal, S.P., and Tsichlis, P.N. (1991). A retroviral oncogene, *akt*, encoding a serine-threonine kinase containing an SH2-like region. *Science* **254**: 274-277.

Birnbaum, M.J., Haspel, H.C., and Rosen, O.M. (1986). Cloning and characterization of a cDNA encoding the rat brain glucose-transporter protein. *Proc. Natl. Acad. Sci. USA* **83**: 5784-5788.

Birnbaum, M.J. (1989). Identification of a novel gene encoding an insulin-responsive glucose transporter protein. *Cell* **57**: 305-315.

Burgering, B.M.T. and Coffer, P.J. (1995). Protein kinase B (c-Akt) in phosphatidylinositol-3-OH kinase signal transduction. *Nature* **376**: 599-602.

Calderhead, D.M., Kitagawa, K., Tanner, L.I., Holman, G.D., and Lienhard, G.E. (1990). Insulin regulation of the two glucose transporters in 3T3-L1 adipocytes. *J. Biol. Chem.* **265**(23): 13800-13808.

Charron, M.J., Brosius III, F.C., Alper, S.L., and Lodish, H.F. (1989). A glucose transport protein expressed predominately in insulin-responsive tissues. *Proc. Natl. Acad. Sci. USA* **86**: 2535-2539.

Cheatham, B., Vlahos, C.J., Cheatham, L., Wang, L., Blenis, J., and Kahn, C.R. (1994). Phosphatidylinositol 3-kinase activation is required for insulin stimulation of pp70 S6 kinase, DNA synthesis, and glucose transporter translocation. *Mol. Cell. Biol.* **14**(7): 4902-4911.

Cheatham, B., Volchuk, A., Kahn, C.R., Wang, L., Rhodes, C.J., and Klip, A. (1996). Insulin-stimulated translocation of GLUT4 glucose transporters requires SNARE-complex proteins. *Proc. Natl. Acad. Sci. USA* **93**: 15169-15173.

Cheng, J.Q., Godwin, A.K., Bellacosa, A., Taguchi, T., Franke, T.F., Hamilton, T.C., Tsichlis, P.N., and Testa, J.R. (1992). *AKT2*, a putative oncogene encoding a member of a subfamily of protein-serine/threonine kinases, is amplified in human ovarian carcinomas. *Proc. Natl. Acad. Sci. USA* **89**: 9267-9271.

Chung, J., Grammer, T.C., Lemon, K.P., Kazlauskas, A., and Blenis, J. (1994). PDGF- and insulin-dependent $pp70^{S6k}$ activation mediated by phosphatidylinositol-3-OH kinase. *Nature* **370**: 71-75.

Clark, A.E. and Holman, G.D. (1990). Exofacial photolabelling of the human erythrocyte glucose transporter with an azitrifluoroethylbenzoyl-substituted bismannose. *Biochem. J.* **269**: 615-622.

Clark, A.E., Holman, G.D., and Kozka, I.J. (1991). Determination of the rates of appearance and loss of glucose transporters at the cell surface of rat adipose cells. *Biochem. J.* **278**: 235-241.

Clarke, J.F., Young, P.W., Yonezawa, K., Kasuga, M., and Holman, G.D. (1994). Inhibition of the translocation of GLUT1 and GLUT4 in 3T3-L1 cells by the phosphatidylinositol 3-kinase inhibitor, wortmannin. *Biochem. J.* **300**: 631-635.

Coffer, P.J. and Woodgett, J.R. (1991). Molecular cloning and characterisation of a novel putative protein-serine kinase related to the cAMP-dependent and protein kinase C families. *Eur. J. Biochem.* **201**: 475-481.

Corvera, S., Jaspers, S., and Pasceri, M. (1991). Acute inhibition of insulin-stimulated glucose transport by the phosphatase inhibitor, okadaic acid. *J. Biol. Chem.* **266**(14): 9271-9275.

Corvera, S., Chawla, A., Chakrabarti, R., Joly, M., Buxton, J., and Czech, M.P. (1994). A double leucine within the GLUT4 glucose transporter COOH-terminal domain functions as an endocytosis signal. *J. Cell Biol.* **126**(4): 979-989.

Cross, D.A.E., Alessi, D.R., Cohen, P., Andjelkovich, M., and Hemmings, B.A. (1995). Inhibition of glycogen synthase kinase-3 by insulin mediated by protein kinase B. *Nature* **378**: 785-789.

Cross, D.A.E., Watt, P.W., Shaw, M., van der Kaay, J., Downes, C.P., Holder, J.C., and Cohen, P. (1997). Insulin activates protein kinase B, inhibits glycogen synthase kinase-3 and activates glycogen synthase by rapamycin-insensitive pathways in skeletal muscle and adipose tissue. *FEBS Lett.* **406**: 211-215.

Cushman, S.W. and Wardzala, L.J. (1980). Potential mechanism of insulin action on glucose transport in the isolated rat adipose cell. *J. Biol. Chem.* **255**(10): 4758-4762.

Czech, M.P., Chawla, A., Woon, C.-W., Buxton, J., Armoni, M., Tang, W., Joly, M., and Corvera, S. (1993). Exofacial epitope-tagged glucose transporter chimeras reveal COOH-terminal sequences governing cellular localization. *J. Cell Biol.* **123**(1): 127-135.

Denton, R.M. and Tavare, J.M. (1995). Does mitogen-activated-protein kinase have a role in insulin action? *Eur. J. Biochem.* **227**: 597-611.

Didichenko, S.A., Tilton, B., Hemmings, B.A., Ballmer-Hofer, K., and Thelen, M. (1996). Constitutive activation of protein kinase B and phosphorylation of p47phox by a membrane-targeted phosphoinositide 3-kinase. *Current Biol.* **6**(10): 1271-1278.

Dudek, H., Datta, S.R., Franke, T.F., Birnbaum, M.J., Yao, R., Cooper, G.M., Segal, R.A., Kaplan, D.R., and Greenberg, M.E. (1997). Regulation of neuronal survival by the serine-threonine protein kinase Akt. *Science* **275**: 661-665.

Ebina, Y., Ellis, L., Jarnagin, K., Edery, M., Graf, L., Clauser, E., Ou, J.-H., Masiarz, F., Kan, Y.W., Goldfine, I.D., Roth, R.A., and Rutter, W.J. (1985). The human insulin receptor cDNA: the structural basis for hormone-activated transmembrane signalling. *Cell* **40**: 747-758.

Eck, M.J., Dhe-Paganon, S., Trub, T., Nolte, R.T., and Shoelson, S.E. (1996). Structure of the IRS-1 PTB domain bound to the juxtamembrane region of the insulin receptor. *Cell* **85**: 695-705.

Farese, R.V., Standaert, M.L., Francois, A.J., Ways, K., Arnold, T.P., Hernandez, H., and Cooper, D.R. (1992). Effects of insulin and phorbol esters on subcellular distribution of protein kinase C isoforms in rat adipocytes. *Biochem. J.* **288**: 319-323.

Fingar, D.C., Hausdorff, S.F., Blenis, J., and Birnbaum, M.J. (1993). Dissociation of pp70 ribosomal protein S6 kinase from insulin-stimulated glucose transport in 3T3-L1 adipocytes. *J. Biol. Chem.* **268**(4): 3005-3008.

Fingar, D.C. and Birnbaum, M.J. (1994a). A role for Raf-1 in the divergent signaling pathways mediating insulin-stimulated glucose transport. *J. Biol. Chem.* **269**(13): 10127-10132.

Fingar, D.C. and Birnbaum, M.J. (1994b). Characterization of the mitogen-activated protein kinase/90-kilodalton ribosomal protein S6 kinase signaling pathway in 3T3-L1 adipocytes and its role in insulin-stimulated glucose transport. *Endocrinol.* **134**(2): 728-735.

Franke, T.F., Kaplan, D.R., Cantley, L.C., and Toker, A. (1997). Direct regulation of the *Akt* proto-oncogene product by phosphatidylinositol-3,4-bisphosphate. *Science* **275**: 665-668.

Frech, M., Andjelkovic, M., Ingley, E., Reddy, K.K., Falck, J.R., and Hemmings, B.A. (1997). High affinity binding of inositol phosphates and phosphoinositides to the pleckstrin homology domain of RAC/protein kinase B and their influence on kinase activity. *J. Biol. Chem.* **272**(13): 8474-8481.

Frevert, E.U. and Kahn, B.B. (1996). Protein kinase C isoforms ε, η, δ and ζ in murine adipocytes: expression, subcellular localization and tissue-specific regulation in insulin-resistant states. *Biochem. J.* **316**: 865-871.

Frevert, E.U. and Kahn, B.B. (1997). Differential effects of constitutively active phosphatidylinositol 3-kinase on glucose transport, glycogen synthase activity, and DNA synthesis in 3T3-L1 adipocytes. *Mol. Cell. Biol.* **17**(1): 190-198.

Fukumoto, H., Kayano, T., Buse, J.B., Edwards, Y., Pilch, P.F., Bell, G.I., and Seino, S. (1989). Cloning and characterization of the major insulin-responsive glucose transporter expressed in human skeletal muscle and other insulin-responsive tissues. *J. Biol. Chem.* **264**(14): 7776-7779.

Gibbs, E.M., Calderhead, D.M., Holman, G.D., and Gould, G.W. (1991). Phorbol ester only partially mimics the effects of insulin on glucose transport and glucose-transporter distribution in 3T3-L1 adipocytes. *Biochem. J.* **275**: 145-150.

Gibson, T.J., Hyvonen, M., Musacchio, A., and Saraste, M. (1994). PH domain: the first anniversary. *Trends Biochem. Sci.* **19**: 349-353.

Gould, G.W. and Holman, G.D. (1993). The glucose transporter family: structure, function and tissue-specific expression. *Biochem. J.* **295**: 329-341.

Gould, G.W., Merrall, N.W., Martin, S., Jess, T.J., Campbell, I.W., Calderhead, D.M., Gibbs, E.M., Holman, G.D., and Plevin, R.J. (1994). Growth factor-induced stimulation of hexose transport in 3T3-L1 adipocytes: evidence that insulin-induced translocation of GLUT4 is independent of activation of MAP kinase. *Cell. Sig.* **6**(3): 313-320.

Harlan, J.E., Hajduk, P.J., Yoon, H.S., and Fesik, S.W. (1994). Pleckstrin homology domains bind to phosphatidylinositol-4,5-bisphosphate. *Nature* **371**: 168-170.

Hausdorff, S.F., Frangioni, J.V., and Birnbaum, M.J. (1994). Role of $p21^{ras}$ in insulin-stimulated glucose transport in 3T3-L1 adipocytes. *J. Biol. Chem.* **269**(34): 21391-21394.

Haystead, T.A.J., Sim, A.T.R., Carling, S.D., Honnor, R.C., Tsukitani, Y., Cohen, P., and Hardie, D.G. (1989). Effects of the tumour promoter okadaic acid on intracellular protein phosphorylation and metabolism. *Nature* **337**: 78-81.

Heller-Harrison, R.A., Morin, M., Guilherme, A., and Czech, M.P. (1996). Insulin-mediated targeting of phosphatidylinositol 3-kinase to GLUT4-containing vesicles. *J. Biol. Chem.* **271**(17): 10200-10204.

Holman, G.D., Kozka, I.J., Clark, A.E., Flower, C.J., Saltis, J., Habberfield, A.D., Simpson, I.A., and Cushman, S.W. (1990). Cell surface labeling of glucose transporter isoform GLUT4 by bis-mannose photolabel. *J. Biol. Chem.* **265**(30): 18172-18179.

Holman, G.D. and Cushman, S.W. (1994). Subcellular localization and trafficking of the GLUT4 glucose transporter isoform in insulin-responsive cells. *BioEssays 16*(10): 753-759.

Holman, G.D., Lo Leggio, L., and Cushman, S.W. (1994). Insulin-stimulated GLUT4 glucose transporter recycling. *J. Biol. Chem.* **269**(26): 17516-17524.

Inglese, J., Koch, W.J., Touhara, K., and Lefkowitz, R.J. (1995). Gβγ interactions with PH domains and Ras-MAPK signaling pathways. *Trends. Biochem. Sci.* **20**: 151-156.

James, D.E., Strube, M., and Mueckler, M. (1989). Molecular cloning and characterization of an insulin-regulatable glucose transporter. *Nature* 338: 83-87.

Jones, P.F., Jakubowicz, T., Pitossi, F.J., Maurer, F., and Hemmings, B.A. (1991). Molecular cloning and identification of a serine/threonine protein kinase of the second-messenger subfamily. *Proc. Natl. Acad. Sci. USA* **88**: 4171-4175.

Jullien, D., Tanti, J.-F., Heydrick, S.J., Gautier, N., Gremeaux, T., Van Obberghen, E., and Le Marchand-Brustel, Y. (1993). Differential effects of okadaic acid on insulin-stimulated glucose and amino acid uptake and phosphatidylinositol 3-kinase activity. *J. Biol. Chem.* **268**(20): 15246-15251.

Kaestner, K.H., Christy, R.J., McLenithan, J.C., Braiterman, L.T., Cornelius, P., Pekala, P.H., and Lane, M.D. (1989). Sequence, tissue distribution, and differential expression of mRNA for a putative insulin-responsive glucose transporter in mouse 3T3-L1 adipocytes. *Proc. Natl. Acad. Sci. USA* **86**: 3150-3154.

Kahn, C.R. (1994). Insulin action, diabetogenes, and the cause of type II diabetes. *Diabetes* 43: 1066-1084.

Kapeller, R. and Cantley, L.C. (1994). Phosphatidylinositol 3-kinase. *BioEssays* **16**(8): 565-576.

Kasuga, M., Zick, Y., Blithe, D.L., Crettaz, M., and Kahn, C.R. (1982). Insulin stimulates tyrosine phosphorylation of the insulin receptor in a cell-free system. *Nature* **298**: 667-669.

Katagiri, H., Asano, T., Inukai, K., Ogihara, T., Ishihara, H., Shibasaki, Y., Murata, T., Terasaki, J., Kikuchi, M., Yazaki, Y., and Oka, Y. (1997). Roles of PI 3-kinase and Ras on insulin-stimulated glucose transport in 3T3-L1 adipocytes. *Am. J. Physiol.* **272**: E326-E331.

Keller, K., Strube, M., and Mueckler, M. (1989). Functional expression of the human HepG2 and rat adipocyte glucose transporters in *Xenopus* oocytes. *J. Biol. Chem.* **264**(32): 18884-18889.

Keller, S.R., Kitagawa, K., Aebersold, R., Lienhard, G.E., and Garner, C.W. (1991). Isolation and characterization of the 160,000-Da phosphotyrosyl protein, a putative participant in insulin signaling. *J. Biol. Chem.* **266**(20): 12817-12820.

Keller, S.R., Aebersold, R., Garner, C.W., and Lienhard, G.E. (1993). The insulin-elicited 160 kDa phosphotyrosine protein in mouse adipocytes is an insulin receptor substrate 1: identification by cloning. *Biochim. Biophys. Acta* **1172**: 323-326.

Keller, S.R. and Lienhard, G.E. (1994). Insulin signalling: the role of insulin receptor substrate 1. *Trends Cell Biol.* **4**: 115-119.

Kelly, K.L. and Ruderman, N.B. (1993). Insulin-stimulated phosphatidylinositol 3-kinase. *J. Biol. Chem.* **268**(6): 4391-4398.

Klippel, A., Reinhard, C., Kavanaugh, W.M., Apell, G., Escobedo, M.-A., and Williams, L.T. (1996). Membrane localization of phosphatidylinositol 3-kinase is sufficient to activate multiple signal-transducing kinase pathways. *Mol. Cell. Biol.* **16(8)**: 4117-4127.

Kohanski, R.A., Frost, S.C., and Lane, M.D. (1986). Insulin-dependent phosphorylation of the insulin receptor-protein kinase and activation of glucose transport in 3T3-L1 adipocytes. *J. Biol. Chem.* **261**(26): 12272-12281.

Kohn, A.D., Kovacina, K.S., and Roth, R.A. (1995). Insulin stimulates the kinase activity of RAC-PK, a pleckstrin homology domain containing ser/thr kinase. *EMBO J.* **14**(17): 4288-4295.

Kohn, A.D., Takeuchi, F., and Roth, R.A. (1996a). Akt, a pleckstrin homology domain containing kinase, is activated primarily by phosphorylation. *J. Biol. Chem.* **271**(36): 21920-21926.

Kohn, A.D., Summers, S.A., Birnbaum, M.J., and Roth, R.A. (1996b). Expression of a constitutively active Akt ser/thr kinase in 3T3-L1 adipocytes stimulates glucose uptake and glucose transporter 4 translocation. *J. Biol. Chem.* **271**(49): 31372-31378.

Konishi, H., Kuroda, S., Tanaka, M., Matsuzaki, H., Ono, Y., Kameyama, K., Haga, T., and Kikkawa, U. (1995). Molecular cloning and characterization of a new member of the rac protein kinase family: association of the pleckstrin homology domain of three types of rac protein kinase with protein kinase C subspecies and βγ subunits of G proteins. *Biochem. Biophys. Res. Commun.* **216**(2): 526-534.

Kozka, I.J., Clark, A.E., and Holman, G.D. (1991). Chronic treatment with insulin selectively down-regulates cell-surface GLUT4 glucose transporters in 3T3-L1 adipocytes. *J. Biol. Chem.* **266**(18): 11726-11731.

Kozka, I.J. and Holman, G.D. (1993). Metformin blocks downregulation of cell surface GLUT4 caused by chronic insulin treatment of rat adipocytes. *Diabetes* **42**: 1159-1165.

Lavan, B.E. and Lienhard, G.E. (1993). The insulin-elicited 60-kDa phosphotyrosine protein in rat adipocytes is associated with phosphatidylinositol 3-kinase. *J. Biol. Chem.* **268**(8): 5921-5928.

Lavan, B.E., Lane, W.S., and Lienhard, G.E. (1997). The 60-kDa phosphotyrosine protein in insulin-treated adipocytes is a new member of the insulin receptor substrate family. *J. Biol. Chem.* **272**(17): 11439-11443.

Lawrence Jr., J.C., Hiken, J.F., and James, D.E. (1990). Stimulation of glucose transport and glucose transporter phosphorylation by okadaic acid in rat adipocytes. *J. Biol. Chem.* **265**(32): 19768-19776.

Lemmon, M.A., Ferguson, K.M., O'Brien, R., Sigler, P.B., and Schlessinger, J. (1995). Specific and high-affinity binding of inositol phosphates to an isolated pleckstrin homology domain. *Proc. Natl. Acad. Sci. USA* **92**: 10472-10476.

Lowe, A.G. and Walmsley, A.R. (1986). The kinetics of glucose transport in human red blood cells. *Biochim. Biophys. Acta* **857**: 146-154.

Marsh, B.J., Alm, R.A., McIntosh, S.R., and James, D.E. (1995). Molecular regulation of GLUT-4 targeting in 3T3-L1 adipocytes. *J. Cell Biol.* **130**(5): 1081-1091.

Martin, S.S., Haruta, T., Morris, A.J., Klippel, A., Williams, L.T., and Olefsky, J.M. (1996). Activated phosphatidylinositol 3-kinase is sufficient to mediate actin rearrangement and GLUT4 translocation in 3T3-L1 adipocytes. *J. Biol. Chem.* **271**(30): 17605-17608.

Morris, A.J., Martin, S.S., Haruta, T., Nelson, J.G., Vollenweider, P., Gustafson, T.A., Mueckler, M., Rose, D.W., and Olefsky, J.M. (1996). Evidence for an insulin receptor substrate 1 independent insulin

signaling pathway that mediates insulin-responsive glucose transporter (GLUT4) translocation. *Proc. Natl. Acad. Sci. USA* **93**: 8401-8406.

Moule, S.K., Welsh, G.I., Edgell, N.J., Foulstone, E.J., Proud, C.G., and Denton, R.M. (1997). Regulation of protein kinase B and glycogen synthase kinase-3 by insulin and β-adrenergic agonists in rat epididymal fat cells. *J. Biol. Chem.* **272**(12): 7713-7719.

Mueckler, M., Caruso, C., Baldwin, S.A., Panico, M., Blench, I., Morris, H.R., Allard, W.J., Lienhard, G.E., and Lodish, H.F. (1985). Sequence and structure of a human glucose transporter. *Science* **229**: 941-945.

Murakami, M.S. and Rosen, O.M. (1991). The role of insulin receptor autophosphorylation in signal transduction. *J. Biol. Chem.* **266**(33): 22653-22660.

Musacchio, A., Gibson, T., Rice, P., Thompson, J., and Saraste, M. (1993). The PH domain: a common piece in the structural patchwork of signalling proteins. *Trends Biochem. Sci.* **18**: 343-348.

Myers Jr., M.G., Grammer, T.C., Brooks, J., Glasheen, E.M., Wang, L.-M., Sun, X.J., Blenis, J., Pierce, J.H., and White, M.F. (1995). The pleckstrin homology domain in insulin receptor substrate-1 sensitizes insulin signaling. *J. Biol. Chem.* **270**(20): 11715-11718.

Nakanishi, H., Brewer, K.A., and Exton, J.H. (1993). Activation of the ζ isozyme of protein kinase C by phosphatidylinositol 3,4,5-trisphosphate. *J. Biol. Chem.* **268**(1): 13-16.

Nave, B.T., Haigh, R.J., Hayward, A.C., Siddle, K., and Shepherd, P.R. (1996a). Compartment-specific regulation of phosphoinositide 3-kinase by platelet-derived growth factor and insulin in 3T3-L1 adipocytes. *Biochem. J.* **318**: 55-60.

Nave, B.T., Siddle, K., and Shepherd, P.R. (1996b). Phorbol esters stimulate phosphatidylinositol 3,4,5-trisphosphate production in 3T3-L1 adipocytes: implications for stimulation of glucose transport. *Biochem. J.* **318**: 203-205.

Nishimura, H., Pallardo, F.V., Seidner, G.A., Vannucci, S., Simpson, I.A., and Birnbaum, M.J. (1993). Kinetics of GLUT1 and GLUT4 glucose transporters expressed in *Xenopus* oocytes. *J. Biol. Chem.* **268**(12): 8514-8520.

Olson, A.L., Knight, J.B., and Pessin, J.E. (1997). Syntaxin 4, VAMP2, and/or VAMP3/cellubrevin are functional target membrane and vesicle SNAP receptors for insulin-stimulated GLUT4 translocation in adipocytes. *Mol. Cell. Biol.* **17**(5): 2425-2435.

Paterson, H.F., Savopoulos, J.W., Perisic, O., Cheung, R., Ellis, M.V., Williams, R.L., and Katan, M. (1995). Phospholipase C δ_1 requires a pleckstrin homology domain for interaction with the plasma membrane. *Biochem. J.* **312**: 661-666.

Patti, M.-E., Sun, X.-J., Bruening, J.C., Araki, E., Lipes, M.A., White, M.F., and Kahn, C.R. (1995). 4PS/Insulin receptor substrate (IRS)-2 is the alternative substrate of the insulin receptor in IRS-1-deficient mice. *J. Biol. Chem.* **270**(42): 24670-24673.

Piper, R.C., Hess, L.J., and James, D.E. (1991). Differential sorting of two glucose transporters expressed in insulin-sensitive cells. *Am. J. Physiol.* **260**: C570-C580.

Piper, R.C., Tai, C., Slot, J.W., Hahn, C.S., Rice, C.M., Huang, H., and James, D.E. (1992). The efficient intracellular sequestration of the insulin-regulatable glucose transporter (GLUT-4) is conferred by the NH_2 terminus. *J. Cell Biol.* **117**(4): 729-743.

Piper, R.C., Tai, C., Kulesza, P., Pang, S., Warnock, D., Baenziger, J., Slot, J.W., Geuze, H.J., Puri, C., and James, D.E. (1993). GLUT-4 NH_2 terminus contains a phenylalanine-based targeting motif that regulates intracellular sequestration. *J. Cell Biol.* **121**(6): 1221-1232.

Pronk, G.J., McGlade, J., Pelicci, G., Pawson, T., and Bos, J.L. (1993). Insulin-induced phosphorylation of the 46- and 52-kDa Shc proteins. *J. Biol. Chem.* **268**(8): 5748-5753.

Pryor, P.R., Liu, S.C.H., and Holman, G.D. (1997). Metformin prevents the down-regulation of signalling intermediates in rat adipocytes that have been chronically treated with insulin. *In press.*

Rice, K.M., Turnbow, M.A., and Garner, C.W. (1993). Insulin stimulates the degradation of IRS-1 in 3T3-L1 adipocytes. *Biochem. Biophys. Res. Commun.* **190**(3): 961-967.

Ricort, J.-M., Tanti, J.-F., Van Obberghen, E., and Le Marchand-Brustel, Y. (1995). Alterations in insulin signalling pathway induced by prolonged insulin treatment of 3T3-L1 adipocytes. *Diabetologia* **38**: 1148-1156.

Ricort, J.-M., Tanti, J.-F., Van Obberghen, E., and Le Marchand-Brustel, Y. (1996). Different effects of insulin and platelet-derived growth factor on phosphatidylinositol 3-kinase at the subcellular level in 3T3-L1 adipocytes. *Eur. J. Biochem.* **239**: 17-22.

Rondinone, C.M., Wang, L.-M., Lonnroth, P., Wesslau, C., Pierce, J.H., and Smith, U. (1997). Insulin receptor substrate (IRS) 1 is reduced and IRS-2 is the main docking protein for phosphatidylinositol 3-

kinase in adipocytes from subjects with non-insulin-dependent diabetes mellitus. *Proc. Natl. Acad. Sci. USA* **94**: 4171-4175.

Rordorf-Nikolic, T., Van Horn, D.J., Chen, D., White, M.F., and Backer, J.M. (1995). Regulation of phosphatidylinositol 3'-kinase by tyrosyl phosphoproteins. *J. Biol. Chem.* **270**(8): 3662-3666.

Rothenberg, P.L., Lane, W.S., Karasik, A., Backer, J., White, M., and Kahn, C.R. (1991). Purification and partial sequence analysis of pp185, the major cellular substrate of the insulin receptor tyrosine kinase. *J. Biol. Chem.* **266**(13): 8302-8311.

Satoh, S., Nishimura, H., Clark, A.E., Kozka, I.J., Vannucci, S.J., Simpson, I.A., Quon, M.J., Cushman, S.W., and Holman, G.D. (1993). Use of bismannose photolabel to elucidate insulin-regulated GLUT4 subcellular trafficking kinetics in rat adipose cells. *J. Biol. Chem.* **268**(24): 17820-17829.

Sawka-Verhelle, D., Tartare-Decker, S., White, M.F., and Van Obberghen, E. (1996). Insulin receptor substrate-2 binds to the insulin receptor through its phosphotyrosine-binding domain and through a newly identified domain comprising amino acids 591-786. *J. Biol. Chem.* **271**(11): 5980-5983.

Shibata, H., Suzuki, Y., Omata, W., Tanaka, S., and Kojima, I. (1995). Dissection of GLUT4 recycling pathway into exocytosis and endocytosis in rat adipocytes. *J. Biol. Chem.* **270**(19): 11489-11495.

Simpson, I.A., Yver, D.R., Hissin, P.J., Wardzala, L.J., Karnieli, E., Salans, L.B., and Cushman, S.W. (1983). Insulin-stimulated translocation of glucose transporters in the isolated rat adipose cells: characterization of subcellular fractions. *Biochim. Biophys. Acta* **763**: 393-407.

Skolnik, E.Y., Lee, C.-H., Batzer, A., Vicentini, L.M., Zhou, M., Daly, R., Myers Jr., M.J., Backer, J.M., Ullrich, A., White, M.F., and Schlessinger, J. (1993a). The SH2/SH3 domain-containing protein GRB2 interacts with tyrosine-phosphorylated IRS1 and Shc: implications for insulin control of ras signalling. *EMBO J.* **12**(5): 1929-1936.

Skolnik, E.Y., Batzer, A., Li, N., Lee, C.-H., Lowenstein, E., Mohammadi, M., Margolis, B., and Schlessinger, J. (1993b). The function of GRB2 in linking the insulin receptor to Ras signaling pathways. *Science* **260**: 1953-1955.

Slot, J.W., Geuze, H.J., Gigengack, S., Lienhard, G.E., and James, D.E. (1991). Immuno-localization of the insulin regulatable glucose transporter in brown adipose tissue of the rat. *J. Cell Biol.* **113**(1): 123-135.

Staubs, P.A., Reichart, D.R., Saltiel, A.R., Milarski, K.L., Maegawa, Berhanu, P., Olefsky, J.M., and Seely, B.L. (1994). Localization of the insulin receptor binding sites for the SH2 domain proteins p85, Syp, and GAP. *J. Biol. Chem.* **269**(44): 27186-27192.

Sun, X.J., Rothenberg, P., Kahn, C.R., Backer, J.M., Araki, E., Wilden, P.A., Cahill, D.A., Goldstein, B.J., and White, M.F. (1991). Structure of the insulin receptor substrate IRS-1 defines a unique signal transduction protein. *Nature* **352**: 73-77.

Sun, X.J., Miralpeix, M., Myers Jr., M.G., Glasheen, E.M., Backer, J.M., Kahn, C.R., and White, M.F. (1992). Expression and function of IRS-1 in insulin signal transmission. *J. Biol. Chem.* **267**(31): 22662-22672.

Sun, X.J., Crimmins, D.L., Myers Jr., M.G., Miralpeix, M., and White, M.F. (1993). Pleiotropic insulin signals are engaged by multisite phosphorylation of IRS-1. *Mol. Cell. Biol.* **13**(12): 7418-7428.

Sun, X.J., Wang, L.-M., Zhang, Y., Yenush, L., Myers Jr, M.G., Glasheen, E., Lane, W.S., Pierce, J.H., and White, M.F. (1995). Role of IRS-2 in insulin and cytokine signalling. *Nature* **377**: 173-177.

Suzuki, K. and Kono, T. (1980). Evidence that insulin causes translocation of glucose transport activity to the plasma membrane from an intracellular storage site. *Proc. Natl. Acad. Sci. USA* **77**: 2542-2545.

Tamemoto, H., Kadowaki, T., Tobe, K., Yagi, T., Sakura, H., Hayakawa, T., Terauchi, Y., Ueki, K., Kaburagi, Y., Satoh, S., Sekihara, H., Yoshioka, S., Horikoshi, H., Furuta, Y., Ikawa, Y., Kasuga, M., Yazaki, Y., and Aizawa, S. (1994). Insulin resistance and growth retardation in mice lacking insulin receptor substrate-1. *Nature* **372**: 182-186.

Tanner, L.I. and Lienhard, G.E. (1989). Localization of transferrin receptors and insulin-like growth factor II receptors in vesicles from 3T3-L1 adipocytes that contain intracellular glucose transporters. *J. Cell Biol.* **108**: 1537-1545.

Tanti, J.-F., Gremeaux, T., Van Obberghen, E., and Le Marchand-Brustel, Y. (1994). Serine/threonine phosphorylation of insulin receptor substrate 1 modulates insulin receptor signaling. *J. Biol. Chem.* **269**(8): 6051-6057.

Tanti, J.-F., Grillo, S., Gremeaux, T., Coffer, P.J., Van Obberghen, E., and Le Marchand-Brustel, Y. (1997). Potential role of protein kinase B in glucose transporter 4 translocation in adipocytes. *Endocrinol.* **138**(5): 2005-2010.

Timmers, K.I., Clark, A.E., Omatsu-Kanbe, M., Whiteheart, S.W., Bennett, M.K., Holman, G.D., and Cushman, S.W. (1996). Identification of SNAP receptors in rat adipose cell membrane fractions and in SNARE complexes co-immunoprecipitated with epitope-tagged N-ethylmaleimide-sensitive fusion protein. *Biochem. J.* **320**: 429-436.

Tobe, K., Tamemoto, H., Yamauchi, T., Aizawa, S., Yazaki, Y., and Kadowaki, T. (1995). Identification of a 190-kDa protein as a novel substrate for the insulin receptor kinase functionally similar to insulin receptor substrate-1. *J. Biol. Chem.* **270**(11): 5698-5701.

Touhara, K., Inglese, J., Pitcher, J.A., Shaw, G., and Lefkowitz, R.J. (1994). Binding of G protein βγ-subunits to pleckstrin homology domains. *J. Biol. Chem.* **269**(14): 10217-10220.

Ui, M., Okada, T., Hazeki, K., and Hazeki, O. (1995). Wortmannin as a unique probe for an intracellular signalling protein, phosphoinositide 3-kinase. *Trends Biochem. Sci.* **20**: 303- 307.

Ullrich, A., Bell, J.R., Chen, E.Y., Herrera, R., Petruzzelli, L.M., Dull, T.J., Gray, A., Coussens, L., Liao, Y.-C., Tsubokawa, M., Mason, A., Seeburg, P.H., Grunfeld, C., Rosen, O.M., and Ramachandran, J. (1985). Human insulin receptor and its relationship to the tyrosine kinase family of oncogenes. *Nature* **313**: 756-761.

Van Horn, D.J., Myers Jr., M.G., and Backer, J.M. (1994). Direct activation of the phosphatidylinositol 3'-kinase by the insulin receptor. *J. Biol. Chem.* **269**(1): 29-32.

Verhey, K.J., Yeh, J.-I., and Birnbaum, M.J. (1995). Distinct signals in the GLUT4 glucose transporter for internalization and for targeting to an insulin-responsive compartment. *J. Cell Biol.* **130**(5): 1071-1079.

Vlahos, C.J., Matter, W.F., Hui, K.Y., and Brown, R.F. (1994). A specific inhibitor of phosphatidylinositol 3-kinase, 2-(4-morpholinyl)-8-phenyl-4H-1-benzopyran-4-one (LY294002). *J. Biol. Chem.* **269**(7): 5241-5248.

Voliovitch, H., Schindler, D.G., Hadari, Y.R., Taylor, S.I., Accili, D., and Zick, Y. (1995). Tyrosine phosphorylation of insulin receptor substrate-1 *in Vivo* depends upon the presence of its pleckstrin homology region. *J. Biol. Chem.* **270**(30): 18083-18087.

Wang, D.-S., Shaw, R., Winkelmann, J.C., and Shaw, G. (1994). Binding of PH domains of β-adrenergic receptor kinase and β-spectrin to WD40/β-transducin repeat containing regions of the β-subunit of trimeric G-proteins. *Biochem. Biophys. Res. Commun.* **203**(1): 29-35.

White, M.F., Maron, R., and Kahn, C.R. (1985). Insulin rapidly stimulates tyrosine phosphorylation of a Mr-185,000 protein in intact cells. *Nature* **318**: 183-186.

White, M.F. and Kahn, C.R. (1994). The insulin signaling system. *J. Biol. Chem.* **269**(1): 1-4.

Whitesell, R.R. and Gliemann, J. (1979). Kinetic parameters of transport of 3-*O*-methylglucose and glucose in adipocytes. *J. Biol. Chem.* **254**(12): 5276-5283.

Wolf, G., Trub, T., Ottinger, E., Groninga, L., Lynch, A., White, M.F., Miyazaki, M., Lee, J., and Shoelson, S.E. (1995). PTB domains of IRS-1 and Shc have distinct but overlapping binding specificities. *J. Biol. Chem.* **270**(46): 27407-27410.

Yang, J., Clark, A.E., Harrison, R., Kozka, I.J., and Holman, G.D. (1992). Trafficking of glucose transporters in 3T3-L1 cells. *Biochem. J.* **281**: 809-817.

Yang, J. and Holman, G.D. (1993). Comparison of GLUT4 and GLUT1 subcellular trafficking in basal and insulin-stimulated 3T3-L1 cells. *J. Biol. Chem.* **268**(7): 4600-4603.

Yang, J., Clarke, J.F., Ester, C.J., Young, P.W., Kasuga, M., and Holman, G.D. (1996). Phosphatidylinositol 3-kinase acts at an intracellular membrane site to enhance GLUT4 exocytosis in 3T3-L1 cells. *Biochem. J.* **313**: 125-131.

Yenush, L., Makati, K., Smith-Hall, J., Ishibashi, O., Myers Jr., M.G., and White, M.F. (1996). The pleckstrin homology domain is the principle link between the insulin receptor and IRS-1. *J. Biol. Chem.* **271**(39): 24300-24306.

Yonezawa, K., Ando, A., Kaburagi, Y., Yamamoto-Honda, R., Kitamura, T., Hara, K., Nakafuku, M., Okabayashi, Y., Kadowaki, T., Kaziro, Y., and Kasuga, M. (1994). Signal transduction pathways from insulin receptors to Ras. *J. Biol. Chem.* **269**(6): 4634-4640.

Zorzano, A., Wilkinson, W., Kotliar, N., Thoidis, G., Wadzinkski, B.E., Ruoho, A.E., and Pilch, P.F. (1989). Insulin-regulated glucose uptake in rat adipocytes is mediated by two transporter isoforms present in at least two vesicle populations. *J. Biol. Chem.* **264**(21): 12358-12363.